

NONLINEAR POLYMERIC
ARCHITECTURES VIA OLEFIN
METATHESIS

Thesis by

Irina A. Gorodetskaya

In Partial Fulfillment of the Requirements for the
degree of

Doctor of Philosophy

CALIFORNIA INSTITUTE OF TECHNOLOGY

Pasadena, California

2009

(Defended November 25, 2008)

© 2009

Irina A. Gorodetskaya

All Rights Reserved

To my grandmother Yadviga

ACKNOWLEDGEMENTS

First, I would like to thank my research advisor, Professor Grubbs, for accepting me into his group. Being a part of the Grubbs groups was everything I sought in a graduate school experience. I am very grateful to Bob for his seemingly infinite patience, which allowed me the time and resources to pursue the projects that were interesting to me at my own pace. Bob's guidance, combined with the consistently diverse and stimulating environment of the group, provided an invaluable learning experience on both scientific and personal levels, and it has made me a smarter, better, stronger person.

I am grateful to Dr. Tae-Lim Choi for believing in me and for being so persistently "annoying" with his suggestions on the potential of olefin metathesis chemistry for hyperbranched polymerization. This thesis would not be quite the same without the research that evolved from the TLC's nagging—thank you so much!

Next, I thank my most immediate collaborators over the years at Caltech. Lucia Fernandez-Ballister from the Kornfield group at Caltech and Jian Wang from the McKenna group at Texas Tech taught me everything I know about the rheology of polymer melts. They greatly contributed to the cyclic polymers research presented in Chapter 5 of this thesis (while making me secretly happy I did not choose chemical engineering as my major). Alon Gorodetsky provided his invaluable expertise in the study of pyrene-functionalized polymers described in Chapter 3. Finally, Katya Vinogradova worked very long hours on the hyperbranched project over the summer of 2007 as a summer undergraduate research fellow. Thank you all! I greatly benefited from your skill, knowledge, and time, and it has been a pleasure to know you and work with you.

I would also like to thank Alon again, Dr. Rose Conrad, and Dr. Ian Stewart for their time and help in proof-reading this thesis. I am sorry, but despite all of the language coaching you provided, I don't have enough fancy English words in my vocabulary to express my gratitude to you for reading it all (including the experimentals!) and providing numerous helpful suggestions. I also enjoyed sharing the lab with Rose and Ian, and our non-thesis- and even non-science-related(!) conversations.

I am very grateful to Professor Tobias Ritter, the most brilliant synthetic chemist I have ever met, for a number of key research suggestions, but also, and more importantly, for teaching me one of the most valuable skills I gained while in graduate school—driving. Having a car not only greatly enriched my life in Southern California, but also, finally, made me feel truly American. On this note, I would also like to thank Dr. Donde Anderson for risking her life as my diving buddy and navigator in my early driving days.

I am at loss of words, again, to describe the depth of my gratitude to my family, whether relatively close (within the US borders) or far abroad (Russia and Ukraine). Your unconditional love and support (moral and financial) made all the difference and got me through the grad school: mom, dad, grandma Lyuba, Natasha, tyetushka, Bobochka—I love you all. Special thanks go to cousin Pitrovich, who is currently the farthest away relative, but used to be the closest in San Francisco, where he was always happy to see me, even if for a few minutes of a practically unannounced, 3 am on a week-night visit of a camping gear emergency. Thank you for all your help, advice, and genuine interest in my well-being; and also for introducing me to Mitya, Olya, Fedor, Sasha, who became my adoptive Pasadena family.

I want to thank my thesis committee: Professor Tirrell, Professor Heath, and Professor Barton.

Finally, I wish to thank all of the friends and acquaintances, who are not singled out on this undeservingly short list, but whose friendships, love, care and kindness have touched my life over the past few years, making my not-so-short stay in Pasadena special and memorable.

ABSTRACT

The research presented in this thesis focuses on application of different forms of olefin metathesis, in conjunction with judicious choices of catalysts and monomers, to the construction of hyperbranched and cyclic macromolecules. This multifaceted reaction is briefly reviewed in Chapter 1, along with ruthenium-based metathesis catalysts and applications of olefin metathesis in polymer synthesis.

Hyperbranched polymers are curious materials which feature multiple end groups and possess a host of desirable physical properties; potential applications stemming from the unique properties of these macromolecules include their use as viscosity lowering additives and analyte carriers. In general, the major drawbacks faced by the classical, AB_n monomer-based hyperbranched polymers are the limited availability of specially designed monomers, harsh synthetic conditions, and poor control of the required step-growth polymerization methods. A very mild, simple, and modular, olefin metathesis-based hyperbranched polymerization route, which addresses some of these challenges, is presented in Chapter 2. This method utilizes the cross metathesis selectivity of the functional group tolerant N-heterocyclic carbene ruthenium catalyst towards different types of alkenes, and it can be applied to the polymerization of many easily prepared AB_n monomers. Moreover, the same method can be used to post-synthetically functionalize such polymers for realization of their substrate carrying potential. Chapter 3 describes one functionalization example—a pyrene analyte is attached to a metathesis derived hyperbranched polymer. This modification of the polymer provides insight into its solution structure relative to a linear analog. In addition, molecular weight control of the metathesis hyperbranched polymerization is discussed in detail in Chapter 4. The careful choice of the catalysts loading and the use of a multifunctional core are found to be important parameters in preparation of polymers which span a range of molecular weights.

Even well-established materials, such as polyethylene, can benefit from olefin metathesis and the unusual polymeric architectures it can efficiently create. For example, a cyclic polymer which lacks end groups, as opposed to having many end groups like a

hyperbranched polymer, is expected to possess unique physical properties. The preparation of cyclic and linear polyethylenes and the study of their relative rheological properties are described in Chapter 5. The polymerization methodology outlined in this Chapter takes advantage of ring-expansion metathesis polymerization—a facile method for the synthesis of cyclic macromolecules. Some efforts directed at molecular weight control of this cyclic polymerization are also discussed.

Taken together, the findings presented in this thesis emphasize the utility of olefin metathesis for the preparation of nonlinear polymers. The unusual polymeric architectures available through this chemical transformation may lead to a host of new materials with unique properties.

TABLE OF CONTENTS

CHAPTER 1: <i>Introduction to Olefin Metathesis and Its Applications in</i>	
<i>Polymer Synthesis</i>	1
Olefin Metathesis.....	2
Polymer Synthesis Applications of Olefin Metathesis.....	6
<i>ADMET</i>	6
<i>ROMP</i>	7
Summary and Thesis Research	8
References.....	11
CHAPTER 2: <i>Hyperbranched Polymers via Acyclic Diene Metathesis</i>	
<i>Polymerization</i>	14
Abstract.....	15
Introduction.....	16
Results and Discussion.....	17
Conclusion	23
Experimental Procedures.....	24
Representative Polymerization Procedure.....	31
References.....	33

CHAPTER 3: <i>An Olefin Metathesis Route to the Preparation of Functionalized Hyperbranched Polymers</i>	35
Abstract	36
Introduction.....	37
Results and Discussion	38
Functionalization of the Hyperbranched Polymer.....	38
Preparation of the Pyrene Modified Linear Analog	43
Fluorescence Properties of Pyrene-Functionalized Hyperbranched and Linear Polymers.....	45
Conclusion	46
Experimental Procedures.....	48
References.....	52
CHAPTER 4: <i>Towards Molecular Weight Control of the Hyperbranched ADMET Polymerization</i>	54
Abstract	55
Introduction.....	56
Results and Discussion	58
Catalyst Loading.....	58
Reaction Time	62
Addition of a Multifunctional Core	64
Conclusion	66
Experimental Procedures.....	67

References.....	68
CHAPTER 5: <i>The Importance of Molecular Weight Control for Cyclic</i>	
<i>Polymers Prepared via Ring-Expansion Metathesis Polymerization</i> 69	
Abstract.....	70
Introduction.....	71
Results and Discussion.....	72
Part 1: Studies of shear-induced crystallization processes in polyethylene and the need for large cyclic polymers.....	72
Part 2: Studies of the viscoelastic properties of cyclic polyethylene and the need for small cyclic polymers	77
Conclusion	82
Polymerization Experimental Procedures.....	84
References.....	86
Appendix A: <i>Towards AB_n-Based Hyperbranched Polyethylene</i>	88
Experimental Procedures.....	91
Notes and References	93

LIST OF FIGURES, SCHEMES AND TABLES

CHAPTER 1

Figures

Figure 1.1. Ruthenium-based olefin metathesis catalysts	5
---	---

Schemes

Scheme 1.1. General mechanism of olefin metathesis.....	2
Scheme 1.2. Types of olefin metathesis reactions.....	3
Scheme 1.3. Selectivity of 1 st and 2 nd generation ruthenium catalysts.	6
Scheme 1.4. Olefin metathesis routes to polyethylene of different architectures.....	9

Tables

Table 1.1. Functional group tolerance of olefin metathesis catalysts.	4
--	---

CHAPTER 2

Figures

Figure 2.1. Acyclic diene metathesis polymerization catalyst.....	18
Figure 2.2. Monomers for hyperbranched ADMET polymerization.....	18
Figure 2.3. ¹ H NMR spectra of monomer 4 and hyperbranched polymer 4a	19
Figure 2.4. Mark-Houwink-Sakurada plots for polymers 2a–7a	21
Figure 2.5. Representative MALS-SEC traces for polymerization of 4 with consecutive batch catalyst addition.	32

Schemes

Scheme 2.1. Synthesis of dendritic polymers.....	16
Scheme 2.2. Synthesis of AB ₂ monomer 4 and its hyperbranched ADMET polymerization.	18

Scheme 2.3. AB ₂ monomers which were found to be challenging for ADMET.....	22
Scheme 2.4. Synthesis of AB ₄ monomer for hyperbranched ADMET polymerization.....	23
Scheme 2.5. Synthesis of monomer 2	24
Scheme 2.6. Synthesis of monomers 3 and 5	25
Scheme 2.7. Synthesis of monomer 6	27
Scheme 2.8. Synthesis of monomer 7	28
Scheme 2.9. Synthesis of monomer 8	30
Scheme 2.10. Synthesis of monomer 9	30

Tables

Table 2.1. Results for polymerization of 2–7	20
---	----

CHAPTER 3

Figures

Figure 3.1. Imidazolynylidene-based ruthenium olefin metathesis catalyst 1	38
Figure 3.2. SEC traces for 3 before and after functionalization with 0.5 equivalents of 10-bromo-1-decene.....	40
Figure 3.3. ¹ H NMR spectra with integration values for 2 , 3 , and 5	42
Figure 3.4. SEC traces for crude 3 , crude and purified 5	43
Figure 3.5. ¹ H NMR spectra with integration values for 6 , 7 , and 8	44
Figure 3.6. (A) UV-visible absorbance and fluorescence emission spectra for 4 , 5 , and 8 . (B) A plot of the monomer to excimer intensity emission ratio at various concentrations.....	46

Schemes

Scheme 3.1. Hyperbranched ADMET polymerization	
--	--

and subsequent end group functionalization.	39
Scheme 3.2. Hyperbranched polymer 3 functionalization with pyrene....	41
Scheme 3.3. Synthesis of the pyrene-functionalized linear polymeric analog.....	44
Scheme 3.4. Synthesis of the monomers for linear ROMP.....	49

CHAPTER 4

Figures

Figure 4.1. ADMET catalyst 1	57
Figure 4.2. SEC traces for 3 made with different amounts of 1	58
Figure 4.3. SEC traces for 5 made with different amounts of 1	60
Figure 4.4. Molecular weight and PDI timeline of 3 at 0.5 mol % of 1 . ..	62
Figure 4.5. Proposed polymerization “error” correction mechanism.	63
Figure 4.6. The dependence of the observed M_w at 0.5 mol % of 1 on the addition time of 8-bromo-1-octene.....	64
Figure 4.7. SEC traces for 3 made with a fixed amount of 1 but different amounts of 4	65

Schemes

Scheme 4.1. Hyperbranched ADMET polymerization.	57
Scheme 4.2. Linear ADMET polymerization.....	59
Scheme 4.3. The “chain-walking” mechanism for hyperbranched ADMET polymerization at low loading of 1	61

CHAPTER 5

Figures

Figure 5.1. The effect of shear stress on polymer chain orientation.	73
Figure 5.2. Catalysts required for the preparation of linear and cyclic polyalkenamers.....	74
Figure 5.3. Polarized optical microscopy of selected samples.....	77

Figure 5.4. The results of the viscoelastic properties investigation of cyclic PE prepared by REMP.....	79
Figure 5.5. Proposed 2 nd generation REMP catalysts.....	80
Figure 5.6. First accomplished 2 nd generation REMP catalyst.....	83

Schemes

Scheme 5.1. Ring-expansion polymerization.....	72
Scheme 5.2. Synthesis of long and short linear PE chains.....	75
Scheme 5.3. Synthesis of large PE rings.....	76
Scheme 5.4. Synthetic route towards 2 nd generation REMP catalyst 4	81
Scheme 5.5. Synthetic route towards 2 nd generation REMP catalyst 5	82

Tables

Table 5.1. Results for REMP of cyclic alkenes with 3	76
---	----

Appendix A

Figures

Figure A1. Hyperbranched ADMET catalysts	90
Figure A2. H NMR evidence for polymerization of 3 to 4	90

Schemes

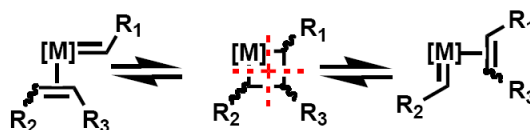
Scheme A1. Synthetic route towards the hyperbranched polyethylene via ADMET.....	90
---	----

CHAPTER 1
Introduction to Olefin Metathesis and Its Applications in Polymer
Synthesis

Olefin Metathesis

Olefin metathesis is a metal-catalyzed transformation, which acts on carbon-carbon double bonds and rearranges them via cleavage and reassembly.¹⁻⁵ While the reaction itself was discovered in the mid-1950s, its now generally accepted mechanism was not proposed until 1971.⁶ According to this mechanism, first introduced by Chauvin, the coordination of an olefin to a metal carbene catalytic species leads to the reversible formation of a metallacyclobutane (Scheme 1.1). This intermediate then proceeds by cycloreversion via either of the two possible paths: 1) non-productive—resulting in the re-formation of the starting materials or 2) product-forming—yielding an olefin that has exchanged a carbon with the catalyst's alkylidene. Since all of these processes are fully reversible (Scheme 1.1), only statistical mixtures of starting materials as well as all of possible rearrangement products are produced in the absence of thermodynamic driving forces.

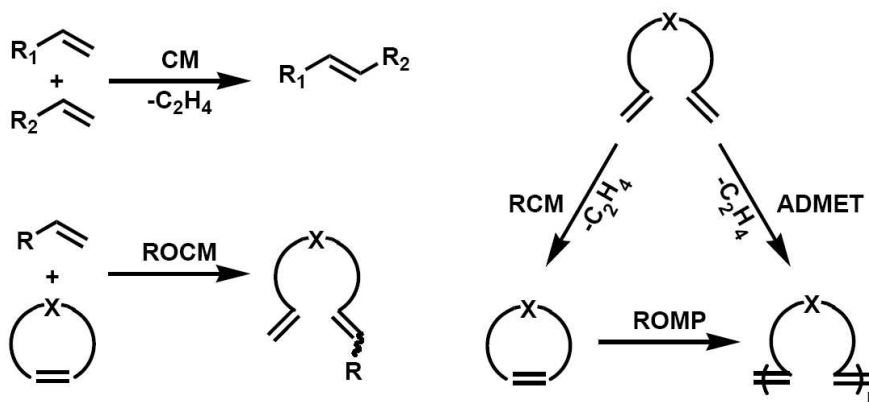
Scheme 1.1. General mechanism of olefin metathesis.⁶



Fortunately for the organic and polymer chemistry communities, the olefin metathesis reaction's thermodynamic equilibrium can be easily influenced. There are two major approaches that are commonly employed to drive the reaction towards the desired products. One tactic is to rely on Le Chatelier's principle by continuously removing one of the products from the reaction system in order to shift the equilibrium in favor of the other product. This method is especially effective in the case of cross metathesis (CM)⁷ reactions involving terminal olefins, ring-closing metathesis (RCM)^{8,9} and acyclic diene metathesis polymerization (ADMET),¹⁰⁻¹⁴ because the volatile ethylene gas by-product formed in these processes can be easily removed (Scheme 1.2). The other approach capitalizes on the ring strain of cyclic olefins such as cyclooctenes and norbornenes. The energy released during the ring-opening of these compounds is sufficient to drive forward reactions such as ring-opening cross metathesis (ROCM)^{15,16} and ring-opening metathesis polymerization

(ROMP)^{2,14,17,18} (Scheme 1.2). In addition, in some instances, substrate concentration (which often distinguishes ADMET from RCM) or the catalysts' sensitivity to olefin substitution can also be taken advantage of to influence product selectivity. All of these methods are currently successfully employed in the synthesis of a large variety of small, medium, and polymeric molecules, as well as novel materials.^{1-5,19-23}

Scheme 1.2. Types of olefin metathesis reactions.⁴



Once an olefin metathesis mechanism consistent with the experimental evidence was established, rational catalyst design became possible. Consequently, several well-defined, single-species catalysts based on different transition metals such as titanium,²⁴ tungsten,^{19,25,26} molybdenum,^{19,27} rhenium,²⁸ osmium,²⁹ and ruthenium^{3,30,31} evolved from the original metathesis-active but ill-defined multi-component mixtures. However, even today, the early transition metal catalysts, although very active, are also sensitive to many functional groups found in organic molecules, as well as moisture and air—a drawback that significantly limits their synthetic applications. For example, as demonstrated in Table 1.1, a metathesis catalyst with a tungsten center will preferentially react with olefins in the presence of esters and amides, but it will ignore all of these functionalities in favor of ketones, aldehydes, alcohols, acids or water.⁴ On the other hand, the late transition metal, ruthenium-based catalysts proved to be very tolerant towards polar functional groups and water, albeit at the expense of activity, early in olefin metathesis research.³² Overall, both Mo and Ru metathesis catalysts gained the most prominence and popularity due to their

versatility, as they provided a good balance between activity and functional group tolerance (Table 1.1). However, only the applications of ruthenium-based catalysts will be discussed in this thesis.

Table 1.1. Functional group tolerance of olefin metathesis catalysts.⁴

Titanium (Ti)	Tungsten (W)	Molybdenum (Mo)	Ruthenium (Ru)	
Acids	Acids	Acids	<i>Olefins</i>	↑ Increasing order of reactivity
Alcohols, Water	Alcohols, Water	Alcohols, Water	Acids	
Aldehydes	Aldehydes	Aldehydes	Alcohols, Water	
Ketones	Ketones	<i>Olefins</i>	Aldehydes	
Esters, Amides	<i>Olefins</i>	Ketones	Ketones	
<i>Olefins</i>	Esters, Amides	Esters, Amides	Esters, Amides	

→
Functional group tolerance

The exceptional selectivity of ruthenium for C–C double bonds secured continuous interest for this line of catalysts despite the low activity of the early versions, relative to the molybdenum catalysts of the time. For example, the activity of bis-triphenylphosphine (PPh₃) predecessors of catalyst **1** (Figure 1.1) was limited to ROMP of strained monomers, yet the catalyst performed remarkably well in polar media such as alcohols.³² However, the subsequent replacement of the PPh₃ ligands with tricyclohexyl phosphines (PCy₃) produced a much more active catalyst **1** (“the 1st generation Grubbs catalyst”), which is capable of cross metathesis of acyclic olefins, while maintaining the stability and high functional group tolerance of earlier ruthenium catalysts.^{31,33} Furthermore, the substitution of one of the phosphine ligands for an even more electron-donating N-heterocyclic carbene (NHC) resulted in a series of 2nd generation catalysts, such as **2**³⁰ and the phosphine-free **3**,³⁴ which now rival Mo catalysts in activity (Figure 1.1). While both **2** and **3** maintain the excellent selectivity for olefins typical of ruthenium catalysts, they have somewhat slower rates of initiation than the first generation catalysts, limiting their application in polymer synthesis. Alternatively, NHC-catalyst **4**,³⁵ which bears a bipyridine ligand in place of a

phosphine (Figure 1.1), has a sufficiently rapid initiation rate to promote ROMP of norbornenes with all of the attributes of a living polymerization. Moreover, the continuing emergence of new catalysts serves to further improve the metathesis reaction to be applicable to asymmetric,³⁶ sterically demanding,³⁷ or aqueous^{38,39} transformations.

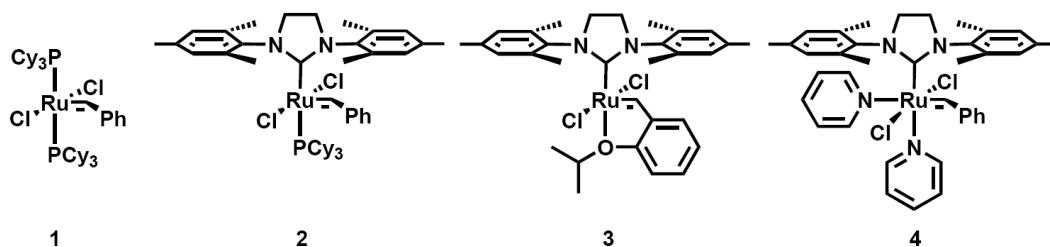
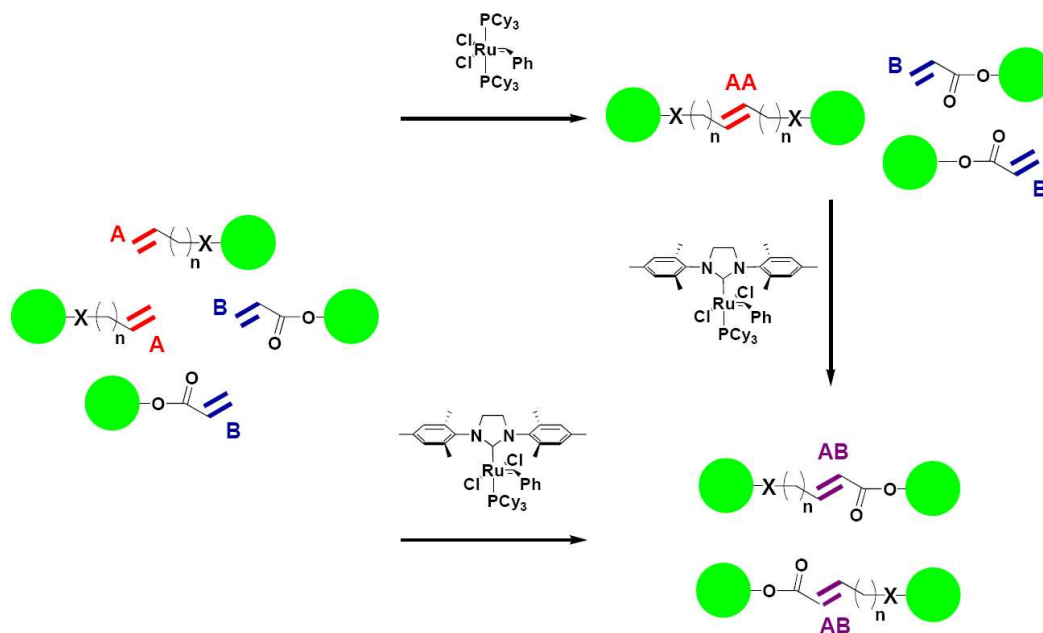


Figure 1.1. Ruthenium-based olefin metathesis catalysts.

One specific example of the improved reactivity of 2nd generation ruthenium catalysts, such as **2** and **3**, is their ability to react with electron-deficient α,β -unsaturated carbonyls, which are inert to **1**. As a result, excellent cross metathesis selectivity can be achieved in the reactions with such substrates.^{40,41} While both types of catalysts will successfully homodimerize “easy,” electron-rich, unsubstituted olefins, such as terminal aliphatic alkenes, even the active NHC-catalysts have very limited ability, if any, to cross a pair of “difficult,” electron-deficient olefins, such as acrylates. Nevertheless, unlike **1**, NHC-catalysts will promote selective cross metathesis between an “easy” and a “difficult” olefin. Therefore, a mixture of compounds, each functionalized with either a terminal alkene or an acrylate, will produce homodimers of the “easy” alkenes exclusively when exposed to **1**, and mixed “easy”-“difficult” cross products when exposed to **2** or **3** (Scheme 1.3). Importantly, although homodimerization of “easy” olefins occurs in the presence of either **2** or **3**, the disubstituted, electron-rich product of this cross is still qualified as “easy” and can proceed through secondary metathesis with acrylates and the NHC-catalyst to form a thermodynamically more stable cross product. In fact, this cross metathesis selectivity of 2nd generation ruthenium catalysts has already been creatively exploited in the synthesis of small molecules,⁴² macrocycles,⁴³ and alternating A,B polymers.⁴⁴

Scheme 1.3. Selectivity of 1st and 2nd generation ruthenium catalysts.



Polymer Synthesis Applications of Olefin Metathesis

Olefin metathesis is a versatile reaction that is becoming an increasingly important tool in the synthesis of small molecules, preparation of natural products, and construction of polymers. Furthermore, recent advances in the development of very active, yet stable catalysts now allows for the facile preparation of various functionalized polyalkenes,¹ alternating block-copolymers,⁴⁴ and even telechelic⁴⁵ polymers. The two synthetic approaches to olefin metathesis polymerizations are acyclic diene metathesis and ring opening metathesis reactions, each of which requires a different set of considerations for successful polymerization.

ADMET

Traditionally, acyclic diene metathesis is considered to be a step-growth⁴⁶ polycondensation-type polymerization reaction, which makes strictly linear chains from unconjugated dienes.¹⁰⁻¹⁴ As such, ADMET requires very high monomer conversion rates to produce polymer chains of considerable size. Therefore, the more active 2nd generation catalysts such as **2** and **3** are usually better suited for ADMET than bisphosphine ones.¹² Since the loss of ethylene is the main driving force behind the cross metathesis of terminal

olefins, the efficient removal of this volatile gas from the reaction vessel is also crucial. Consequently, although olefin metathesis with ruthenium catalysts is, in general, very mild and does not require stringent air removal, ADMET greatly benefits from conditions which promote the diffusion and expulsion of ethylene (i.e., higher reaction temperatures, application of vacuum, and rigorous stirring). In addition, the use of concentrated or even neat solutions of monomers is usually helpful to polycondensation reactions but, in the case of ADMET, a very viscous solution might be detrimental to efficient stirring and ethylene removal. Furthermore, as a consequence of the poor molecular weight control of step-growth reactions, the polydispersity index (PDI) of polymers obtained by this method is usually quite large. However, an important advantage of ADMET is that it allows a large variety of monomers to be polymerized since terminal olefins are quite easy to install. Many functional groups and moieties of interest can be incorporated into such polymers directly through monomer design, due to the excellent tolerance of ruthenium catalysts.

ROMP

Ring opening metathesis polymerization exhibits very different reaction kinetics from the ADMET approach to polymeric materials. ROMP is a chain-growth type polymerization which relies on monomer ring strain and, thus, it can be efficiently controlled by catalyst loading. The equilibrium molecular weight of the resulting polymer chains is, therefore, essentially independent of the extent of conversion. Moreover, a variety of olefin metathesis catalysts effect ROMP and sufficiently fast initiating ones can even lead to a living polymerization of appropriately chosen monomers. For example, the polymerization of norbornenes with the fast initiating bipyridine species **4** produces well-defined polymers with PDIs close to 1.0.⁴⁷ The employment of these strained, bi-cyclic alkenes as monomers ensures that both depolymerization via competing RCM and chain fragmentation via “back-biting” of the catalyst into the growing chain are significantly suppressed. However, the limited availability of suitable monomers is the main disadvantage of this method. Although a variety of backbones can be created through monomer functionalization, such alterations sometimes negatively affect the ring strain and, thus, success of ROMP.

Summary and Thesis Research

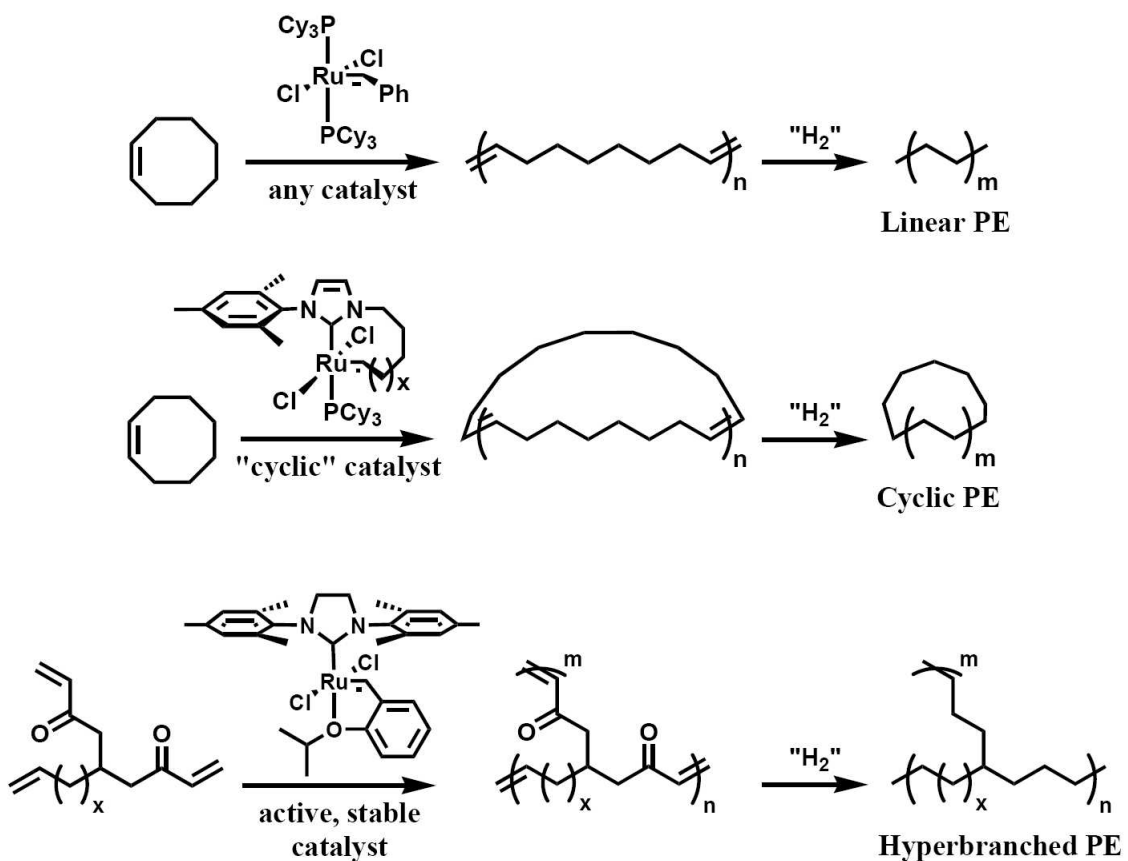
Olefin metathesis is a mild, yet powerful, method for carbon-carbon bond formation. Although metathesis is mediated by a variety of metals, ruthenium-based catalysts demonstrate unprecedented functional group, air, and moisture tolerance and greatly expand the scope of this reaction. Furthermore, recent advances in catalyst development have produced a variety of well-defined and very active catalysts, some of which are tuned for specific applications. This progress has allowed for new and creative uses of olefin metathesis in the preparation of novel synthetic products.

With so many olefin metathesis catalyst options at hand, a number of factors, most importantly the nature of the substrate, need to be considered for each specific application in order to fully realize the potential of this chemical transformation. For example, in the case of polymerization via ADMET, the pool of monomers can be practically unlimited if a very active and stable species such as phosphine-free **3** is chosen as the catalyst. On the other hand, when polymerizing via ROMP, any ruthenium catalyst can produce satisfactory results, if the monomer of choice has sufficient ring strain. In addition, to achieve “living polymerization” with ruthenium catalysts, the use of fast-initiating **4** and norbornene-based monomers are required. However, despite certain limitations, ADMET and ROMP together provide a bottomless toolbox for the synthesis of polymeric materials.

Notably, even well-established materials such as polyethylene (PE) can benefit from the advances in olefin metathesis. This polymer is already one of the largest-volume polymers produced world-wide, with more than 22 billion pounds made yearly in the United States alone.⁴⁸ The demand for this plastic is driven by a stunning range of desirable properties provided by the simplest polymeric backbone imaginable. Furthermore, all of the diversity in physical properties (crystallinity, mechanical strength, and thermal stability) stems from the different architecture of the individual polymeric chains, specifically chain branching and chain size, rather than variations in chemical composition.^{48,49} Therefore, the synthesis and study of polymers with different structural design and a variety of molecular weights is important for promoting a better understanding of structure-property relationships and, consequently, broadening the applications of polymeric materials.⁵⁰

In spite of the progress in polymer synthesis techniques, some important chain architectures remain inaccessible for PE with current synthetic methods. For example, both coordination and, to some extent, radical polymerization of α -olefins currently employed in industry allow for very good statistical control over the number and length of branches along the chain backbone, but these reactions cannot produce absolutely linear PE or place branches of exact desirable length at precise locations along the polymer chain. In contrast, ROMP of cyclooctene or cyclooctadiene, followed by hydrogenation of the resulting internal alkenes, can effortlessly accomplish the perfectly linear polymerization; ADMET of a diene with a desired side chain can ensure precise branching.⁵⁰ Finally, today's state of the art olefin metathesis catalysts and methods also allow the synthesis of cyclic⁵¹ and, potentially, hyperbranched PE (Scheme 1.4).

Scheme 1.4. Olefin metathesis routes to polyethylene of different architectures.



This thesis explores the application of ruthenium catalyzed olefin metathesis in the synthesis of polymers with nonlinear architectures. The hyperbranched and cyclic polymers described herein are made possible by means of either judicious substrate or catalyst design (Scheme 1.4). The fact that both of these polymeric architectures can be extended to the synthesis of polyethylene further demonstrates the power of olefin metathesis as a synthetic tool because neither cyclic⁵¹ nor truly hyperbranched PE⁵² is currently available via any other method.

Chapter 2 of this thesis describes the method for the synthesis of hyperbranched polymers via ADMET of specially designed, yet very simple monomers. Chapter 3 explores the post-synthetic functionalization of these polymers by secondary olefin metathesis and probes their potential application as substrate carriers. Chapter 4 investigates the molecular weight control of this polymerization technique (effects of the catalyst loading, reaction time, end-capping, and multifunctional core molecules). Chapter 5 of this thesis summarizes the recent developments in the synthesis and study of cyclic polymers and catalysts. In addition, Appendix 1 outlines the extension of the hyperbranched ADMET polymerization methodology towards the synthesis of hyperbranched polyethylene.

References

- (1) *Handbook of Metathesis*; Grubbs, R. H., Ed.; Wiley-VCH: Weinheim, Germany, 2003.
- (2) Ivin, K. J.; Mol, J. C. *Olefin Metathesis and Metathesis Polymerization*; Academic Press: San Diego, CA, 1997.
- (3) Grubbs, R. H. *Tetrahedron* **2004**, *60*, 7117-7140.
- (4) Trnka, T. M.; Grubbs, R. H. *Acc. Chem. Res.* **2001**, *34*, 18-29.
- (5) Fürstner, A. *Angew. Chem. Int. Ed.* **2000**, *39*, 3012-3043.
- (6) Hérrison, J.-L.; Chauvin, Y. *Makromol. Chem.* **1971**, *141*, 161-167.
- (7) Connon, S. J.; Blechert, S. *Angew. Chem. Int. Ed.* **2003**, *42*, 1900-1923.
- (8) Deiters, A.; Martin, S. F. *Chem. Rev.* **2004**, *104*, 2199-2238.
- (9) McReynolds, M. D.; Dougherty, J. M.; Hanson, P. R. *Chem. Rev.* **2004**, *104*, 2239-2258.
- (10) Baughman, T. W.; Wagener, K. B. *Adv. Polym. Sci.* **2005**, 1-42.
- (11) Lehman, E.; Wagener, K. B. In *Handbook of Metathesis*; Grubbs, R. H., Ed.; Wiley-VCH: Weinheim, Germany, 2003; Vol. 3, p 283-353.
- (12) Lehman, S. E.; Wagener, K. B. In *Late Transition Metal Polymerization Catalysis*; Rieger, B., Baugh, L. S., Kacker, S., Striegler, S., Eds.; Wiley-VCH: Weinheim, 2003, p 193-229.
- (13) Lehman, S. E.; Wagener, K. B. *Macromolecules* **2002**, *35*, 48-53.
- (14) Buchmeiser, M. R. *Chem. Rev.* **2000**, *100*, 1565-1604.
- (15) Morgan, J. P.; Morrill, C.; Grubbs, R. H. *Org. Lett.* **2002**, *4*, 67-70.
- (16) Mayo, P.; Tam, W. *Tetrahedron* **2002**, *58*, 9513-9525.
- (17) Frenzel, U.; Nuyken, O. *J. Polym. Sci., Part A: Polym. Chem.* **2002**, *40*, 2895-2916.
- (18) Schrock, R. R. *Acc. Chem. Res.* **1990**, *23*, 158-165.
- (19) Schrock, R. R.; Hoveyda, A. H. *Angew. Chem. Int. Ed.* **2003**, *42*, 4592-4633.
- (20) Roy, R.; Das, S. K. *Chem. Commun.* **2000**, *7*, 519-529.
- (21) Gorodetskaya, I. A.; Choi, T. L.; Grubbs, R. H. *J. Am. Chem. Soc.* **2007**, *129*, 12672-12673.
- (22) Guidry, E. N.; Li, J.; Stoddart, J. F.; Grubbs, R. H. *J. Am. Chem. Soc.* **2007**, *129*, 8944-8945.

- (23) Matson, J. B.; Grubbs, R. H. *J. Am. Chem. Soc.* **2008**, *130*, 6731-6733.
- (24) Gilliom, L. R.; Grubbs, R. H. *J. Am. Chem. Soc.* **1986**, *108*, 733-742.
- (25) Schrock, R. R.; DePue, R. T.; Feldman, J.; Schaverien, C. J.; Dewan, J. C.; Liu, A. H. *J. Am. Chem. Soc.* **1988**, *110*, 1423-1435.
- (26) Agüero, A.; Kress, J.; Osborn, J. A. *J. Chem. Soc. Chem. Commun.* **1985**, *12*, 793-794.
- (27) Bazan, G. C.; Schrock, R. R.; O'Regan, M. B. *Organometallics* **1991**, *10*, 1062-1067.
- (28) Toreki, R.; Schrock, R. R. *J. Am. Chem. Soc.* **1990**, *112*, 2448-2449.
- (29) Castarlenas, R.; Esteruelas, M. A.; Onate, E. *Organometallics* **2005**, *24*, 4343-4346.
- (30) Scholl, M.; Ding, S.; Lee, C. W.; Grubbs, R. H. *Org. Lett.* **1999**, *1*, 953-956.
- (31) Schwab, P.; Grubbs, R. H.; Ziller, J. W. *J. Am. Chem. Soc.* **1996**, *118*, 100-110.
- (32) Novak, B. M.; Grubbs, R. H. *J. Am. Chem. Soc.* **1988**, *110*, 960-961.
- (33) Schwab, P.; France, M. B.; Ziller, J. W.; Grubbs, R. H. *Angew. Chem. Int. Ed. Engl.* **1995**, *34*, 2039-2041.
- (34) Garber, S. B.; Kingsbury, J. S.; Gray, B. L.; Hoveyda, A. H. *J. Am. Chem. Soc.* **2000**, *122*, 8168-8179.
- (35) Sanford, M. S.; Love, J. A.; Grubbs, R. H. *Organometallics* **2001**, *20*, 5314-5318.
- (36) Funk, T. W.; Berlin, J. M.; Grubbs, R. H. *J. Am. Chem. Soc.* **2006**, *128*, 1840-1846.
- (37) Berlin, J. M.; Campbell, K.; Ritter, T.; Funk, T. W.; Chlenov, A.; Grubbs, R. H. *Org. Lett.* **2007**, *9*, 1339-1342.
- (38) Jordan, J. P.; Grubbs, R. H. *Angew. Chem. Int. Ed.* **2007**, *46*, 5152-5155.
- (39) Hong, S. H.; Grubbs, R. H. *J. Am. Chem. Soc.* **2006**, *128*, 3508-3509.
- (40) Chatterjee, A. K.; Choi, T. L.; Sanders, D. P.; Grubbs, R. H. *J. Am. Chem. Soc.* **2003**, *125*, 11360-11370.
- (41) Chatterjee, A. K.; Morgan, J. P.; Scholl, M.; Grubbs, R. H. *J. Am. Chem. Soc.* **2000**, *122*, 3783-3784.
- (42) Choi, T.-L.; Grubbs, R. H. *Chem. Commun.* **2001**, *24*, 2648-2649.
- (43) Lee, C. W.; Choi, T. L.; Grubbs, R. H. *J. Am. Chem. Soc.* **2002**, *124*, 3224-3225.
- (44) Choi, T.-L.; Rutenberg, I. M.; Grubbs, R. H. *Angew. Chem. Int. Ed.* **2002**, *41*, 3839-3841.

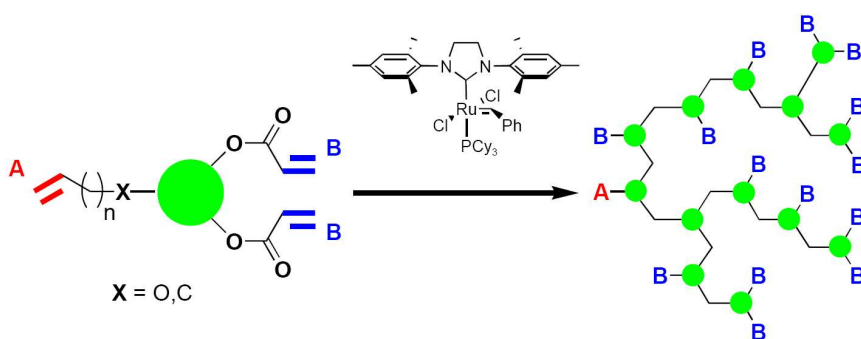
- (45) Bielawski, C. W.; Benitez, D.; Morita, T.; Grubbs, R. H. *Macromolecules* **2001**, *34*, 8610-8618.
- (46) Wagener, K. B.; Boncella, J. M.; Nel, J. G. *Macromolecules* **1991**, *24*, 2649-2657.
- (47) Choi, T.-L.; Grubbs, R. H. *Angew. Chem. Int. Ed.* **2003**, *42*, 1743-1746.
- (48) Odian, G. *Principles of Polymerization*; 4th ed.; Wiley: Hoboken, 2004.
- (49) Rojas, G.; Berda, E. B.; Wagener, K. B. *Polymer* **2008**, *49*, 2985-2995.
- (50) Sworen, J. C.; Smith, J. A.; Wagener, K. B.; Baugh, L. S.; Rucker, S. P. *J. Am. Chem. Soc.* **2003**, *125*, 2228-2240.
- (51) Bielawski, C. W.; Benitez, D.; Grubbs, R. H. *Science* **2002**, *297*, 2041-2044.
- (52) Voit, B. I. *C. R. Chimie* **2003**, *6*, 821-832.

CHAPTER 2
Hyperbranched Polymers via Acyclic Diene Metathesis Polymerization

Portions of this chapter have previously appeared as: Gorodetskaya, I. A.; Choi, T. L.;
Grubbs, R. H. *J. Am. Chem. Soc.* **2007**, *129*, 12672-12673.

Abstract

A facile route to hyperbranched polymers via acyclic diene metathesis is described. According to this new methodology, a variety of molecules functionalized with two or more acrylate groups and one terminal aliphatic alkene can serve as an AB_n monomer when exposed to an imidazolinyldene-based ruthenium olefin metathesis catalyst, due to the cross metathesis selectivity of this catalyst. For the polymers obtained by this method, both ^1H NMR spectroscopy and triple detector size exclusion chromatography conclusively indicate a branched architecture.

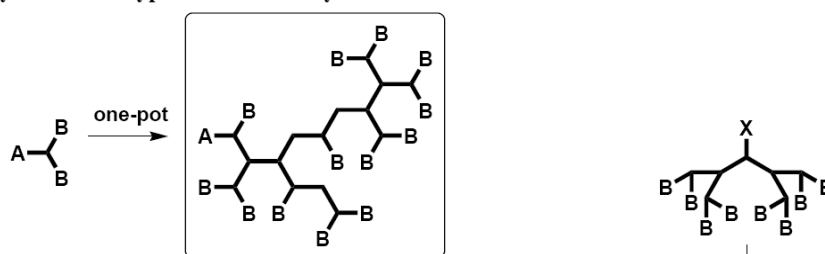


Introduction

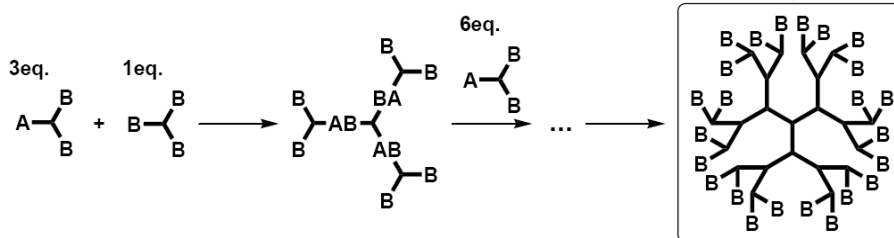
Hyperbranched polymers are highly branched macromolecules typically prepared via a one-pot polymerization of $AB_{n \geq 2}$ monomers (Scheme 2.1A).¹⁻⁶ The A and B functionalities of these monomers readily react with each other (A reacts with B and vice versa) but not with themselves (A does not react with A and B does not react with B). The approach to the preparation of hyperbranched polymers was originally described by Flory as early as 1952, but, at the time, such an architecture was mainly of theoretical interest.⁷ However, it has since been discovered that the unique macromolecular architecture of these polymers gives rise to many attractive, practical features such as multiple end groups, improved solubility, and lower solution viscosity (relative to linear analogues of the same molecular weight).¹⁻⁶ Moreover, dendrimers⁸⁻¹⁰—structurally perfect, monodisperse hyperbranched macromolecules—have already found applications in medicine,^{11,12} catalysis,^{13,14} and nanofabrication.^{15,16} Unfortunately, dendrimer iterative synthesis and purification can be rather labor-intensive and, thus, expensive (Scheme 2.1B).⁸⁻¹⁰ As such, the preparation and study of hyperbranched polymers, which typically exhibit properties similar to those of monodisperse dendrimers,^{17,18} have been extensively pursued in recent years.³⁻⁶

Scheme 2.1. Synthesis of dendritic polymers.

A. Synthesis of Hyperbranched Polymers



B. Synthesis of Dendrimers



In the 55 years since Flory's theoretical report, as interest in dendrimers and hyperbranched polymers increased, a large number of synthetic approaches to these macromolecules have been reported. Moreover, the range of methods available for hyperbranched synthesis has expanded well beyond classical step-growth condensations and additions of AB₂ monomers⁶ to include such notable examples as self-condensing vinyl polymerization (SCVP) of AB* monomers,¹⁹ various ring-opening polymerizations of latent AB_n monomers,²⁰⁻²² and proton-transfer polymerization.²³ However, many of these methods have significant drawbacks such as harsh reaction conditions and the need for complex monomers. Although olefin metathesis has never previously been used to prepare hyperbranched architectures, it is well-suited for the task because it requires very mild reaction conditions and possesses good functional group tolerance, which allows access to a great variety of polymer backbones from readily available monomers. This chapter describes a simple method for the preparation of hyperbranched polymers via acyclic diene metathesis polymerization (ADMET).²⁴

Results and Discussion

Catalyst **1** (Figure 2.1) was selected for the ADMET hyperbranched polymerization. This imidazolinyliene-based catalyst is tolerant of many functional groups, stable to air and moisture, and readily promotes cross metathesis between electron-rich primary olefins. Furthermore, it can catalyze cross metathesis involving low metathesis-reactive olefins, such as electron-deficient alkenes. When treated with **1**, electron-poor olefins do not homodimerize (or do so very slowly), but do participate in a secondary metathesis reaction with homodimers of more reactive olefins.²⁵ Therefore, a molecule functionalized with one electron-rich olefin, such as a terminal alkene, and two or more electron-poor olefins, such as acrylates, is an AB_n-type monomer (Figure 2.2) that can be polymerized into a hyperbranched structure using catalyst **1** (Scheme 2.2). In fact, a similar concept has been previously demonstrated in the synthesis of alternating copolymers²⁶ and various small molecules.^{27,28}

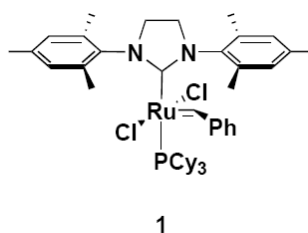


Figure 2.1. Acyclic diene metathesis polymerization catalyst.

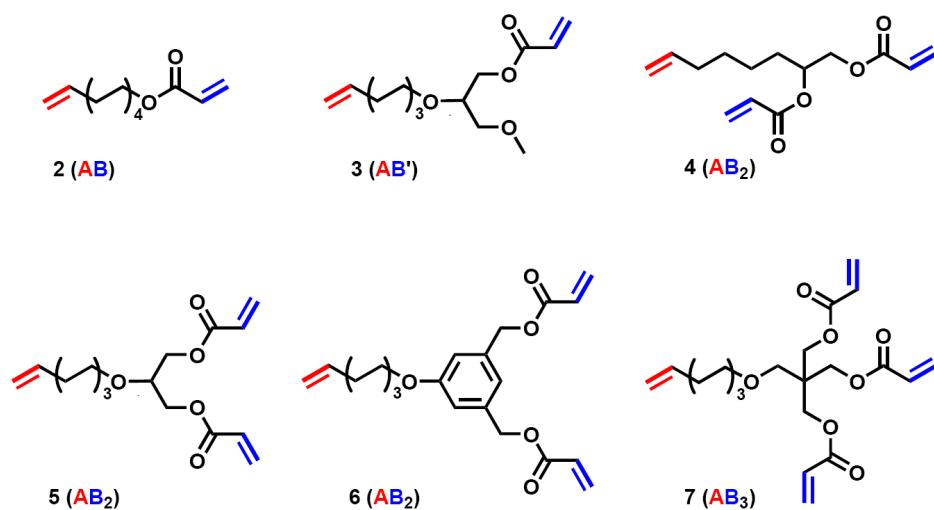
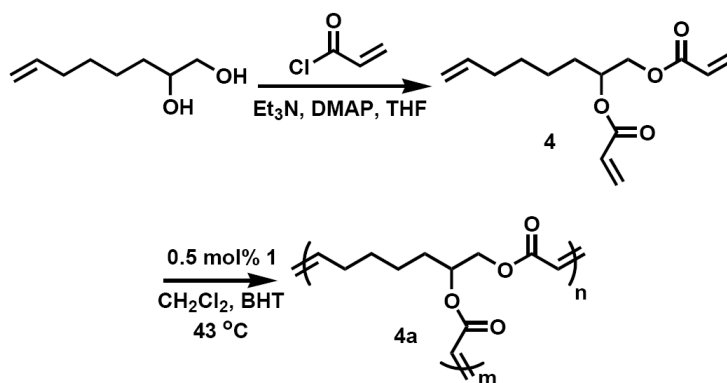


Figure 2.2. Monomers for hyperbranched ADMET polymerization

Scheme 2.2. Synthesis of AB₂ monomer **4** and its hyperbranched ADMET polymerization.



Monomers **2–7** (Figure 2.2) were utilized for the ADMET hyperbranched polymerization. They were prepared in one to four steps from commercially available,

inexpensive starting materials such as glycerol, pentaerythritol, and 5-hydroxyisophthalic acid. **2** and **3** were prepared as linear analogues to AB₂ monomers **4** and **5**, as well as the AB₃ monomer **7**. To further demonstrate the inherent flexibility of the presented method, monomer **6** was also synthesized to make a hyperbranched polymer with a different backbone.

The polymerization of each monomer is easily monitored by ¹H NMR spectroscopy.^{26,29} For example, Figure 2.3 shows the ¹H NMR spectra of **4** and the resulting crude polymer **4a**. Some peak broadening due to formation of macromolecules can be observed in the spectrum of **4a**, especially for the backbone proton **b**. It can also be seen that the terminal olefins (**a**) completely disappear during the polymerization. Moreover, as expected, a new peak (**g**), a doublet of triplets, appears at 6.95 ppm due to formation of internal acrylates (AB olefins). Furthermore, if polymerization proceeds to completion, as is the case here, all of the terminal aliphatic alkenes are consumed and there should be half of the free acrylate groups left in the final polymer. Since there are twice as many B groups as A groups in an AB₂ monomer, an integration ratio of 1 (**g**) to 1 (**c** or **d**) should hold for the product of complete polymerization. Indeed, a 1:1 ratio is observed for **4a** (Figure 2.3), as well as **5a** and **6a**; it is 2:1 for **7a**. Peaks **d**, **c**, and **e** completely disappear, along with the peaks for protons **a**, during the polymerizations of **2** and **3**, and the integration ratio of the corresponding polymer peaks **g** and **f** is 1:1.

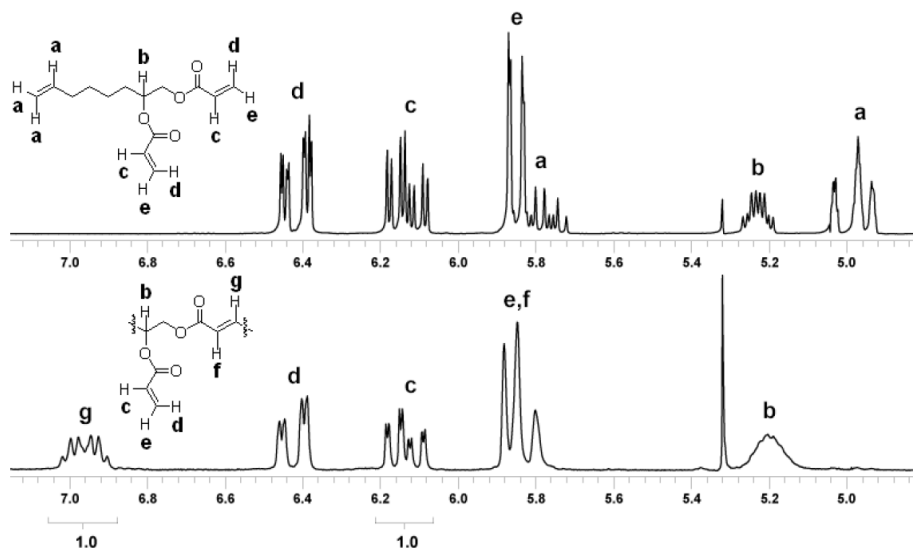


Figure 2.3. ¹H NMR spectra of monomer **4** (top) and hyperbranched polymer **4a** (bottom).

A multiangle light-scattering (MALS) detector combined with a differential refractometer and an on-line viscometer following size exclusion chromatography (SEC) was used to determine the molecular weights and PDIs of the obtained polymers. Additionally, viscometer data helped to characterize branching of the macromolecules resulting from ADMET of **2–7**. Table 2.1 summarizes the typical crude polymerization results. The observed PDI values are quite high, which is typical for a hyperbranched step-growth type polymerization.³⁰

Table 2.1. Results of polymerization of **2–7**.^a

Polymer	M_w (kDa)	M_n (kDa)	PDI	$\alpha \times 10^{-1}$
2a	4.31	2.07	2.1	4.45 ± 0.01
3a	21.43	4.44	4.8	4.12 ± 0.02
4a	3.61	0.55	6.5	3.82 ± 0.02
5a	14.77	3.08	4.8	3.24 ± 0.02
6a	10.24	3.17	3.2	3.34 ± 0.03
7a	30.90	5.00	6.2	2.69 ± 0.02

^a Polymerization conditions: 0.5 mol % of **1** was used and the polymerizations were conducted in near-refluxing methylene chloride (43 °C) with venting. M_w , M_n , and PDI were calculated from triple-angle laser light scattering and refractive index measurements. α was measured with an on-line differential viscometer.

Figure 2.4 compares the plots of intrinsic viscosity (IV) vs. molecular weight (Mark–Houwink–Sakurada plots) for polymers **2a–7a**. As expected, the IV of branched polymers **4a–7a** is much lower than that of the linear polymer **2a** for any given molecular weight. Interestingly, the supposedly linear polymer **3a** has a drastically reduced intrinsic viscosity compared to that of **2a**, although not quite as low as the viscosities of branched polymers. This property of **3a** can be attributed to the presence of a methoxy-methyl pendant group in each monomer unit. This group is inert during the polymerization, but its length is comparable to the monomer’s overall size. Such an architecture results in a “comb”-type polymer with a lower than expected IV (relative to that of a linear analogue).³¹ Across the molecular weight range studied, the viscosity of polymer **7a**, based

on an AB₃ monomer **7**, is even lower than that of AB₂ polymers **4a–6a**. This observation indicates even more branching in the AB₃-based polymer. On the other hand, the intrinsic viscosity does not change dramatically with slight variations in the backbone; it can be seen from Figure 2.4 that the Mark–Houwink plots for **4a–6a** completely overlap.

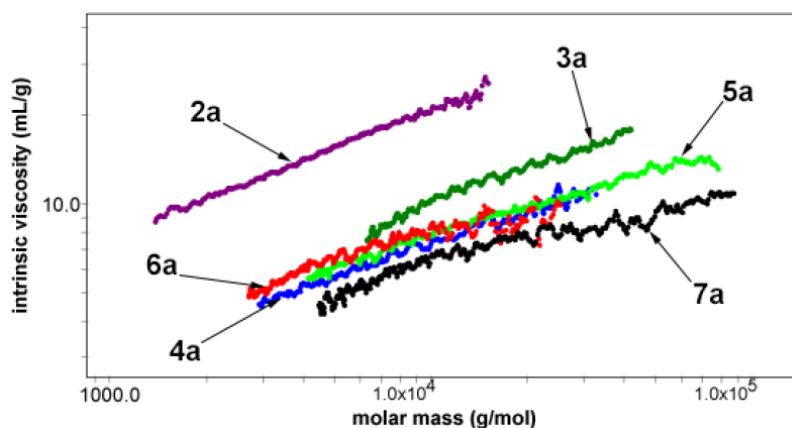


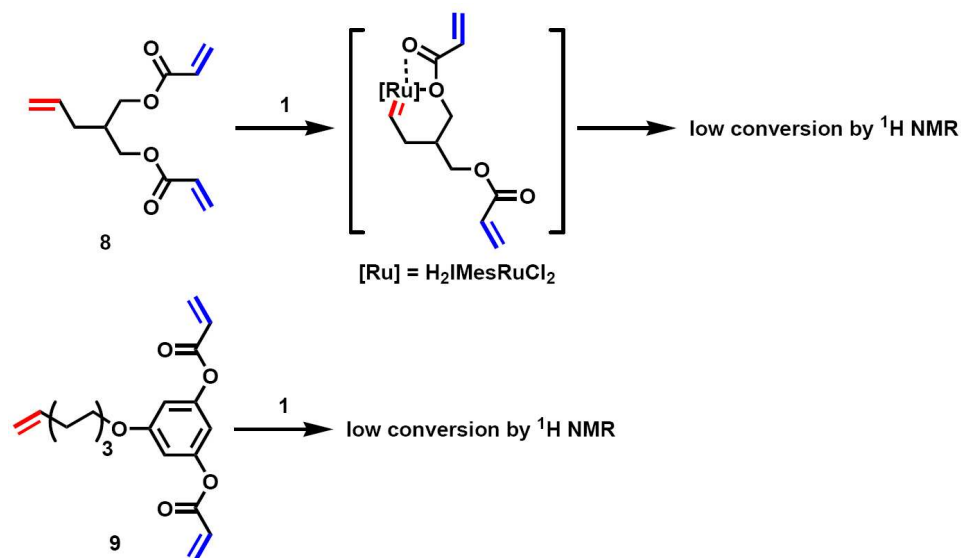
Figure 2.4. Mark-Houwink-Sakurada plots for polymers **2a–7a**.

To extend the analysis, the Mark–Houwink shape parameter α ($[\eta] = KM^\alpha$) for polymers **2a–7a** were compared (Table 2.1). An α parameter of 0.5–1.0 is typical for randomly coiled linear polymers.³² Polymers with a rigid-rod shape have an α of 2.0, and spherically shaped macromolecules are expected to have an $\alpha < 0.5$.³² The linear polymer **2a** was found to have the highest α value of 0.45 (Table 2.1), closely followed by an α of 0.41 for **3a**. This observation confirms that **3a** is a linear polymer despite its low viscosity. It also validates that polymers **4a–7a** are not simply linear, alternating A,B comb-shaped polymers. Branched AB₂-based polymers **4a**, **5a**, and **6a** all have α parameters indicative of a spherical shape in solution. Moreover, polymer **7a** yielded the lowest α value, which is in agreement with the AB₃-based polymer having the lowest intrinsic viscosity and, thus, the most branching. Overall, the α values found strongly suggest a spherical shape in solution and, therefore, a hyperbranched architecture for polymers **4a–7a**.

Interestingly, some of the structurally altered ADMET AB₂ monomers were found to test the general utility of this method. Both substrates **8** and **9** (Scheme 2.3) produced poor polymerization results when exposed to **1**. In the case of **8**, the decreased reactivity

must stem from the shortened length of the aliphatic chain between the tertiary carbon and the terminal alkene, since it is the only feature distinguishing this monomer from **4** or **5**, both of which underwent ADMET successfully. It can be speculated that the chain length of **8** allows for the formation of a stable, 6-membered chelates between the ruthenium and the polar acrylate moiety upon cross metathesis (Scheme 2.3). This deactivates the catalyst and prevents or slows down the polymerization process.³³ On the other hand, the low conversion observed with **9** must be a result of the poor metathesis reactivity of the aryl acrylate groups. The acrylates directly attached to the aryl ring are too electron-poor to undergo olefin metathesis efficiently even with the highly active NHC-catalyst. This explanation is supported by the fact that removing the acrylate groups from the aromatic ring by just one carbon, as is the case with **6**, completely restores their metathesis reactivity. The observed metathesis behavior of **6** and **8**, as compared to **5** and **6** correspondingly, shows that although there are certain limitations to ADMET polymerization with **1**, they can be easily overcome by careful monomer design.

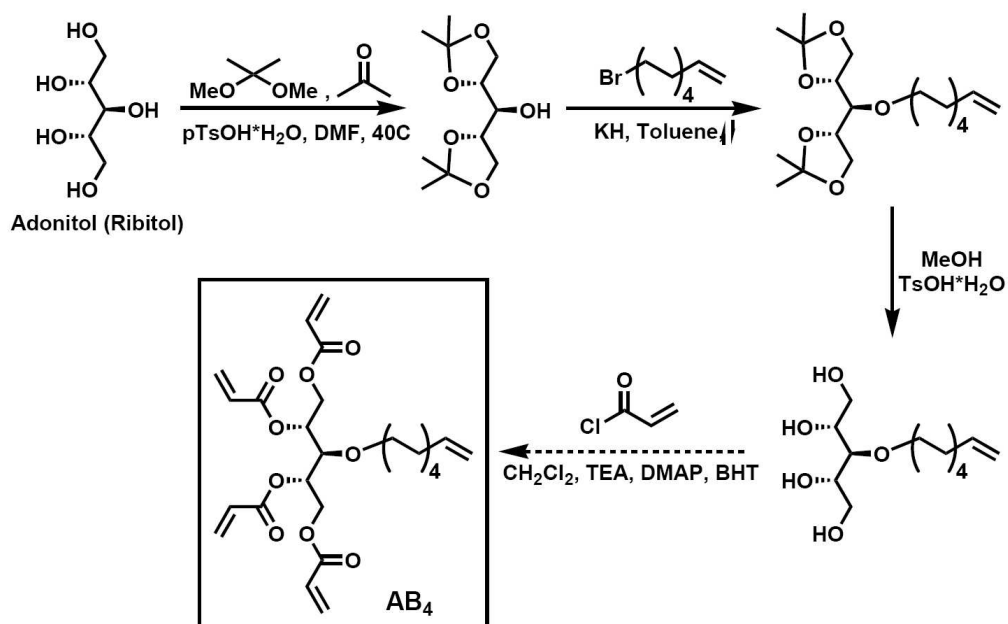
Scheme 2.3. AB₂ monomers which were found to be challenging for ADMET.



In general, despite the minor limitations noted above, the structural diversity and availability of monomer cores that can be used in the hyperbranched ADMET

polymerization present unprecedented opportunities for fine-tuning the properties of dendritic polymers. For example, the evidence presented in this chapter indicates that polymers prepared from AB_3 monomers have an even lower viscosity and a more compact structure in solution than the ones prepared from the analogous AB_2 monomers. Consequently, it would be interesting to extend the comparison to AB_n -based polymers, where $n > 3$. For example, an AB_4 monomer should be readily available via a straightforward 4-step route described in Scheme 2.4. Such explorations should provide even greater insight into the properties of hyperbranched polymers.

Scheme 2.4. Synthesis of AB_4 monomer for hyperbranched ADMET polymerization.



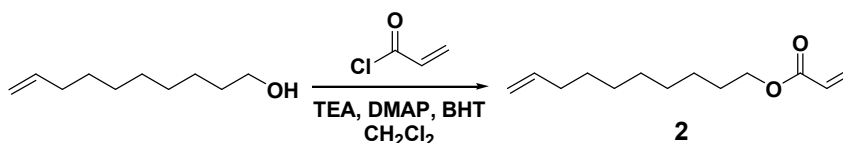
Conclusion

This chapter demonstrates that olefin metathesis can be used to prepare hyperbranched polymers with a variety of backbones in a very simple and truly modular fashion. Moreover, the method presented here is amenable to the synthesis of functionalized hyperbranched polymers that can be employed in biological and material applications. Therefore, as an extension of this work, Chapter 3 investigates functionalization of the peripheral groups (acrylates) of the hyperbranched polymers presented here.

Experimental Procedures

Materials and Instrumentation. All reagents (except catalyst **1** and phloroglucinol) were purchased from Aldrich at the highest available purity grade and used without further purification. Catalyst **1** was obtained from Materia, Inc. and phloroglucinol was bought from Fluka. NMR spectra were obtained using a Varian Mercury-300 spectrometer; samples were dissolved in (methylene chloride)-d₂, unless noted otherwise. Size exclusion chromatography (SEC) analysis was performed using a Wyatt triple detector system equipped with a refractive index (Optilab rex) detector, a viscometer (ViscoStar) detector, and a triple angle light scattering (miniDAWN TREOS, with laser wavelength of 658 nm) detector all operating at 25°C. Viscotek ViscoGEL I-Series (one mixed bed medium MW and one mixed bed high MW) columns were used for SEC with THF as the eluent and a Shimadzu LC-10AD pump operating at 1 mL/minute.

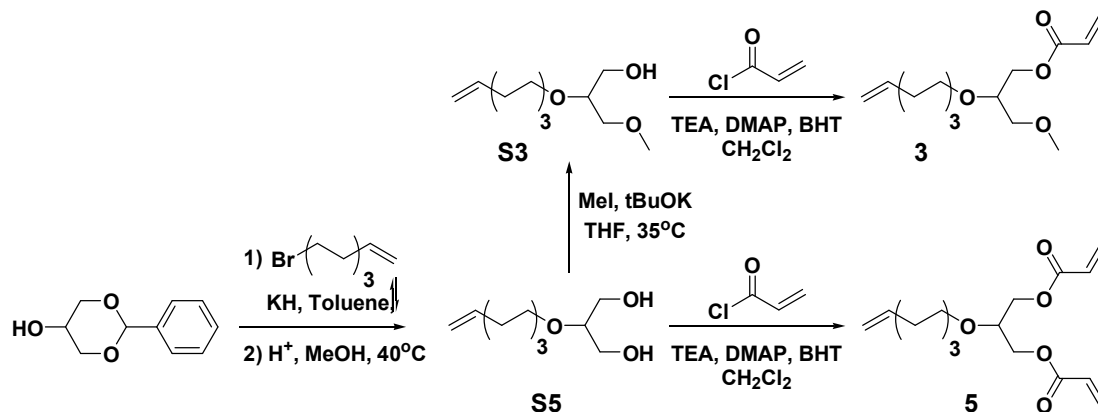
Scheme 2.5. Synthesis of monomer **2**.



Representative procedure for the addition of acryloyl chloride to alcohol groups (2). Acryloyl chloride (0.8 mL, 9.6 mmol) was slowly added via syringe to a stirring solution of 9-decene-1-ol (1 g, 6.4 mmol), triethylamine (TEA) (2.2 mL, 16 mmol), and a small amount of 2,6-di-*tert*-butyl-4-methoxyphenol (BHT) in dry THF (2 mL) at 0 °C (Scheme 2.5). After the solution was allowed to warm to room temperature, a catalytic amount of 4-(dimethylamino)pyridine (DMAP) (3.9 mg, 0.06 mmol) was added, and the flask was stirred for an additional 2 h. The reaction mixture was then filtered, and the solvent was removed under reduced pressure. The crude product was purified by silica gel (TSI) chromatography, eluting with 95:5 hexane:ethyl acetate to afford 0.99 g (73% yield) of a viscous colorless oil **2**. ¹H NMR (300 MHz, CD₂Cl₂, ppm): δ 6.36 (dd, J = 17.5 Hz, J = 1.6 Hz, 1H), 6.11 (dd, J = 17.5 Hz, J = 10.2 Hz, 1H), 5.89–5.75 (m, 1H), 5.80 (dd, J = 10.2 Hz, J = 1.6 Hz, 1H), 5.03–4.89 (m, 2H), 4.12 (t, J = 6.9 Hz, 2H), 2.04 (m, 2H), 1.65 (m, 2H), 1.31 (m, 10H). ¹³C NMR (300 MHz, CD₂Cl₂, ppm): δ 166.62, 139.81, 130.58,

129.27, 114.42, 65.15, 34.35, 29.91, 29.77, 29.61, 29.49, 29.17, 26.47. HRMS(EI+) m/z : 210.1617 [M]⁺.

Scheme 2.6. Synthesis of monomers **3** and **5**.



(**3**). Monomer **3** was derived from the same starting material as **5** (see synthesis of **5** below). The intermediate **S5** (Scheme 2.6) was treated with 0.5 equivalents of MeI and tBuOK each in THF at 35°C for 10 h. The unreacted base was then neutralized with tBuOH, and the reaction mixture was concentrated and purified by silica gel chromatography (4:1 hexane:EtOAc). A clear viscous oil **S3** was produced in 54% yield. ¹H NMR (300 MHz, CD₂Cl₂, ppm): δ 5.82 (m, 1H), 5.03–4.90 (m, 2H), 3.67–4.41 (m, 7H), 3.33 (s, 3H), 2.28 (broad s, 1H), 2.04 (m, 2H), 1.55 (m, 2H), 1.34 (m, 6H). ¹³C NMR (300 MHz, CD₂Cl₂, ppm): δ 139.73, 114.47, 79.03, 73.10, 70.69, 63.09, 59.56, 34.28, 30.60, 29.50, 29.44, 26.48. HRMS(FAB+) m/z : 217.1813 [M+H]⁺.

Colorless oil **3** (Scheme 2.6) was made from **S3** according to the representative procedure outlined above for **2** in 79% yield. ¹H NMR (300 MHz, CD₂Cl₂, ppm): δ 6.38 (dd, $J = 17.1$ Hz, $J = 1.8$ Hz, 1H), 6.14 (dd, $J = 17.4$ Hz, $J = 10.5$ Hz, 1H), 5.89–5.75 (m, 1H), 5.84 (dd, $J = 10.2$ Hz, $J = 1.8$ Hz, 1H), 5.02–4.89 (m, 2H), 4.25 (dd, $J = 11.4$ Hz, $J = 4.3$ Hz, 1H), 4.13 (dd, $J = 11.4$ Hz, $J = 5.7$ Hz, 1H), 3.63 (doublet of quintets, $J = 5.4$ Hz, $J = 4.5$ Hz, 1H), 3.53 (t, $J = 6.6$ Hz, 2H), 3.44 (d, $J = 4.8$ Hz, 2H), 3.34 (s, 3H), 2.04 (m, 2H), 1.53 (m, 2H), 1.42–1.27 (m, 6H). ¹³C NMR (300 MHz, CD₂Cl₂, ppm): δ 166.35, 139.75, 131.12, 128.89, 114.44, 76.95, 72.65, 70.97, 64.53, 59.57, 34.28, 30.53, 29.48, 29.46, 26.43. HRMS(EI+) m/z : 271.1907 [M+H]⁺.

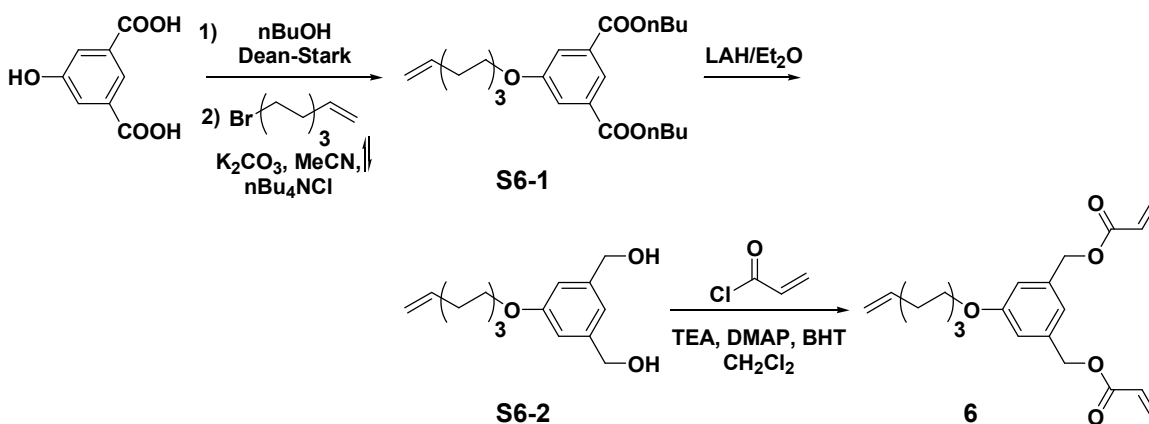
(4). Colorless oil **4** was prepared using the same procedure as described for **2** from 7-octene-1,2-diol (Scheme 2.2) in 67% yield. ^1H NMR (300 MHz, CD_2Cl_2 , ppm): 6.37 (ddd, $J = 17.1$ Hz, $J = 4.2$ Hz, $J = 1.2$ Hz, 2H), 6.11 (ddd, $J = 17.1$ Hz, $J = 10.5$ Hz, $J = 2.7$ Hz, 2H), 5.85–5.73 (m, 1H), 5.83 (dd, $J = 10.5$ Hz, $J = 1.8$ Hz, 2H), 5.17 (m, 1H), 5.05–4.91 (m, 2H), 4.30 (dd, $J = 12.0$ Hz, $J = 3.6$ Hz, 1H), (dd, $J = 12.0$ Hz, $J = 6.5$ Hz, 1H), 2.05 (m, 2H), 1.65 (m, 2H), 1.43–1.36 (m, 6H). ^{13}C NMR (300 MHz, CD_2Cl_2 , ppm): δ 166.21, 166.06, 139.28, 131.44, 131.20, 129.00, 128.61, 114.79, 72.13, 65.60, 34.03, 31.10, 29.16, 25.08. HRMS(EI+) m/z : 253.1441 $[\text{M}]^+$.

(5). *cis*-1,3-*O*-Benzylidenglycerol (2 g, 11.1 mmol) was combined with potassium hydride (35% suspension in oil, 2.5 g, 22.2 mmol) in 8 mL of toluene (Scheme 2.6) in a 50 mL round bottom flask equipped with a stir bar. The solution was stirred at room temperature until gas evolution ceased, at which point 7-bromo-octene (2 mL, 12.2 mmol) was slowly added to the reaction flask. The reaction was subsequently heated to reflux for 10 h. The reaction mixture was then cooled to room temperature, and the unreacted potassium hydride was neutralized with a small amount of *i*PrOH before the solution was filtered and concentrated. The crude product was redissolved in 5 mL of methanol, a catalytic amount of *p*TsOH monohydrate was added, and the mixture was stirred at 40°C for 2 h (Scheme 2.6). Subsequently, the solution was basified with 1M aqueous NaOH. The resulting mixture was filtered and the filtrate was concentrated *en vacuo*. The product was purified by silica gel chromatography, eluting with 95:5 CH_2Cl_2 :MeOH, to give 1.20 g (53% overall yield) of viscous colorless oil **S5**. ^1H NMR (300 MHz, CD_2Cl_2 , ppm): δ 5.81 (m, 1H), 5.02–4.89 (m, 2H), 3.64 (m, 4H), 3.52 (t, $J = 6.6$ Hz, 2H), 3.41 (m, 1H), 3.37 (t, $J = 5.1$ Hz, 2H; OH), 2.04 (m, 2H), 1.57 (m, 2H), 1.34 (m, 6H). ^{13}C NMR (300 MHz, CD_2Cl_2 , ppm): δ 139.62, 114.55, 80.53, 70.65, 62.12, 34.27, 30.54, 29.52, 29.43, 26.45. HRMS(EI+) m/z : 202.1569 $[\text{M}]^+$.

Clear colorless oil **5** was made from **S5** according to the representative procedure outlined above for **2** (Scheme 2.6) in 72% yield. ^1H NMR (300 MHz, CD_2Cl_2 , ppm): δ 6.39 (dd, $J = 17.1$ Hz, $J = 1.2$ Hz, 2H), 6.14 (dd, $J = 17.3$ Hz, $J = 10.5$ Hz, 2H), 5.88–5.75 (m, 1H), 5.85 (dd, $J = 10.5$ Hz, $J = 1.2$ Hz, 2H), 5.02–4.89 (m, 2H), 4.23 (m, 4H), 3.77

(quintet, $J = 5.3$ Hz, 1H), 3.56 (t, $J = 6.6$ Hz, 2H), 2.03 (m, 2H), 1.54 (m, 2H), 1.32 (m, 6H). ^{13}C NMR (300 MHz, CD_2Cl_2 , ppm): δ 166.22, 139.74, 131.46, 128.65, 114.43, 75.70, 71.14, 63.88, 34.26, 30.41, 29.44, 26.37. HRMS(FAB+) m/z : 311.1855 $[\text{M}+\text{H}]^+$.

Scheme 2.7. Synthesis of monomer **6**.

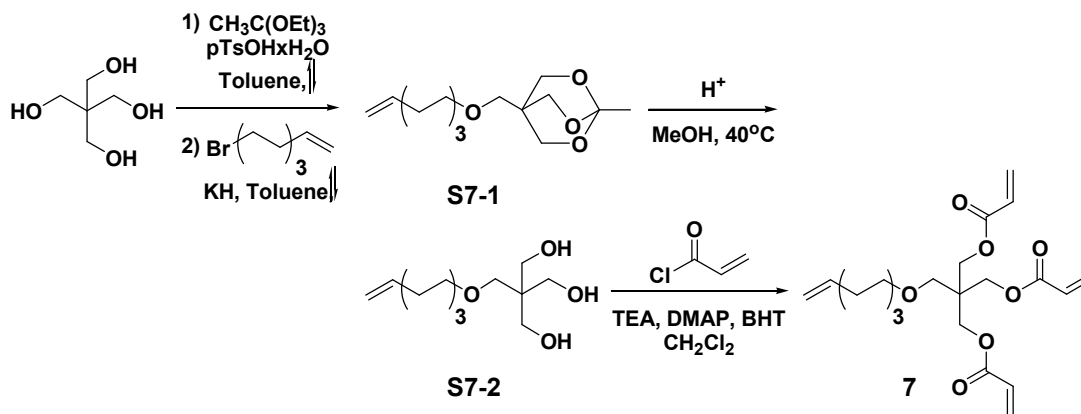


(**6**). 5-Hydroxyisophthalic acid (5.46 g, 30 mmol) was combined with n-butyl alcohol (10 mL), benzene (10 mL), and pTsOH monohydrate (57 mg, 0.3 mmol) in a 50 mL round bottom flask which was equipped with a Dean-Stark trap and a reflux condenser (Scheme 2.7). The reaction was refluxed until the white suspension in the reaction flask completely dissolved and water collection in the Dean-Stark trap had ceased (12 h). The reaction solution was then concentrated under reduced pressure and dried under high vacuum for an additional 6 h. The very thick, yellow residue obtained (1.5 g, 5 mmol) was redissolved in MeCN (7 mL) before being combined with 7-bromo-octene (1 mL, 5.35 mmol), potassium carbonate (1.17 g, 8.46 mmol) and a catalytic amount of tetra-n-butylammonium chloride; this reaction was refluxed for 10 h. The mixture was then cooled to room temperature, filtered, concentrated, and purified by silica gel chromatography. Elution with 95:5 hexane:EtOAc afforded **S6-1** (Scheme 2.7) in quantitative yield. NMR (300 MHz, CD_2Cl_2 , ppm): δ 8.21 (t, $J = 1.5$ Hz, 1H), 7.72 (d, $J = 1.5$ Hz, 2H), 5.83 (m, 1H), 5.04–4.91 (m, 2H), 4.32 (t, $J = 6.8$ Hz, 4H), 4.05 (t, $J = 6.6$ Hz, 2H), 2.07 (m, 2H), 1.77 (m, 6H), 1.55–1.37 (m, 10H), 0.99 (t, $J = 7.4$ Hz, 6H). ^{13}C NMR (300 MHz, CD_2Cl_2 , ppm): δ 166.16, 159.80, 139.66, 132.75, 122.90, 119.96, 114.55, 69.17, 65.74, 34.26, 31.27, 29.61, 29.40, 29.37, 26.35, 19.84, 14.11. HRMS(FAB+) m/z : 405.2645 $[\text{M}+\text{H}]^+$.

S6-1 (2.06 g, 5.1 mmol) was added to a stirring 1M solution of LAH in ethyl ether (11 mL) at 0 °C; the mixture was allowed to slowly warm up to room temperature, before being heated to reflux. After 6 hours, the reaction was cooled to room temperature, and sodium sulfate decahydrate was slowly added to the reaction mixture with vigorous stirring until gas evolution had ceased. The suspension was then stirred for 0.5 h, filtered through Celite (the filter cake was washed with Et₂O and boiling hot THF), and concentrated under reduced pressure. **S6-2** was further purified by recrystallization from EtOH/hexane to afford 1.27 g (94% yield) of a white solid. ¹H NMR (300 MHz, CD₂Cl₂, ppm): δ 6.89 (s, 1H), 6.80 (s, 2H), 5.83 (m, 1H), 5.03–4.90 (m, 2H), 4.61 (s, 4H), 3.96 (t, J = 6.6 Hz, 2H), 2.05 (m, 2H), 1.77 (m, 2H), 1.64 (broad s, 2H; OH), 1.40 (m, 6H). ¹³C NMR (300 MHz, CDCl₃, ppm): δ 160.12, 143.55, 139.18, 117.64, 114.49, 112.35, 68.55, 65.42, 34.25, 29.75, 29.40, 26.40. HRMS(FAB+) *m/z*: 264.1723 [M]⁺.

Colorless viscous oil **6** was made from **S6-2** according to the standard procedure outlined above for **2**. ¹H NMR (300 MHz, CD₂Cl₂, ppm): δ 6.95 (s, 1H), 6.87 (s, 2H), 6.43 (dd, J = 17.6 Hz, J = 1.4 Hz, 2H), 6.18 (dd, J = 17.6 Hz, J = 10.5 Hz, 2H), 5.90-5.77 (m, 1H), 5.87 (dd, J = 10.5 Hz, J = 1.4 Hz, 2H), 5.15 (s, 4H), 5.05-4.91 (m, 2H), 3.97 (t, J = 6.6 Hz, 2H), 2.11-2.04 (m, 2H), 1.83-1.73 (m, 2H), 1.52-1.35 (m, 6H). ¹³C NMR (300 MHz, CD₂Cl₂, ppm): δ 166.28, 160.10, 139.68, 138.44, 131.47, 128.79, 120.04, 114.54, 114.32, 68.66, 66.41, 34.27, 29.71, 29.41, 26.40. HRMS(EI+) *m/z*: 372.1924 [M]⁺.

Scheme 2.8. Synthesis of monomer **7**.



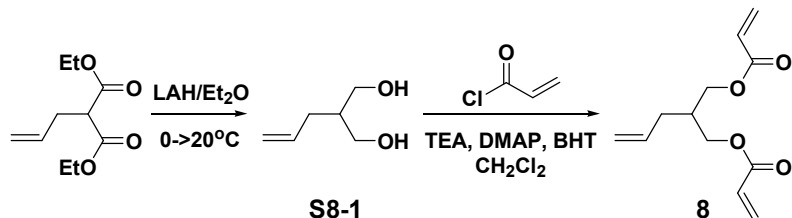
(7). Pentaerythritol (2 g, 14.7 mmol.) and pTsOH monohydrate (28 mg, 0.15 mmol) were combined in 25 mL of dry toluene and heated to reflux (Scheme 2.8). Triethyl orthoacetate (2.7 mL, 14.7 mmol) was added to the flask, and the resulting suspension was refluxed until the solution went clear and no solid residue was visible (24-48 hours). A few drops of TEA were added to the reaction, and the solution was filtered while still hot. The solution was concentrated under reduced pressure, and white, soft crystals were obtained (1.9 g, 80% yield). This orthoacetate protected product (11.7 mmol) was redissolved in hot dry toluene, and potassium hydride (35% suspension in oil, 2 g, 17.6 mmol) was added to the reaction flask followed by 8-bromo-octene (2.2 mL, 12.9 mmol). The reaction mixture was then heated to reflux. After 10 hours, the reaction was cooled to room temperature and unreacted potassium hydride was quenched with a small amount of iPrOH. The solution was filtered and concentrated. (**S7-1** could be purified at this stage by silica gel chromatography, eluting with 95:5 hexane:EtOAc. ^1H NMR (300 MHz, CD_2Cl_2 , ppm): δ 5.82 (m, 1H), 5.03-4.90 (m, 2H), 3.95 (s, 6H), 3.32 (t, $J = 6.5$ Hz, 2H), 3.13 (s, 2H), 2.04 (m, 2H), 1.50 (m, 2H), 1.40-1.27 (m, 9H). ^{13}C NMR (300 MHz, CD_2Cl_2 , ppm): δ 139.73, 114.49, 108.91, 72.35, 70.07, 69.58, 35.44, 34.27, 29.88, 29.42, 26.43, 23.91).

The crude **S7-1** was redissolved in 5 mL of methanol, a few drops of hydrochloric acid were added, and the mixture was stirred at 40°C for 2 h (Scheme 2.8). The basified with 1M aqueous NaOH solution was filtered, concentrated, and purified by silica gel chromatography. The product was eluted with 95:5 CH_2Cl_2 :MeOH and **S7-2** was obtained in 31% overall yield (in three steps from pentaerythritol). ^1H NMR (300 MHz, CD_2Cl_2 , ppm): δ 5.89-5.75 (m, 1H), 5.03-4.90 (m, 2H), 3.65 (d, $J = 5.7$ Hz, 6H), 3.42 (s, 2H), 3.41 (t, $J = 6.3$ Hz, 2H), 2.76 (t, $J = 5.7$ Hz, 3H; OH), 2.08-2.00 (m, 2H), 1.58-1.51 (m, 2H), 1.41-1.29 (m, 6H). ^{13}C NMR (300 MHz, CD_2Cl_2 , ppm): δ 139.72, 114.47, 73.88, 72.54, 65.07, 45.30, 34.24, 29.98, 29.41, 29.38, 26.48. HRMS(EI+) m/z : 247.1898 [$\text{M}+\text{H}$] $^+$.

Clear viscous oil **7** was made from **7S-2** according to the typical procedure outlined for **2** above in 57% yield. ^1H NMR (300 MHz, CD_2Cl_2 , ppm): δ 6.37 (dd, $J = 17.6$ Hz, $J = 1.7$ Hz, 3H), 6.11 (dd, $J = 17.6$ Hz, $J = 10.5$ Hz, 3H), 5.88-5.74 (m, 1H), 5.84 (dd, $J = 10.5$ Hz, $J = 1.7$ Hz, 3H), 5.02-4.89 (m, 2H), 4.24 (s, 6H), 3.46 (s, 2H), 3.38 (t, $J = 6.6$ Hz, 2H), 2.06-1.99 (m, 2H), 1.57-1.47 (m, 2H), 1.40-1.26 (m, 6H). ^{13}C NMR (300 MHz, CD_2Cl_2 ,

ppm): δ 166.08, 139.73, 131.39, 128.60, 114.45, 72.19, 69.47, 63.64, 43.42, 34.27, 29.91, 29.41, 29.40, 26.44. HRMS(EI+) m/z : 408.2149 $[M]^+$.

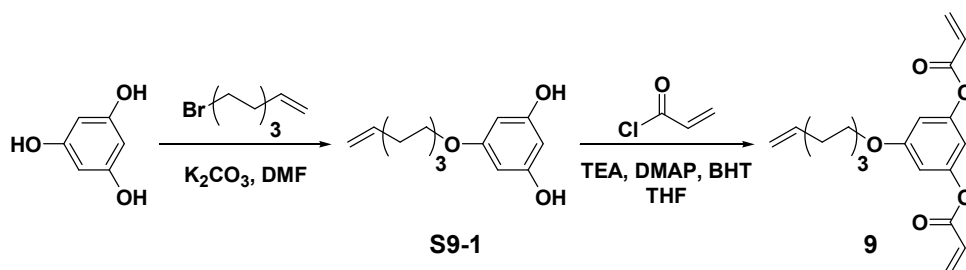
Scheme 2.9. Synthesis of monomer **8**.



(8). Diethyl allylmalonate (2.0 g, 10 mmol) was added to a stirring 1M solution of LAH in ethyl ether (21 mL) at 0°C; the mixture was allowed to slowly warm up to room temperature and stirred for 12 h (Scheme 2.9). After this time, the reaction was cooled to room temperature, and sodium sulfate decahydrate was slowly added to the reaction mixture with vigorous stirring until gas evolution had ceased. The suspension was then stirred for 0.5 h, filtered through Celite (the filter cake was washed with Et₂O and boiling hot THF), and concentrated under reduced pressure. **S8-1** was further purified by silica gel chromatography, eluting with 4:1 hexane:ethyl acetate to afford 0.65 g (56% yield) of a colorless oil. ¹H NMR (300 MHz, CD₂Cl₂, ppm): δ 5.82 (m, 1H), 5.03 (m, 2H), 3.69 (m, 4H), 2.21 (broad m, 2H; OH), 2.04 (m, 2H), 1.81 (m, 1H). ¹³C NMR (300 MHz, CDCl₃, ppm): δ 137.12, 116.65, 66.06, 42.53, 33.04.

Clear viscous oil **8** was made from **S8-1** according to the typical procedure outlined for **2** above in 59% yield. ¹H NMR (300 MHz, CD₂Cl₂, ppm): δ 6.37 (dd, J = 17.6 Hz, J = 1.7 Hz, 2H), 6.12 (dd, J = 17.6 Hz, J = 10.5 Hz, 2H), 5.82 (dd, J = 10.5 Hz, J = 1.7 Hz, 2H), 5.80 (m, 1H), 5.12-5.06 (m, 2H), 4.16 (m, 4H), 2.21 (m, 3H). ¹³C NMR (300 MHz, CD₂Cl₂, ppm): δ 166.41, 135.75, 131.12, 128.86, 117.68, 64.47, 37.77, 33.26.

Scheme 2.10. Synthesis of monomer **9**.



(9). 8-Bromo-1-octene (2.65 mL, 15.9 mmol) was added to a flask charged with phloroglucinol (2 g, 15.9 mmol) and potassium carbonate (3.3 g, 23.9 mmol) in DMF (30 mL) and the reaction mixture was stirred at room temperature for 12 h (Scheme 2.10). The solvent was then removed under reduced pressure, the products redissolved in ether and washed with water three times. The aqueous layers were combined, acidified to pH~2 with 1N HCl, and extracted in ether 3 times. The combined organic layers were washed with saturated solution of sodium chloride and dried over anhydrous MgSO₄. The solution was then filtered, concentrated, and purified by silica gel chromatography. The product was eluted with 3:1 hexane:ethyl acetate and **S9-1** (Scheme 2.9) was obtained as 0.96 g (26% yield) of a soft, white solid. ¹H NMR (300 MHz, CDCl₃, ppm): δ 6.00 (d, J = 2.1 Hz, 2H), 5.95 (t, J = 2.1 Hz, 1H), 5.82 (m, 1H), 5.04–4.92 (m, 2H), 3.87 (t, J = 6.4 Hz, 2H), 2.06 (m, 2H), 1.74 (m, 2H), 1.38 (m, 6H). ¹³C NMR (300 MHz, CDCl₃, ppm): δ 161.44, 157.50, 139.26, 114.52, 95.77, 95.16, 68.34, 33.91, 29.27, 29.03, 29.00, 26.04.

9 was prepared from compound **S9-1** (0.86 g, 4.4 mmol), acryloyl chloride (1.08 mL, 13.3 mmol), TEA (3.08 mL, 22.1 mmol), and DMAP (0.054 g, 0.4 mmol) in dry THF (15 mL) according to the procedure for the synthesis of **2** outlined above (THF had to be used as a solvent instead of CH₂Cl₂ due to the solubility properties of **S9-1**). ¹H NMR (300 MHz, CDCl₃, ppm): δ 6.60 (s, 3H), 6.59 (dd, J = 17.3 Hz, J = 1.2 Hz, 2H), 6.25 (dd, J = 17.3 Hz, J = 10.5 Hz, 2H), 5.95 (dd, J = 10.06 Hz, J = 1.2 Hz, 2H), 5.83 (m, 1H), 5.09–4.98 (m, 2H), 3.91 (t, J = 6.44 Hz, 2H), 2.26 (m, 2H), 1.74 (m, 2H), 1.45 (m, 6H). ¹³C NMR (300 MHz, CD₂Cl₂, ppm): δ 164.60, 160.98, 152.24, 139.68, 133.25, 128.22, 114.56, 108.12, 106.41, 69.16, 34.26, 29.56, 29.41, 29.37, 26.35.

Representative Polymerization Procedure (4a). Monomer **4** (0.1 g, 0.4 mmol) and a small amount of radical quencher BHT (0.4 μmol) were dissolved in dry CH₂Cl₂ (1 ml, 0.4 M) under an argon atmosphere. Catalyst **1** (1.7 mg, 2 μmol) was added to the reaction flask, and the solution was stirred at 45°C for 3–8 days (see explanation below) with venting through a bubbler (Scheme 2.2) Subsequently, the solvent was removed *en vacuo* and the product was characterized by ¹H NMR spectroscopy and triple detector–SEC with no further purification. ¹H NMR (300 MHz, CD₂Cl₂, ppm): δ 6.95 (dt, J = 15.6 Hz, J

= 5.8 Hz, 1H), 6.40 (ddd, $J = 17.4$ Hz, $J = 4.9$ Hz, $J = 1.3$ Hz, 1H), 6.11 (m, 1H), 5.82 (m, 2H), 5.20 (m, 1H), 4.35-4.17 (m, 2H), 2.2 (broad m, 2H), 1.67-1.38 (broad m, 6H).

Figure 2.5 demonstrates the progress of a typical polymerization as monitored by SEC. It was observed that longer polymerization times result in higher molecular weights. However, the catalyst lifetime in the reaction solution limits the polymerization time to 3 days. Consequently, it was found that the best results are obtained when the catalyst is added to the reaction vessel in small portions at about 2 to 3 day intervals. In Figure 2.5, trace A corresponds to a progress of the polymerization at 3 days and 0.5% of mole equivalents of the catalyst, trace B corresponds to 2 more days with a fresh batch of 0.5% of mole equivalents of the catalyst, and trace C corresponds to 3 more days with yet another catalyst batch. The gradual peak shift to the left (from A to C) indicates an increase in polymer molecular weight. Moreover, the trace also becomes more narrow and uniform with time, signaling the narrowing of the PDI. Further optimization of polymerization conditions is currently underway.

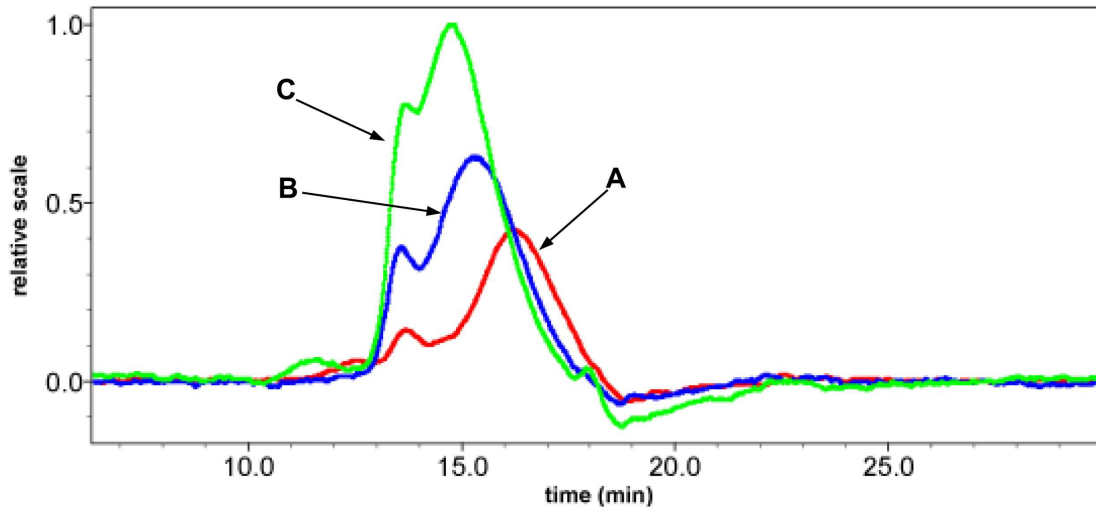


Figure 2.5. Representative MALS-SEC traces for polymerization of **4** with consecutive batch catalyst addition.

References

- (1) Hult, A.; Johansson, M.; Malmström, E. *Adv. Polym. Sci.* **1999**, *143*, 1-34.
- (2) Kim, Y. H. *J. Polym. Sci., Part A: Polym. Chem.* **1998**, *36*, 1685-1698.
- (3) Voit, B. *J. Polym. Sci., Part A: Polym. Chem.* **2000**, *38*, 2505-2525.
- (4) Voit, B. *J. Polym. Sci., Part A: Polym. Chem.* **2005**, *43*, 2679-2699.
- (5) Voit, B. I. *Comptes Rendus Chimie* **2003**, *6*, 821-832.
- (6) Yates, C. R.; Hayes, W. *Eur. Polym. J.* **2004**, 1257-1281.
- (7) Flory, P. J. *J. Am. Chem. Soc.* **1952**, *74*, 2718-2723.
- (8) Newkome, G. R.; Moorefield, C. N.; Vögtle, F. *Dendrimers and Dendrons: Concepts, Synthesis, Applications*; VCH: Weinheim, Germany, 2001.
- (9) Grayson, S. M.; Fréchet, J. M. J. *Chem. Rev.* **2001**, *101*, 3819-3868.
- (10) Bosman, A. W.; Janssen, H. M.; Meijer, E. W. *Chem. Rev.* **1999**, *99*, 1665-1688.
- (11) Stiriba, S.-E.; Frey, H.; Haag, R. *Angew. Chem. Int. Ed.* **2002**, *41*, 1329-1334.
- (12) Grinstaff, M. W. *Chem. Eur. J.* **2002**, *8*, 2838-2846.
- (13) Astruc, D.; Chardac, F. *Chem. Rev.* **2001**, *101*, 2991-3024.
- (14) Piotti, M. E.; Rivera, F.; Bond, R.; Hawker, C. J.; Frechet, J. M. J. *J. Am. Chem. Soc.* **1999**, *121*, 9471-9472.
- (15) Gibson, H. W.; Yamaguchi, N.; Hamilton, L.; Jones, J. W. *J. Am. Chem. Soc.* **2002**, *124*, 4653-4665.
- (16) Zeng, F.; Zimmerman, S. C. *Chem. Rev.* **1997**, *97*, 1681-1712.
- (17) Fréchet, J. M. J.; Hawker, C. J.; Gitsov, I.; Leon, J. W. *J. Macromol. Sci., Pure Appl. Chem.* **1996**, *A33*, 1399-1425.
- (18) Hobson, L. J.; Feast, W. J. *Chem. Commun.* **1997**, *21*, 2067-2068.
- (19) Fréchet, J. M. J.; Henmi, M.; Gitsov, I.; Aoshima, S.; Leduc, M. R.; Grubbs, R. B. *Science* **1995**, *269*, 1080-1083.
- (20) Liu, M.; Vladimirov, N.; Fréchet, J. M. J. *Macromolecules* **1999**, *32*, 6881-6884.
- (21) Suzuki, M.; Yoshida, S.; Shiraga, K.; Saegusa, T. *Macromolecules* **1998**, *31*, 1716-1719.
- (22) Suzuki, M.; Ii, A.; Saegusa, T. *Macromolecules* **1992**, *25*, 7071-7072.
- (23) Chang, H. T.; Frechet, J. M. J. *J. Am. Chem. Soc.* **1999**, *121*, 2313-2314.

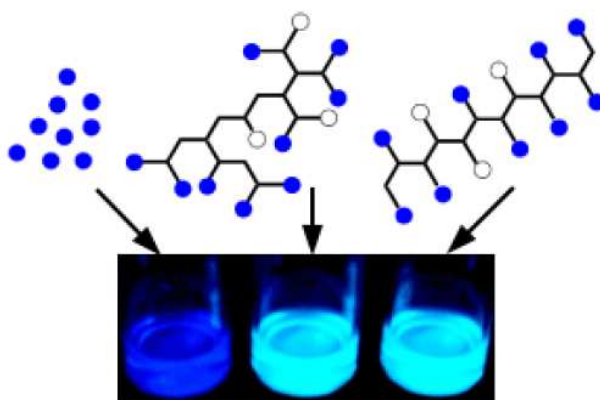
- (24) Lehman, E.; Wagener, K. B. In *Handbook of Metathesis*; Grubbs, R. H., Ed.; Wiley-VCH: Weinheim, Germany, 2003; Vol. 3, p 283-353.
- (25) Chatterjee, A. K.; Choi, T. L.; Sanders, D. P.; Grubbs, R. H. *J. Am. Chem. Soc.* **2003**, *125*, 11360-11370.
- (26) Choi, T.-L.; Rutenberg, I. M.; Grubbs, R. H. *Angew. Chem. Int. Ed.* **2002**, *41*, 3839-3841.
- (27) Choi, T.-L.; Grubbs, R. H. *Chem. Commun.* **2001**, *24*, 2648-2649.
- (28) Lee, C. W.; Choi, T. L.; Grubbs, R. H. *J. Am. Chem. Soc.* **2002**, *124*, 3224-3225.
- (29) Konzelman, J.; Wagener, K. B. *Macromolecules* **1995**, *28*, 4686-4692.
- (30) Odian, G. *Principles of Polymerization*; 4th ed.; Wiley: Hoboken, 2004.
- (31) Radke, W.; Muller, A. H. E. *Macromolecules* **2005**, *38*, 3949-3960.
- (32) Sperling, L. H. In *Introduction to Physical Polymer Science*; 2nd ed.; Wiley: New York, 1992, p 104-105.
- (33) Fürstner, A.; Langemann, K. *J. Am. Chem. Soc.* **1997**, *119*, 9130-9136.

CHAPTER 3
**An Olefin Metathesis Route to the Preparation of Functionalized
Hyperbranched Polymers**

Portions of this chapter have previously appeared as: Gorodetskaya, I. A.; Gorodetsky, A. A.; Vinogradova, E. V.; Grubbs, R. H. *Macromolecules* **2009**, *42*, 2895-2898.

Abstract

A method for the post-synthetic functionalization of hyperbranched polymers prepared by olefin metathesis is reported. This modification is performed by a second metathesis step and can be used to introduce a variety of small molecules, including fluorophores, into the polymer's periphery. Hyperbranched macromolecules functionalized with pyrene demonstrate high local concentrations of the analyte relative to the unbound fluorophore. The comparison of the photophysical properties of the hyperbranched polymer decorated with pyrene to an analogous linear polymer suggests a different distribution of the analyte within the dendritic architecture.



Introduction

Hyperbranched polymers are highly branched, three-dimensional macromolecules which are closely related to dendrimers and are typically prepared via a one-pot polycondensation of $AB_{n \geq 2}$ monomers.¹⁻⁶ Although hyperbranched macromolecules lack the uniformity of monodisperse dendrimers, they still possess many attractive dendritic features such as good solubility, low solution viscosity, globular structure, and multiple end-groups.¹⁻⁸ Furthermore, the usually inexpensive, one-pot synthesis of these polymers makes them particularly desirable candidates for both bulk-material and specialty applications. Toward this end, hyperbranched polymers have been investigated as both rheology-modifying additives to conventional polymers and as substrate-carrying supports or multifunctional macroinitiators, where a large number of functional sites within a compact space becomes beneficial.^{1,2,7,9}

The properties of a polymeric material are considerably influenced by its end groups.¹⁰ Compared to a linear polymer, this effect is more pronounced for a hyperbranched architecture simply because of a significantly larger number of end groups per single polymer chain (there is one end-group per every monomer) and their exposed placement (most of the ends are thought to be located on the periphery of the spherically-shaped units). In fact, it has been demonstrated that the chemical nature of the end-group functionalities of a hyperbranched polymer dominates not only the material's solubility in various solvents,^{7,11-13} but also melt and thermal properties such as the glass transition temperature,^{5,7,11-14} and crystallinity.¹⁴ Consequently, it is desirable to have a simple, convenient, and modular method for post-synthetic functionalization of hyperbranched polymers.

Within the past 10 years, the development of new synthetic routes to hyperbranched polymers has surpassed the detailed investigation of these materials. As a result, a great variety of dendritic backbones is now available, while information on their physical properties, especially when compared to linear analogs, remains limited.¹⁵ In particular, despite the importance of the end-groups for both property-tuning and substrate-carrying applications of hyperbranched polymers, little is known about the dendritic chain termini microenvironments and branch folding.^{9,16}

Chapter 2 described a facile approach to the synthesis of hyperbranched polymers via acyclic diene metathesis polymerization (ADMET).¹⁷ This method is based on the selectivity of N-heterocyclic carbene catalyst **1** (Figure 3.1) in the cross metathesis of different types of olefins. Since **1** promotes a selective reaction between an electron rich terminal aliphatic alkene and an electron poor acrylate, compounds such as AB₂ monomer **2** (Scheme 3.1) form highly branched structures such as **3** (Scheme 3.1) in its presence. Moreover, given that there are twice as many acrylates (B functionalities) as terminal alkenes (A functionalities) in the reaction mixture during the polymerization of **2**, half of the acrylates remain available for further manipulation.

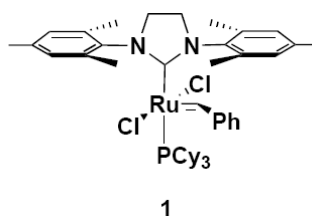


Figure 3.1. Imidazolinylidene-based ruthenium olefin metathesis catalyst **1**.

This chapter reports on the advances in the functionalization of **3** by a second cross metathesis reaction with a small fluorescent analyte—alkene modified pyrene. Although there have been numerous reports on the fluorescent properties of pyrene functionalized dendritic and linear macromolecules, these studies have typically focused on comparing polymers to small molecules.¹⁸⁻²⁷ Here, the information gathered from the comparison of the absorption and emission spectra of the decorated hyperbranched polymer with not only the spectra for a monomeric fluorophore but also the spectra of a similarly labeled linear polymeric analog can provide improved insight into the environment of the polymer's end-groups.

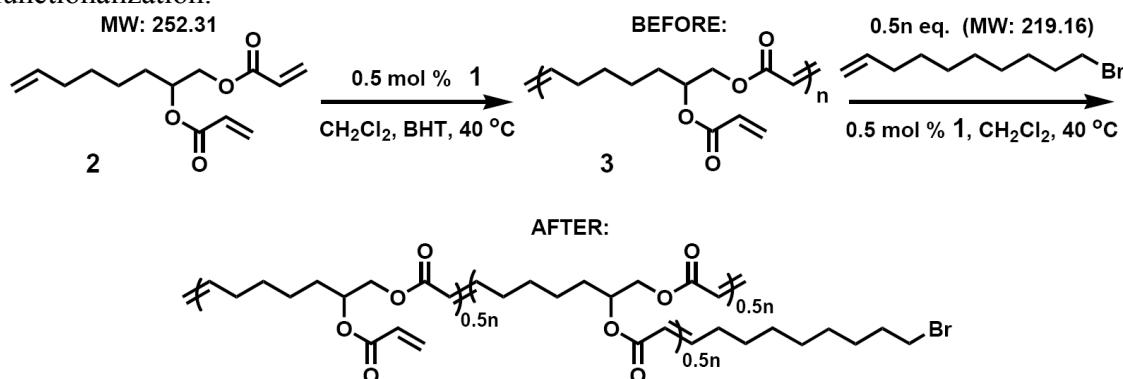
Results and Discussion

Functionalization of the Hyperbranched Polymer. Although a variety of chemical transformations can be employed in the functionalization of the terminal acrylates of **3**, olefin cross metathesis with **1** and an aliphatic alkene is the most advantageous route

for several reasons. First, and most importantly, this selective reaction proceeds in excellent yields and does not produce any non-volatile, stoichiometric by-products. Second, this method is inherently compatible with any functionality incorporated within the polymer backbone because it is the same reaction as the polymerization itself; notably, the synthesis and functionalization can be efficiently performed in tandem. Finally, substrates with functionalities not already present in the polymer can be introduced into the polymer because of the excellent functional group tolerance of **1**.

The cross metathesis functionalization of the end group acrylates was initially tested with a simple, commercially available aliphatic alkene—10-bromo-1-decene (Scheme 3.1). This molecule's molecular weight is very close to that of the monomer **2**, which aided the Size Exclusion Chromatography (SEC) analysis of the modified products. Since the hyperbranched polymer **3** has as many available end-groups as monomers in its backbone, complete functionalization with bromodecene should approximately double its molecular weight. However, only half of the necessary amount of the alkene was utilized to reduce the need for sample purification and further simplify the interpretation of SEC data. As can be seen from the SEC traces of the “before” and “after” samples in Figure 3.2, the modification of **3** with 0.5 equivalents of bromodecene proceeded to completion without any backbone degradation; the polymer's molecular weight increased from 4.73 kDa to 7.9 kDa. Importantly, thus functionalized **3** is susceptible to further manipulations by S_N2 chemistry of the peripheral bromine groups.

Scheme 3.1. Hyperbranched ADMET polymerization¹⁷ and subsequent end group functionalization.



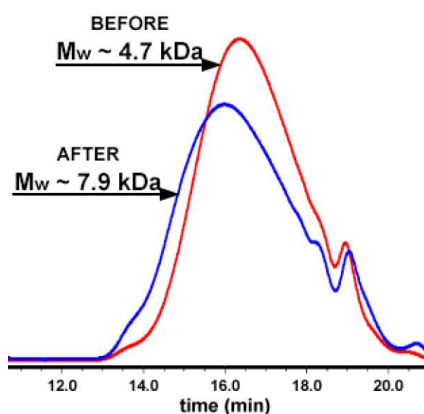
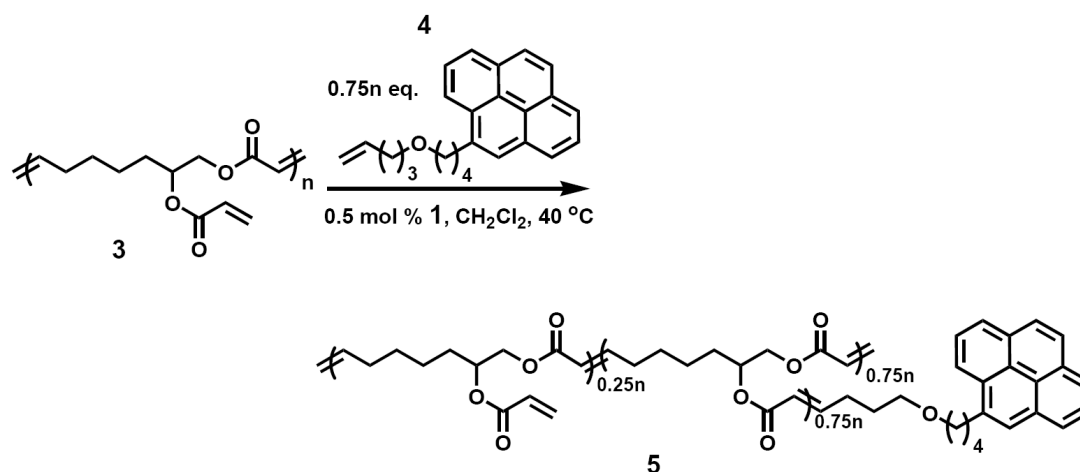


Figure 3.2. SEC (RI) traces for **3** before (red) and after (blue) functionalization with 0.5 equivalents of 10-bromo-1-decene.

Modified pyrene **4** (Scheme 3.2) was subsequently selected for functionalization of the hyperbranched polymer **3** due to its attractive fluorescent properties. Pyrene is recognized as a particularly useful handle for the study of polymer dynamics and structure in solution.¹⁸⁻²⁵ This well-studied fluorophore is characterized by long lifetimes and sensitive solvatochromic shifts.^{26,27} Furthermore, pyrene is known to associate through π -stacking interactions at millimolar concentrations, leading to the formation of highly stable excimers with red shifted emission.^{26,27} Consequently, this analyte allows for a ratiometric and quantitative measurement of pyrene-pyrene interactions, such as those resulting from a high local concentration of the substrate enforced by a covalent attachment to a polymeric backbone.¹⁸⁻²⁵ Therefore, the functionalization of dendritic end-groups with pyrene is instrumental for the study of their microenvironments.

Scheme 3.2. Hyperbranched polymer **3** functionalization with pyrene.



1-Pyrenebutanol was modified with an aliphatic alkene to produce **4**, which is suitable for selective cross metathesis with an acrylate and **1**. The functionalization method works according to the same principles as the polymerization itself: **1** selectively crosses the electron deficient acrylates with the electron rich alkene of **4**. Furthermore, this approach only affects the terminal acrylates, since the internal, di-substituted acrylates of the polymer backbone are too sterically hindered to participate in cross metathesis. In fact, if the internal acrylates could participate in the cross metathesis with **4**, degradation of the backbone would be unavoidable. However, the polymer modification proceeds to completion, and **5** is produced cleanly according to analysis by ^1H NMR and SEC (Figures 3.3 and 3.4).

The ^1H NMR spectra in Figure 3.3 show the polymerization progression of **2** to **3** and the subsequent modification of crude **3** with **4** (Scheme 3.2). In the spectrum of **2**, the peaks downfield of the solvent peak correspond to the six acrylate protons (**a**) and one terminal alkene proton (**d**). As polymer **3** is formed, all of the terminal alkenes of **2** are consumed (**d** disappears) and half of the free acrylates are internalized, thereby producing peaks **b** in the corresponding integration ratios.¹⁷ Finally, when the remaining terminal acrylates of **3** are reacted with ~ 0.75 equivalents (per end group) of **4**, the amount of free acrylates is reduced to ~ 0.25 equivalents (for each peak **a**). Consequently, ~ 0.75

equivalents of internal, pyrene-functionalized acrylates (for each peak **c**) are added to the existing internal acrylates within the polymer backbone (1 equivalent for each peak **b**). As expected, the integration values for the backbone protons **e** of **2** remain constant throughout all of these transformations (Figure 3.3). However, although the presented ^1H NMR analysis strongly supports successful functionalization of **3**, it provides little definitive information on the integrity of the polymer's backbone.

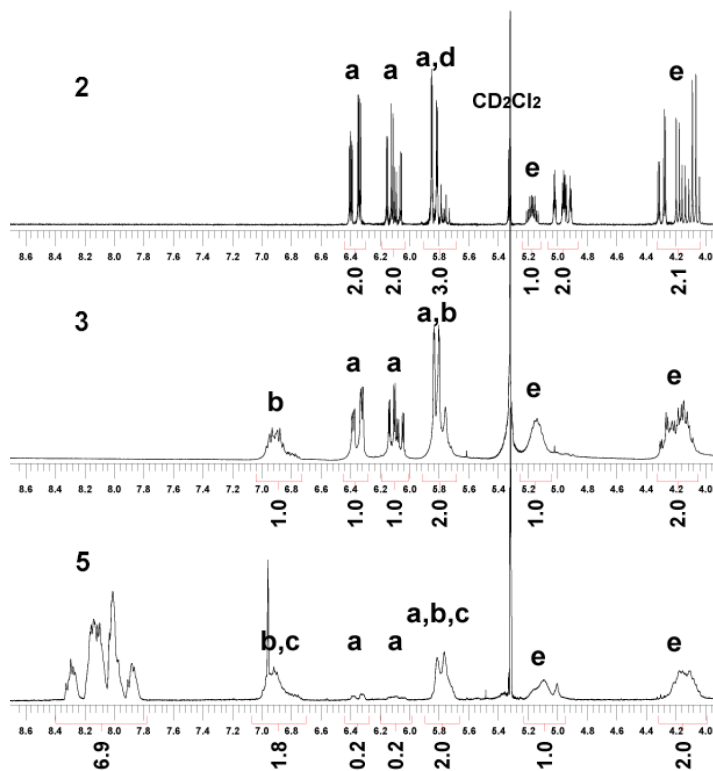


Figure 3.3. ^1H NMR spectra with integration values for **2**, **3**, and **5**. Peaks **a** correspond to the protons of the free terminal acrylate groups. Peaks **b** correspond to the protons of the internal acrylates within the polymer backbone. Peaks **c** correspond to the protons of the internal acrylates resulting from functionalization with **4**. Peak **d** is due to the proton of the terminal alkene of **2** (which is consumed during the polymerization), and peaks **e** correspond to the backbone protons of **2**.

Figure 3.4 compares the SEC traces of the polymer before (**3**) and after functionalization with **4** (**5**). Although crude **3** (purple trace) was used in the functionalization studies, the resulting **5** (pink trace) was later purified (red trace) for further fluorescence investigations. In spite of the broad polydispersity typical of

hyperbranched polymers, the evaluation of the SEC traces obtained for crude **3** and **5** clearly demonstrates that no observable backbone degradation occurs as a result of functionalization. Moreover, the absolute molecular weight corresponding to the major peak of **5** ($M_w \sim 7.87$ kDa, measured by a triple angle light scattering technique) is approximately double that of the major peak of **3** ($M_w \sim 3.33$ kDa), which is in agreement with the postulate that $\sim 75\%$ of the end groups of **3** have reacted with **4** (Figure 3.4). In addition, as expected for a compact dendritic architecture, only a very slight elution time shift is observed for **5** relative to **3** despite the significant molecular weight difference between the two. Overall, both ^1H NMR and SEC analysis indicate that only free, terminal acrylates participate in the post-synthetic functionalization of hyperbranched polymer **3**.

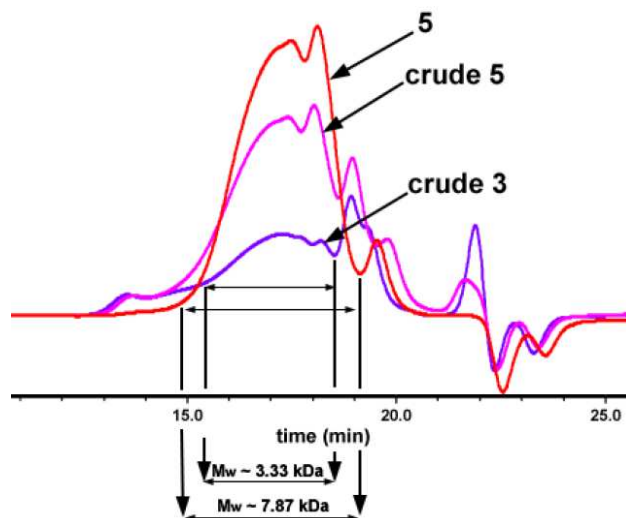


Figure 3.4. SEC (RI) traces for crude **3** (purple), crude (pink) and purified (red) **5**. The molecular weight of the major peak is approximately doubled after functionalization.

Preparation of the Pyrene Modified Linear Analog. Another significant advantage of the olefin metathesis route to the synthesis and functionalization of hyperbranched polymers is that very similar linear polymers can be prepared via the same methodology. This aspect of the synthetic strategy outlined here is crucial for the direct comparison of hyperbranched polymers to suitable linear analogs. Moreover, there is more than one way to approach this task, as either ADMET of AB monomers¹⁷ or ring opening

metathesis polymerization (ROMP) of appropriately functionalized cyclic monomers can be utilized.

We chose to prepare our linear analog by ROMP of pyrene-functionalized cyclooctene (**6**), in order to simplify the molecular weight control over the polymerization reaction (Scheme 3.3). Since ROMP is a chain-growth type polymerization which relies on monomer ring strain, it can be simply and efficiently controlled by the catalyst loading. In addition, to ensure that the linear polymer had a similar pyrene-per-chain content as the hyperbranched version, **6** was co-polymerized with a corresponding amount of “blank” methoxy-functionalized monomer **7**. The resulting random co-polymer **8** had approximately 75 pyrenes per 100 monomers, as did the hyperbranched polymer **5** (Figure 3.5).

Scheme 3.3. Synthesis of the pyrene-functionalized linear polymeric analog.

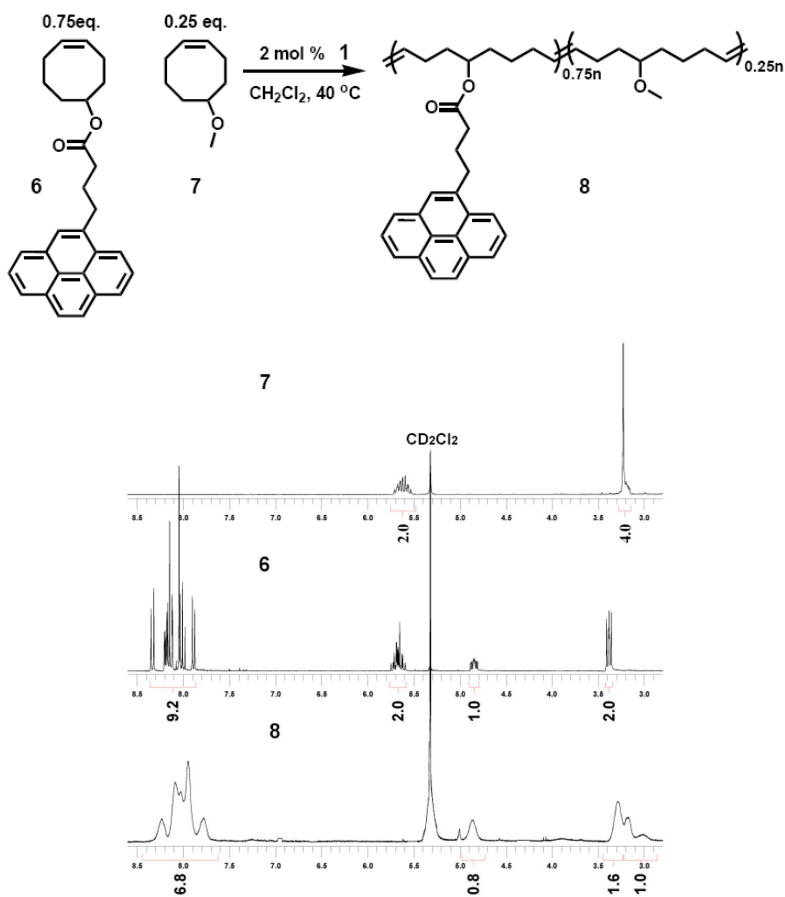


Figure 3.5. ¹H NMR spectra with integration values for **6**, **7**, and **8**.

Fluorescence Properties of Pyrene-Functionalized Hyperbranched and Linear Polymers. Figure 3.6A compares the UV-visible absorbance and steady-state fluorescence emission spectra for solutions of monomeric pyrene **4**, pyrene-functionalized hyperbranched polymer **5**, and similarly functionalized linear analog **8**. The normalized UV-Vis spectra of all three compounds overlap almost perfectly with no observed spectral broadening or red shift of the linear and hyperbranched polymer (relative to the pyrene monomer). This indicates that the polymeric scaffold does not dramatically influence the interaction of the pyrene moieties in the ground state. On the other hand, the fluorescence emission spectra of the three compounds at the identical concentrations are quite distinct. For all three samples, peaks which correspond to emission from the monomeric pyrene are evident at 380 nm and 400 nm. In addition, for the hyperbranched polymer **5** and linear analog **8**, a broad and featureless excimer emission centered at 480–500 nm is also evident. Therefore, the pyrene moieties must interact strongly in the excited state due to constraints imposed by the backbones of **5** and **8**.

As can be seen in Figure 3.6B, the ratios of the monomer to excimer emission intensity indicate that the degree of pyrene association is different for **5** and **8**. At a low pyrene concentration of $\sim 80 \mu\text{M}$, the ratio of the excimer to monomer emission intensity (I_E/I_M) is 1.5 for the hyperbranched polymer and 7.9 for the linear analog. As expected, no stacking is observed for free pyrene **4** at micromolar concentrations. For both **5** and **8**, over the concentration range tested, there is only a slight change in the excimer to monomer ratio, indicating that the pyrene interactions are intramolecular rather than intermolecular. Therefore, although both polymers do serve to effectively increase the local pyrene concentration, the hyperbranched architecture promotes stacking less effectively than the linear scaffold. Given the nearly identical backbone chemical compositions, concentrations, and degrees of functionalization for samples **5** and **8**, these observations suggest that some of the pyrene moieties are confined to the interior of the hyperbranched polymer and are, thus, shielded from adjacent pyrenes.

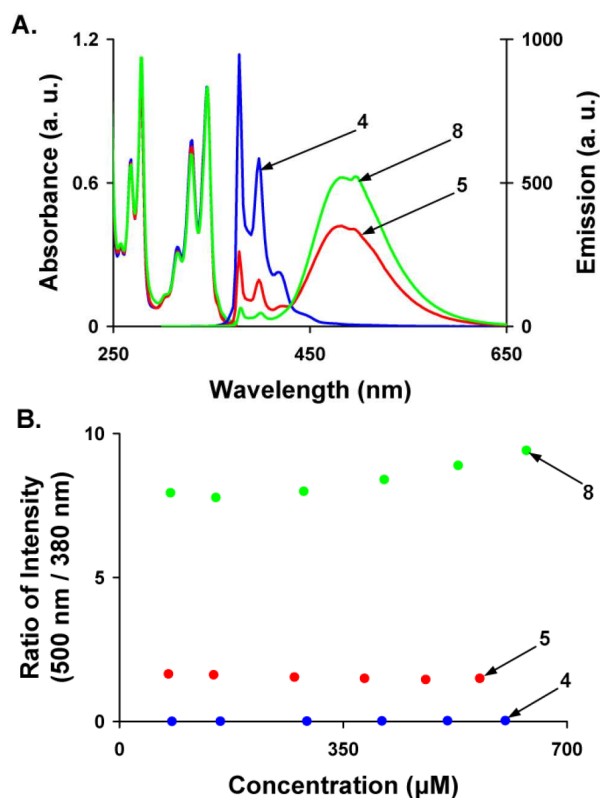


Figure 3.6. (A) UV-visible absorbance and fluorescence emission spectra for **4** (blue), **5** (red), and **8** (green) in dichloromethane. The absorbance spectra have been normalized for clarity, and the fluorescence spectra were obtained at an 80 μM concentration. (B) A plot of the monomer (380 nm) to excimer (500 nm) intensity emission ratio at various concentrations.

Conclusion

In conclusion, hyperbranched polymers were prepared via ADMET with catalyst **1** and efficiently functionalized at their periphery by further cross metathesis. This strategy should prove general for the post-polymerization modification of ADMET hyperbranched polymers with a variety of terminal alkene modified substrates. Moreover, this simple olefin metathesis approach to the synthesis of functionalized hyperbranched polymers can be easily extended to the preparation of linear analogs, which are useful for the investigations of the influence of different polymeric architectures on material properties. In particular, our studies of pyrene-functionalized hyperbranched and linear polymers showed that while both polymeric backbones enforce higher local concentrations of a

bound fluorophore relative to its free form, only the hyperbranched scaffold appears to partially shield the analytes from each other, possibly through absorption into the dendritic interior. These observations may hold implications for the use of hyperbranched polymers as drug-delivery systems.²⁸

Experimental Procedures

Materials. All reagents, except for catalyst **1** and 1-pyrenebutyric acid were purchased from Aldrich at the highest available purity and used without further purification. Catalyst **1** was obtained from Materia, Inc., and 1-pyrenebutyric acid ($\geq 97\%$) was purchased from Fluka. The synthesis of **2** and its polymerization to **3** with **1** have been reported previously.¹⁷

Instrumentation. NMR spectra were obtained using a Varian Mercury-300 spectrometer; samples were dissolved in CD_2Cl_2 .

Size exclusion chromatography (SEC) analysis was performed using a Wyatt triple detector system equipped with a triple angle light scattering (miniDAWN TREOS, with laser wavelength of 658 nm) detector, a viscometer (ViscoStar) detector, and a refractive index (Optilab rEX) detector—all operating at 25°C. Viscotek ViscoGEL I-Series (one mixed bed medium MW and one mixed bed high MW) columns were used for SEC with THF as the eluent and a Shimadzu LC-10AD pump operating at 1 mL/minute.

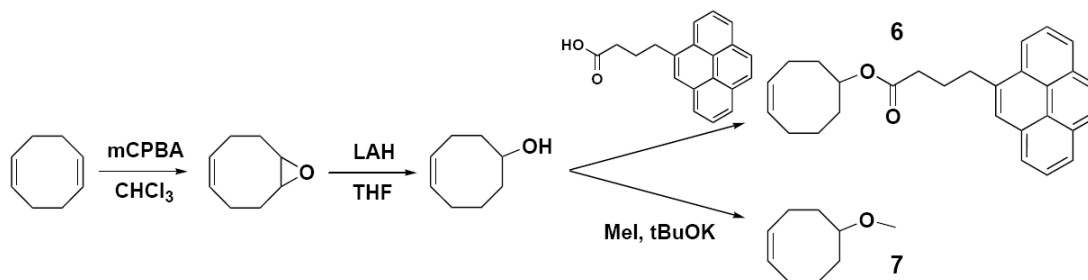
Fluorescence measurements were conducted using an ISS K2 fluorimeter (5 mm path length), equipped with a 250 W xenon lamp as excitation source. Emission spectra were obtained by exciting at 346 nm and monitoring the emission between 300 and 700 nm. UV-Vis spectra were recorded on a Beckman DU 7400 spectrophotometer.

Synthesis of 4-(4-pent-4-enyloxy-butyl)-pyrene (4). 1-Pyrenebutanol (1.0 g, 3.6 mmol) was combined with potassium hydride (35% suspension in oil, 1 g, 8.7 mmol) in 10 mL of toluene in a 50 mL round bottom flask equipped with a stir bar. The solution was stirred at room temperature until it had stopped evolving gas, at which point 5-bromopentene (0.6 mL, 5 mmol) was slowly added to the reaction flask. The reaction was subsequently heated to reflux for 10 h. The reaction mixture was then cooled to room temperature, and the unreacted potassium hydride was neutralized with a small amount of *i*PrOH before the solution was filtered and concentrated. The product was purified by silica gel chromatography, eluting with 5% EtOAc in hexane, and recrystallized from cold (0°C) hexane to give a quantitative yield of pure **4** as a yellowish crystalline solid. ¹H NMR (300 MHz, CD_2Cl_2 , ppm): 8.32 (d, *J* = 9 Hz, 1H), 8.19–7.97 (m, 7H), 7.90 (d, *J* = 7.8

Hz, 1H), 5.83 (m, 1H), 5.04–4.91 (m, 2H), 3.49–3.35 (m, 6H), 2.09 (m, 2H), 1.93 (m, 2H), 1.79–1.59 (m, 4H). ^{13}C NMR (300 MHz, CD_2Cl_2 , ppm): δ 139.17, 137.80, 131.99, 131.50, 129.33, 128.04, 127.89, 127.58, 126.99, 126.37, 125.49, 125.33, 125.18, 125.04, 124.11, 114.82, 71.08, 70.66, 33.81, 30.95, 30.40, 29.62, 29.11.

Synthesis of pyrene functionalized hyperbranched polymer (5). **3** (163 mg, 0.646 mmol in monomer), **4** (167 mg, 0.485 mmol, 0.75 equivalents), and **1** (3 mg, 3.53 μmol) were combined in 2 mL of dry CH_2Cl_2 under an inert atmosphere. The reaction mixture was stirred at 40°C for 10 h with venting through a bubbler. Subsequently, the reaction was concentrated and the product was characterized by ^1H NMR spectroscopy with no further purification. NMR analysis indicated clean and complete addition of all of the added **4** (0.75 equivalents per repeat unit in **3**).

Scheme 3.4. Synthesis of the monomers for linear ROMP.



Synthesis of linear pre-monomer, cyclooct-4-enol. A 250 mL round bottom flask equipped with a stir bar and an addition funnel was charged with 1,5-cyclooctadiene (8.6 g, 79.1 mmol). The solution of mCPBA (11.1 g, 64.1 mmol) in chloroform (180 mL) was added to the reaction flask drop-wise via the addition funnel (Scheme 3.4). The reaction mixture was stirred for 10 h and then filtered; it was then washed with aqueous solutions of NaHSO_3 (3 times), NaHCO_3 (once), and brine (once) consequently. The purification by silica gel chromatography, eluting with 10% EtOAc in hexane, gave 4.2 g (43% yield) of the epoxide product. ^1H NMR (300 MHz, CD_2Cl_2 , ppm): δ 5.57 (m, 2H), 3.00–2.95 (m, 2H), 2.46–2.36 (m, 2H), 2.18–1.93 (m, 6H). ^{13}C NMR (300 MHz, CD_2Cl_2 , ppm): δ 129.35, 56.95, 28.68, 24.20.

A 1M THF solution of LAH (17.0 mL, 17.0 mmol) was slowly added to the solution of the epoxide (4.21 g, 33.9 mmol) in THF (23 mL) at room temperature and the mixture was stirred for 10 h (Scheme 3.4). The reaction was then quenched with sodium sulfate decahydrate, stirred very well for 20 minutes, filtered through Celite, and concentrated. The purification by silica gel chromatography with a 30% EtOAc in hexane eluent afforded 4.0 g (95% yield) of a clear colorless oil. ^1H NMR (300 MHz, CD_2Cl_2 , ppm): δ 5.73–5.53 (m, 2H), 3.75 (m, 1H), 2.33–2.23 (m, 2H), 2.17–2.03 (m, 2H), 1.94–1.75 (m, 2H), 1.71–1.44 (m, 4H). ^{13}C NMR (300 MHz, CD_2Cl_2 , ppm): δ 130.67, 129.95, 73.09, 38.29, 36.92, 26.13, 25.47, 23.30.

(6). Cyclooct-4-enol (0.3 g, 2.4 mmol), 1-pyrenebutyric acid (1.0 g, 3.5 mmol), DMAP (0.6 g, 4.8 mmol), and Et_3N (1.3 mL, 9.5 mmol) were dissolved in 10 mL of dry methylene chloride (Scheme 3.4). 2,4,6-Trichlorobenzoyl chloride (1.16 g, 4.8 mmol) was then slowly added to the reaction mixture, and the reaction was stirred for 10 h. The unreacted benzoyl chloride was neutralized with a small amount of *i*PrOH before the solution was filtered and concentrated. The product was then purified by silica gel chromatography, eluting with 5% EtOAc in hexane, to give 0.9 g (95% yield) of a semi-crystalline, bright yellow material. ^1H NMR (300 MHz, CD_2Cl_2 , ppm): δ 8.33 (d, $J = 9.6$, 1H), 8.21–7.98 (m, 7H), 7.89 (d, $J = 8.1$, 1H), 5.76–5.60 (m, 2H), 4.86 (m, 1H), 3.38 (t, $J = 7.6$, 2H), 2.44–2.29 (m, 4H), 2.22–2.08 (m, 4H), 1.98–1.56 (m, 6H). ^{13}C NMR (300 MHz, CD_2Cl_2 , ppm): δ 173.04, 136.77, 131.98, 131.49, 130.47, 130.34, 130.20, 129.28, 128.02, 128.00, 127.77, 127.15, 126.43, 125.54, 125.45, 125.42, 125.37, 125.28, 124.01, 76.01, 34.83, 34.33, 33.30, 28.45, 27.54, 26.14, 25.49, 22.88.

(7). Cyclooct-4-enol (0.5 g, 4.0 mmol) was combined with *t*BuOK (0.7 g, 6.0 mmol) in dry THF (8 mL) (Scheme 3.4). Upon addition of MeI (0.4 mL, 6 mmol) the reaction mixture was stirred at 35 °C for 10 h. The remaining unreacted *t*BuOK was neutralized with a small amount of *i*PrOH before the solution was filtered and concentrated. Purification by silica gel chromatography, eluting with 5% EtOAc in hexane,

afforded 0.15 g (27% yield) of clear colorless oil **7**. ^1H NMR (300 MHz, CD_2Cl_2 , ppm): δ 5.71 (m, 2H), 3.23 (s, 3H), 3.20 (m, 1H), 2.39–2.27 (m, 2H), 2.17–1.36 (m, 8H)
 ^{13}C NMR (300 MHz, CD_2Cl_2 , ppm): δ 130.67, 129.90, 82.52, 56.15, 34.48, 33.33, 26.31, 26.20, 23.17.

Synthesis of pyrene functionalized linear polymer (8). Monomers **6** (100 mg, 0.25 mmol) and **7** (12.0 mg, 0.08 mmol) were dissolved in dry CH_2Cl_2 (1 ml) under an argon atmosphere. Catalyst **1** (5 mg, 6 μmol) was added to the reaction flask, and the solution was stirred at 45°C for 24 hours. Upon consumption of the monomers, the volatiles were removed under reduced pressure. The product was then redissolved in a small amount of CH_2Cl_2 , loaded on a short silica plug, rinsed with CH_2Cl_2 , and eluted with THF. The purified product was characterized by ^1H NMR spectroscopy and triple detector–SEC ($M_w \sim 38\text{K}$, $M_w/M_n \sim 1.45$).

References

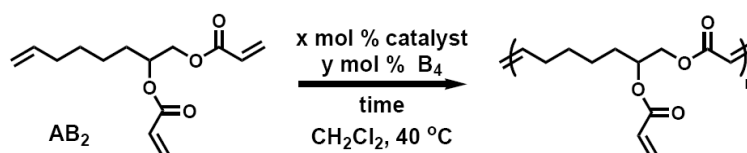
- (1) Voit, B. *J. Polym. Sci., Part A: Polym. Chem.* **2005**, *43*, 2679-2699.
- (2) Yates, C. R.; Hayes, W. *Eur. Polym. J.* **2004**, 1257-1281.
- (3) Voit, B. *I. C. R. Chimie* **2003**, *6*, 821-832.
- (4) Voit, B. *J. Polym. Sci., Part A: Polym. Chem.* **2000**, *38*, 2505-2525.
- (5) Hult, A.; Johansson, M.; Malmström, E. *Adv. Polym. Sci.* **1999**, *143*, 1-34.
- (6) Kim, Y. H. *J. Polym. Sci., Part A: Polym. Chem.* **1998**, *36*, 1685-1698.
- (7) Wooley, K. L.; Hawker, C. J.; Lee, R.; Fréchet, J. M. J. *Polymer J.* **1994**, *26*, 187-197.
- (8) Wooley, K. L.; Fréchet, J. M. J.; Hawker, C. J. *Polymer* **1994**, *35*, 4489-4495.
- (9) Johansson, M.; Malmström, E.; Hult, A. *Trends in polymer science* **1996**, *4*, 398-403.
- (10) *Cyclic Polymers*; 2nd ed.; Semlyen, J. A., Ed.; Kluwer Academic Publishers: Dordrecht, The Netherlands, 2000.
- (11) Kim, Y. H.; Webster, O. W. *Macromolecules* **1992**, *25*, 5561-5572.
- (12) Uhrich, K. E.; Hawker, C. J.; Fréchet, J. M. J.; Turner, S. R. *Macromolecules* **1992**, *25*, 4583-4587.
- (13) Hawker, C. J.; Chu, F. *Macromolecules* **1996**, *29*, 4370-4380.
- (14) Malmström, E.; Johansson, M.; Hult, A. *Macromol. Chem. Phys.* **1996**, *197*, 3199-3207.
- (15) Stiriba, S. E.; Kautz, H.; Frey, H. *J. Am. Chem. Soc.* **2002**, *124*, 9698-9699.
- (16) Lescanec, R. L.; Muthukumar, M. *Macromolecules* **1990**, *23*, 2280-2288.
- (17) Gorodetskaya, I. A.; Choi, T. L.; Grubbs, R. H. *J. Am. Chem. Soc.* **2007**, *129*, 12672-12673.
- (18) Winnik, M. A.; Bystryak, S. M.; Liu, Z.; Siddiqui, J. *Macromolecules* **1998**, *31*, 6855-6864.
- (19) Baker, L. A.; Crooks, R. M. *Macromolecules* **2000**, *33*, 9034-9039.
- (20) Brauge, L.; Caminade, A. M.; Majoral, J. P.; Slomkowski, S.; Wolszczak, M. *Macromolecules* **2001**, *34*, 5599-5606.
- (21) Gao, C.; Yan, D.; Zhang, B.; Chen, W. *Langmuir* **2002**, *18*, 3708-3713.
- (22) Chen, J.; Jiang, M.; Zhang, Y.; Zhou, H. *Macromolecules* **1999**, *32*, 4861-4866.
- (23) Wilson, J. N.; Teo, Y. N.; Kool, E. T. *J. Am. Chem. Soc.* **2007**, *129*, 15426-15427.

- (24) Ingratta, M.; Duhamel, J. *Macromolecules* **2007**, *40*, 6647-6657.
- (25) Ingratta, M.; Hollinger, J.; Duhamel, J. *J. Am. Chem. Soc.* **2008**, *130*, 9420-9428.
- (26) Winnik, F. M. *Chem. Rev.* **1993**, *93*, 587-614.
- (27) Klessinger, M.; Michl, J. *Excited States and Photochemistry of Organic Molecules*; VCH: New York, N. Y., 1995.
- (28) Paleos, C. M.; Tsiourvas, D.; Sideratou, Z. *Mol. Pharmaceutics* **2007**, *4*, 169-188.

CHAPTER 4
Towards Molecular Weight Control of the Hyperbranched ADMET
Polymerization

Abstract

This chapter presents an investigation of the factors thought to be capable of influencing a hyperbranched ADMET polymerization. More specifically, the catalyst loading, reaction time, and use of mono- and multi-functional additives were considered in this study. Unexpectedly, the polymerization system response to these tests strongly suggested pseudo-chain-growth, rather than clear step-growth, kinetics expected of addition polymerizations. A catalyst “branch-hopping” mechanism consistent with the observed polymerization behavior is proposed.



Introduction

Hyperbranched polymers are polydisperse, three-dimensional macromolecules with a densely functionalized semi-globular periphery.¹⁻⁶ These structures are closely related to monodisperse dendrimers and are also typically prepared from $AB_{n \geq 2}$ type monomers. However, unlike the latter, hyperbranched polymers are synthesized by a one-pot, poorly controlled polymerization, in which unprotected functional groups A and B react with each other but not with themselves. Although hyperbranched polymers lack the uniformity of dendrimers, they possess many of the attractive dendritic features such as good solubility, low viscosity, and multiple end groups. Consequently, the available simple synthetic routes to hyperbranched architectures make these polymers especially appealing candidates for bulk property applications, as components of blends, additives, and coatings.^{1,2,7}

Regardless of the type of application, a thoroughly understanding and controlling the molecular weight and polydispersity of a polymer is essential for deriving structure–property relationships and tuning material properties.⁸ Among numerous reported hyperbranched polymerization methods,¹⁻⁶ polycondensations and polyadditions of AB_n monomers are usually the simplest and the least expensive, but these step-growth processes are also the most difficult to control.⁸ Nevertheless, a number of factors which improve the efficiency of these reactions (such as high temperatures,^{1,7,9} extended reaction times,^{1,7} and the choice of solvent)⁹ have been shown to increase the size of the resulting polymers. On the other hand, the addition of end-capping reagents has been demonstrated to decrease the molecular weight of hyperbranched chains.¹⁰ In addition, and more specific to dendritic growth control, multifunctional B_f core molecules have also been utilized, and they appear to reduce the polydispersity index (PDI) of the hyperbranched products, although at the expense of size.¹¹⁻¹⁵ However, catalyst loading as a regulatory tool for transition metal catalyzed hyperbranched polyadditions remains undeservingly overlooked.

We have recently reported a facile approach to the synthesis of hyperbranched polymers via ruthenium catalyzed acyclic diene metathesis polymerization (ADMET).¹⁶ This transition metal catalyzed polyaddition is based on the selectivity of the imidazolinylidene catalyst **1** (Figure 4.1) in the cross metathesis of different types of olefins. Since **1** effects a selective cross between an electron rich terminal aliphatic alkene

and an electron poor acrylate, compounds such as the AB₂ monomer **2** (Scheme 4.1) form highly branched structures (**3**) in its presence.¹⁶ The previously described reaction conditions, which employ a fixed amount of the catalyst and no additives, reliably afford the polydisperse, modestly sized polymer **3** in excellent yields. However, in an attempt to gain a better understanding of this polymerization process and, ultimately, better control it, we have investigated several potentially influential factors. Herein, we report our advances in the optimization of the hyperbranched ADMET polymerization conditions by exploring the effect that catalyst loading, reaction time, and inclusion of multifunctional core molecule (**4**) have on the molecular weight and polydispersity of **3**.

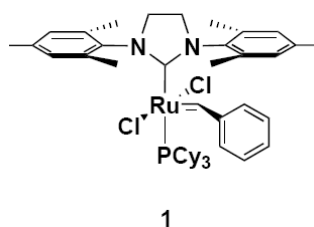
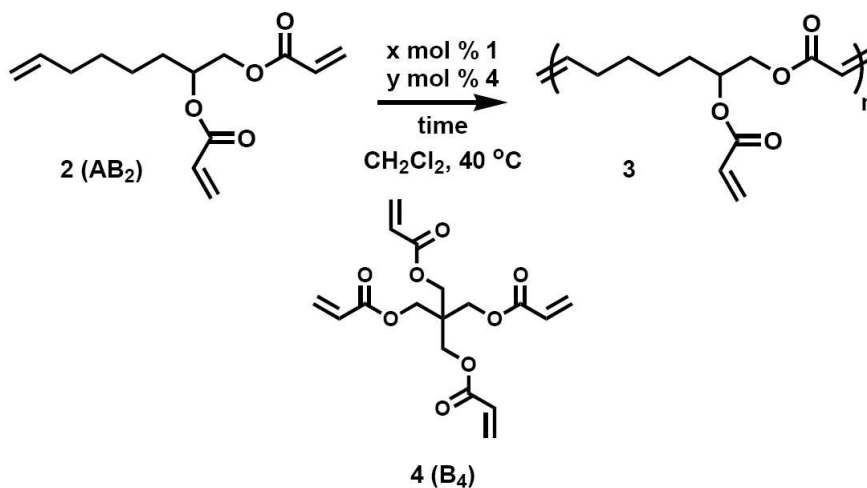


Figure 4.1. ADMET catalyst **1**.

Scheme 4.1. Hyperbranched ADMET Polymerization.



Results and Discussion

Catalyst Loading. Addition polymerizations of AB₂ monomers are traditionally thought of as step-growth processes, in which a build-up of oligomers precedes a sharp increase in molecular weight at high conversions. Consequently, the efficiency of the chosen polymerization reaction is crucial for obtaining high molecular weight polymers. Therefore, if a larger amount of the catalyst increases the effectiveness of the catalyzed reaction, it should also boost the molecular weight of the produced polymers. In fact, this trend was observed for some hyperbranched polycondensations.^{1,2,7} However, contrary to any such expectations, increasing the amount of catalyst **1** from 0.5 mol % (red trace) to 1.0 mol % (blue trace) and 5.0 mol % (green trace) caused the molecular weight of **3** to diminish from 6.8 kDa to 4.1 kDa and 1.4 kDa respectively (Figure 4.2A).

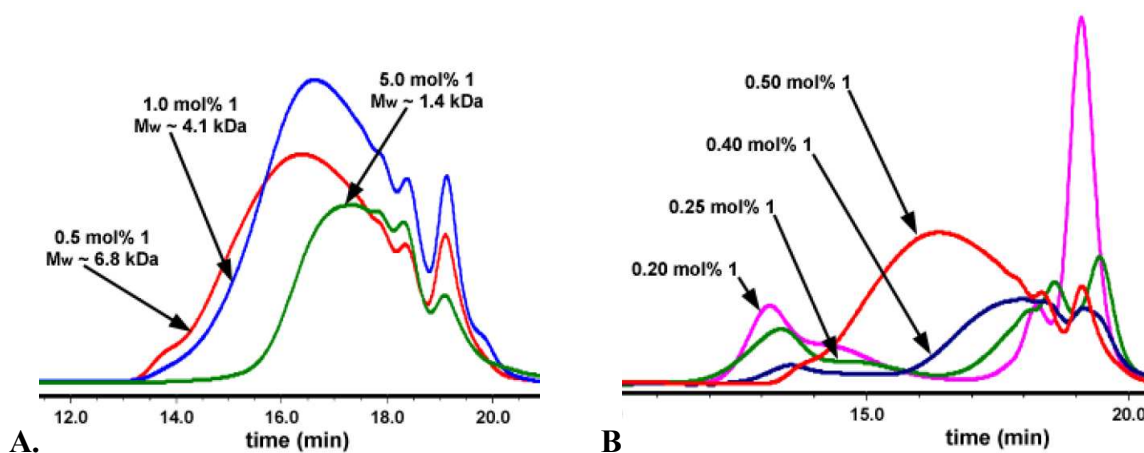


Figure 4.2. SEC (RI) traces for **3** made with different amounts of **1**.

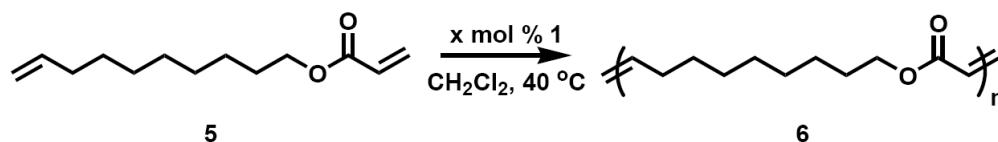
To expand upon our findings, we reduced the amount of catalyst in the polymerization of **2**. As shown in Figure 4.2B, increasing the monomer to catalyst ratio yielded materials with not only much larger chains in the reaction mixture, but also with quite different SEC profiles. The most prominent feature of these traces is their enormous polydispersity; the broad PDI is visually evident in Figure 4.2B, where the samples obtained from the polymerizations with less than 0.5 mol % of **1** appear to contain almost no intermediate sized polymers but, rather, contain only high molecular weight chains

(peaks at ~ 13 min) and small oligomers (~ 19 min). By comparison, at a 0.5 mol % catalyst loading, all the peaks merge into a smoother, average trace with an improved PDI.

An important feature of catalyst **1** is benzylidene moiety. The benzylidene transfers to the growing polymer or monomer as a styrene group, potentially end-capping the growing chain after the first catalytic cycle of **1**. Consequently, some of the molecular weight behavior observed for **3** can be attributed to changes in the number of these growth terminating groups, which correlates with changes in the amount of catalyst. Therefore, a higher catalyst loading also furnishes more end-capping species during the polymerization and, thus, results in shorter polymer chains, but less catalyst has the opposite effect on the polymerization. However, it is unlikely that the catalyst and its counterparts are solely responsible for all of the observed behavior because the molecular weight fluctuations are too large.

A “linear” polymerization of an AB monomer **5** (Scheme 4.2) was investigated next in order to 1) probe the influence of the architecture of the growing chain on the polymerization kinetics and 2) separate any such effects from those associated with specifics of ADMET with **1**. Figure 4.3 presents the SEC traces for **5** produced with different amounts of **1**. As expected of an addition polymerization, more catalyst promotes more efficient cross metathesis and higher molecular weights. In particular, increasing the catalyst loading from 0.25 mol % (green trace) to 0.50 mol % (red trace) and 1.00 mol % (blue trace) resulted in the molecular weight of **5** increasing from 7.3 kDa to 8.5 kDa and 9.1 kDa, respectively. However, more than 2.5 mol % of **1** causes the molecular weight to drop dramatically, which is, most plausibly, the manifestation of end-capping by the styrene produced from catalysis with **1**.

Scheme 4.2. Linear ADMET polymerization.



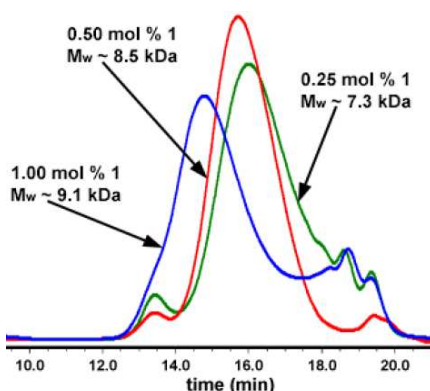


Figure 4.3. SEC (RI) traces for **5** made with different amounts of **1**.

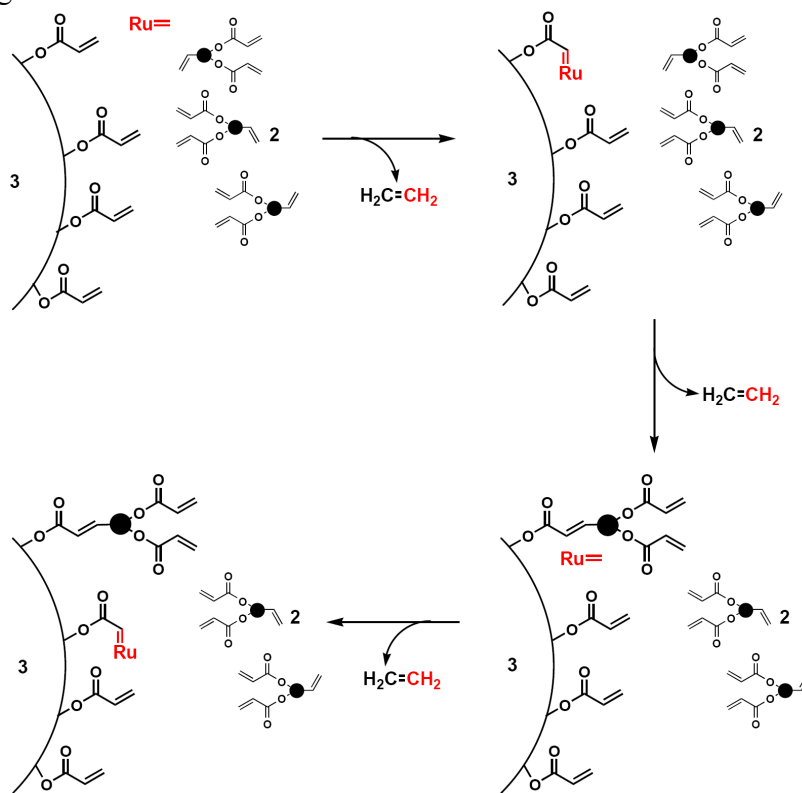
The linear ADMET polymerization of **5** clearly indicates that the unusual polymerization behavior of AB_2 monomers is due to hyperbranched architecture of the growing polymer and not catalyst **1** or the ADMET reaction itself. Furthermore, the dependence of the molecular weight on the catalyst loading demonstrated by **3** is strongly reminiscent of chain-growth kinetics—the monomers (from the small molecular weight peak) are added to the growing chain (large molecular weight peak). This differs from the step-growth kinetics expected for an addition polymerization and, indeed, observed for **5**. Moreover, less **1** seems to produce fewer but larger chains than does more catalyst, and it appears from the SEC analysis that for very low catalyst loadings, **1** decomposes before all of the monomers and smaller oligomers are consumed (Figure 4.2B).

The important difference of the hyperbranched architecture of emerging **3** is its multiple end-groups, which allow for more monomer addition opportunities, relative to the linear architecture of **6**, where only two end-groups are available for addition at any given time. Consequently, once an initial multifunctional, hyperbranched oligomer is formed, a high local concentration of acrylates is created, and the probability of a monomer adding to the growing chain is higher, than the probability of two independent monomers finding each other in solution. However, other factors must also influence the observed molecular weight–catalyst loading relationship; otherwise, more catalyst would be expected to further increase the monomer addition efficiency and produce larger, not smaller polymers.

An additional rationale may underlie the catalyst loading dependence of the hyperbranched ADMET polymerization: at low catalyst loading, the majority of the active

catalytic species in the reaction mixture are “stuck” to the densely acrylate populated periphery of the growing chain. In this case, monomer additions in the polymerization of **2** are only occurring along the polymer chain’s outer sphere, as the catalyst “walks” around it—a chain-growing mechanism depicted in Scheme 4.3. According to this mechanism, as **1** initially reacts with any of the peripheral acrylates of **3**, it becomes physically attached to the growing chain. Although the metal carbene is then quickly released through addition of a monomer (**2**) to the polymer, the freed catalytic species remain surrounded by many more peripheral acrylates. Therefore, it is much more likely that the catalyst is recaptured by **3** and continues its chain-growing “walk” along the periphery, instead of completely dissociating from the polymer to connect two independent monomers in a step-growth fashion. On the other hand, the larger amount of **1** in the reaction mixture increases the probability of unbound catalytic species in the polymerization solution, which, in turn, ensues competitive step-grows.

Scheme 4.3. The “chain-walking” mechanism for hyperbranched ADMET polymerization at low loading of **1**.



Reaction Time. Another important factor in the molecular weight control of a hyperbranched polymerization is reaction time. The duration of the polymerization reaction is particularly important in the case of step-growth, since high monomer conversion is crucial for progressing the polymerization beyond oligomers. Indeed, the molecular weight of **3** does seem to increase with prolonged reaction times, and the PDI is also improved (Figure 4.4); but these changes are modest. Furthermore, the uncertainty of the SEC measurements might be partially responsible for the apparent “jagged” shape of the traces in Figure 4.4A. On the other hand, the molecular weight dips in the time plot (which are especially pronounced for the higher molecular weight polymers obtained at lower catalyst loadings in Figure 4.5A) could also be caused by polymerization “errors”—internal aliphatic alkenes (A-A links). As these undesirable backbone connections are cleaved by the “correct” A to B monomer additions, more thermodynamically stable and olefin cross metathesis resistant A-B links are formed (Figure 4.5B). If the “error correction” assumption is true, it further substantiates the catalyst “branch-hopping” hypothesis. Any A-A defect would quickly become buried in the polymer backbone during the polymerization and would be hard to reach for the cross metathesis catalyst, unless the catalyst directly stumbles onto such a “weak” link during the periphery walk.

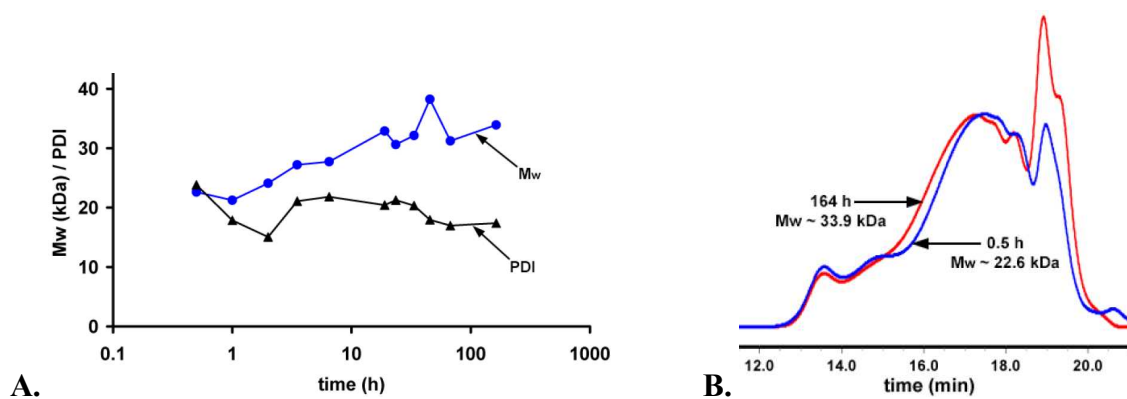


Figure 4.4. Molecular weight and PDI timeline of **3** at 0.5 mol % of **1**.

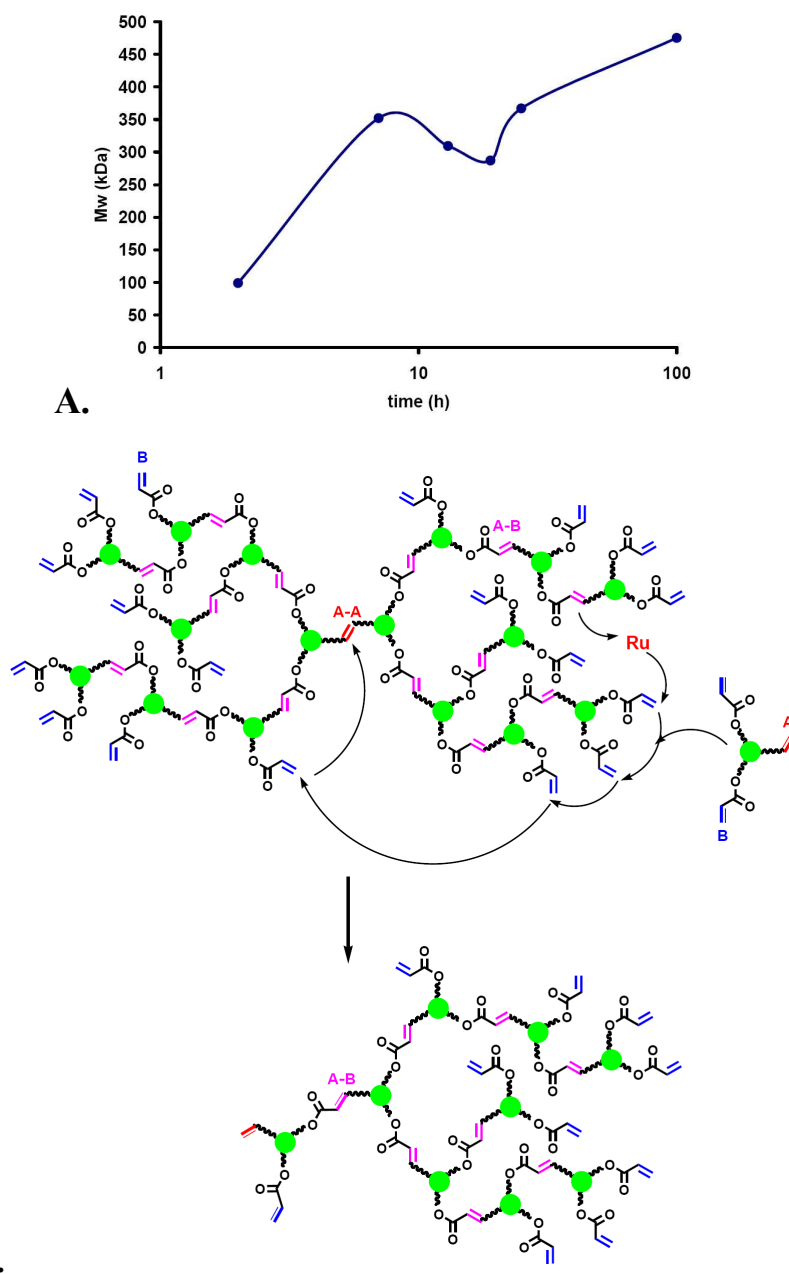


Figure 4.5. Proposed polymerization "error" correction mechanism.

Figure 4.6 illustrates additional experiments, which relate molecular weight to both reaction time and end-capping; here, a polymerization is quenched at different times by addition of 8-bromo-1-octene. As evident from the presented SEC traces, the addition of 1 equivalent of bromooctene (relative to the monomer) efficiently stops the molecular weight build-up. Specifically, when the polymerization of **2** with 0.5 mol % of **1** was allowed to

proceed for 72 hours without the addition of bromooctene, the molecular weight of **3** reached 7.1 kDa (red trace). However, addition of end-caps at 12 hours (green trace) or 24 hours (blue trace) reduced this value (still measured at 72h) to only 3.3 kDa and 4.2 kDa, respectively. One of the important implications of these quenching experiments is that the one-pot synthesis and functionalization of **3** might be possible, if the end-capping reagent also carries an analyte.

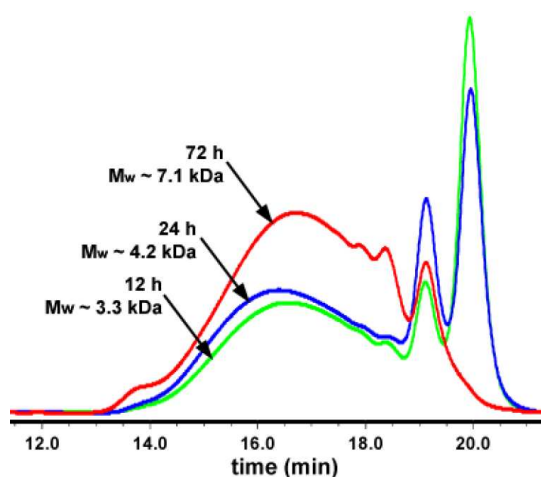


Figure 4.6. The dependence of the observed M_w at 0.5 mol % of **1** on the addition time of 8-bromo-1-octene.

Addition of a Multifunctional Core. Finally, the effect of a B_4 core (**4**) on the molecular weight and PDI of **3** was investigated. Figure 4.7 illustrates the outcome of the introduction of different amounts of **4** to the polymerization of **2** with 0.5 mol % (Figure A) and 0.2 mol % (Figure B) of **1**. According to Figure 4.6A, polymerization with a larger amount of catalyst appears to be influenced by the core molecules as expected, and increasing the amount of **4** lowers the molecular weight of **3**, while slightly improving its PDI.¹¹⁻¹⁵ In essence, **4** acts as a multifunctional growth terminator unit, which quenches the polymerization when present at high concentrations (low monomer to core ratio).¹⁵

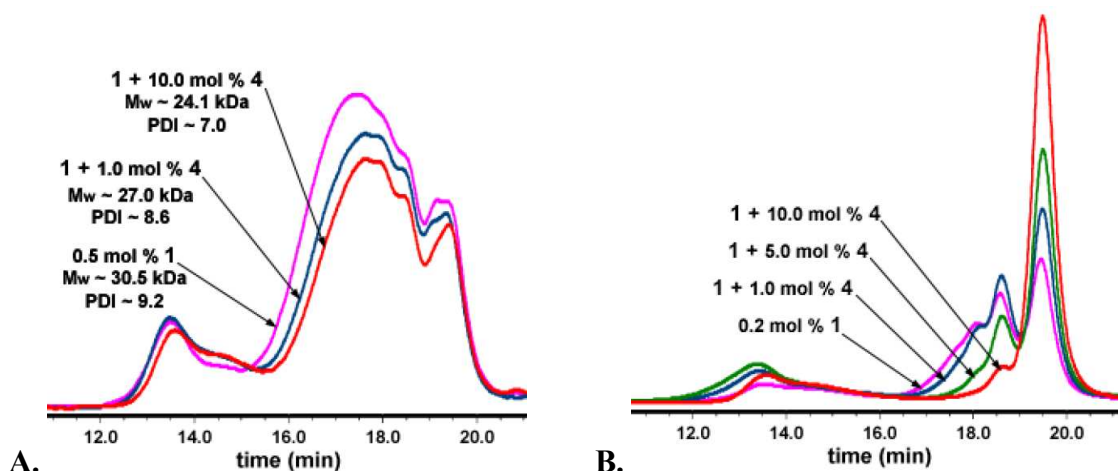


Figure 4.7. SEC (RI) traces for **3** made with a fixed amount of **1** (0.5 mol % in Figure A and 0.2 mol % in Figure B) but different amounts of **4**: none (pink), 1.0 mol % (blue), 5.0 mol % (green), and 10.0 mol % (red).

The situation is quite different for polymerization with smaller amounts of **1** (Figure 4.7B); the SEC traces for these samples have a bi-modal distribution of molecular weights. The addition of increasing amounts of **4** (pink to blue to green traces) results in 1) an increased molecular weight for the left-hand, already high molecular weight peaks (they shift further to the left), and 2) the simultaneous narrowing of the right-hand, oligomeric peak. At very high concentration of **4** (10 mol %, red trace) this relationship breaks down (left side of the trace), with smaller polymers produced in the polymerization.

We believe that the observed effect of the B₄ core on the ADMET polymerization of AB₂ **2** further confirms the catalyst “branch-hopping” hypothesis, especially at low catalyst concentrations. In line with this hypothesis, it appears that the multifunctional core molecules serve as catalyst sponges, and, consequently, chain-growth initiators (Scheme 4.3). At low concentrations of **1**, and at concurrent high concentrations of **4** in the polymerization solution, the catalyst capture is very efficient, and the oligomer build-up is restricted. Fewer oligomers results in a larger pool of monomers for chain growth addition to the periphery of the hyperbranched macromolecule and larger polymers are produced. An excess of B₄ quenches the polymerization entirely and produces much smaller chains, but, still, almost no oligomers (red trace in Figure 4.6B). However, at higher catalyst

loadings, some catalyst can escape trapping and promote the competing step-processes of oligomer formation.

Conclusion

The utility of hyperbranched polymers can be greatly expanded by controlling molecular weight and polydispersity during their production. To accomplish this goal, the factors implicated in influencing the molecular weight and PDI of the ruthenium catalyzed hyperbranched ADMET polymerization were investigated. It appears that at low catalyst loading the polymerization follows pseudo-chain-growth kinetics, rather than the step-growth kinetics expected for polyadditions of AB_n monomers. Moreover, the synthesis of these polymers can be controlled by the catalyst loading, the use of multifunctional cores, and, to some extent, the reaction time. This polymerization behavior seems to stem from the hyperbranched architecture of the growing chains, and a mechanism, which relies on high local concentration of the multiple end groups associated with such an architecture, is proposed. An important implication of the purported mechanism is that the chains obtained from lower catalyst loadings might be more uniform and dendrimer-like. Although the studies described in this report were conducted specifically for ADMET, the findings may prove general to transition metal catalyzed hyperbranched polymerization methods.

Experimental Procedures

Materials. All reagents, except for catalyst **1**, were purchased from Aldrich at the highest available purity and used without further purification. Catalyst **1** was obtained from Materia, Inc. The synthetic procedures with full characterization for **2** and **5**, along with the procedures for their polymerization with **1** (to **3** and **6** respectively), have all been previously reported.¹⁶ When working with hyperbranched polymers of higher molecular weight, it is highly advisable to use the properly silylated glass or plastic tare, to prevent any acid-catalyzed crosslinking of the multiple acrylate groups present on the periphery of the chains.

Instrumentation. NMR spectra were obtained using a Varian Mercury-300 spectrometer; samples were dissolved in CD₂Cl₂.

Size exclusion chromatography (SEC) analysis was performed using a Wyatt triple detector system equipped with a triple angle light scattering (miniDAWN TREOS, with a laser wavelength of 658 nm) detector, a viscometer (ViscoStar) detector, and a refractive index (Optilab rEX) detector—all operating at 25 °C. Viscotek ViscoGEL I-Series (one mixed bed medium MW and one mixed bed high MW) columns were used for SEC with THF as the eluent and a Shimadzu LC-10AD pump operating at 1.0 mL/minute.

Synthesis of B4 core (4). Clear, yellowish oil **4** was made from a well-dried pentaerythritol according to the general procedure previously outlined for **2**.¹⁶ ¹H NMR (300MHz, CD₂Cl₂, ppm): δ 6.38 (dd, J = 17.1 Hz, J = 1.5 Hz, 4H), 6.12 (dd, J = 17.4 Hz, J = 10.5 Hz, 4H), 5.86 (dd, J = 10.2 Hz, J = 1.2 Hz, 4H), 4.28 (s, 8H). ¹³C NMR (300MHz, CD₂Cl₂, ppm): δ 165.97, 131.83, 128.31, 63.18, 42.73. HRMS(FAB+) m/z: 353.1247 [M+H].

References

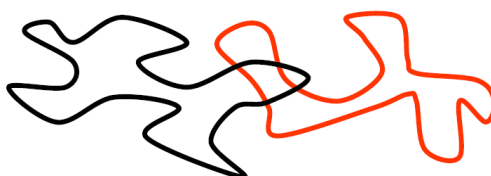
- (1) Voit, B. *J. Polym. Sci., Part A: Polym. Chem.* **2005**, *43*, 2679-2699.
- (2) Yates, C. R.; Hayes, W. *Eur. Polym. J.* **2004**, 1257-1281.
- (3) Voit, B. *C. R. Chimie* **2003**, *6*, 821-832.
- (4) Voit, B. *J. Polym. Sci., Part A: Polym. Chem.* **2000**, *38*, 2505-2525.
- (5) Hult, A.; Johansson, M.; Malmström, E. *Adv. Polym. Sci.* **1999**, *143*, 1-34.
- (6) Kim, Y. H. *J. Polym. Sci., Part A: Polym. Chem.* **1998**, *36*, 1685-1698.
- (7) Wooley, K. L.; Hawker, C. J.; Lee, R.; Fréchet, J. M. J. *Polymer J.* **1994**, *26*, 187-197.
- (8) Sunder, A.; Heinemann, J.; Frey, H. *Chem. Eur. J.* **2000**, *6*, 2499-2506.
- (9) Kim, Y. H.; Webster, O. W. *Macromolecules* **1992**, *25*, 5561-5572.
- (10) Lach, C.; Müller, P.; Frey, H.; Mülhaupt, R. *Macromol. Rapid Commun.* **1997**, *18*, 253-260.
- (11) Bernal, D. P.; Bedrossian, L.; Collins, K.; Fossum, E. *Macromolecules* **2003**, *36*, 333-338.
- (12) Malmström, E.; Hult, A. *Macromolecules* **1996**, *29*, 1222-1228.
- (13) Malmström, E.; Johansson, M.; Hult, A. *Macromolecules* **1995**, *28*, 1698-1703.
- (14) Kricheldorf, H. R.; Stoeber, O.; Luebbers, D. *Macromolecules* **1995**, *28*, 2118-2123.
- (15) Feast, W. J.; Stainton, N. M. *J. Mater. Chem.* **1995**, *5*, 405-411.
- (16) Gorodetskaya, I. A.; Choi, T. L.; Grubbs, R. H. *J. Am. Chem. Soc.* **2007**, *129*, 12672-12673.

CHAPTER 5

The Importance of Molecular Weight Control for Cyclic Polymers Prepared via Ring Expansion Metathesis Polymerization

Abstract

This chapter describes the synthesis of cyclic and linear polyethylenes of various molecular weights, and the study of their physical properties. Molecular weight control of ring-opening and ring-insertion metathesis polymerizations is also discussed. In addition, two potentially more stable and active, new generation ruthenium catalysts, which might provide better molecular weight control of cyclic polymerization, are presented; and advances in their synthesis are reported.



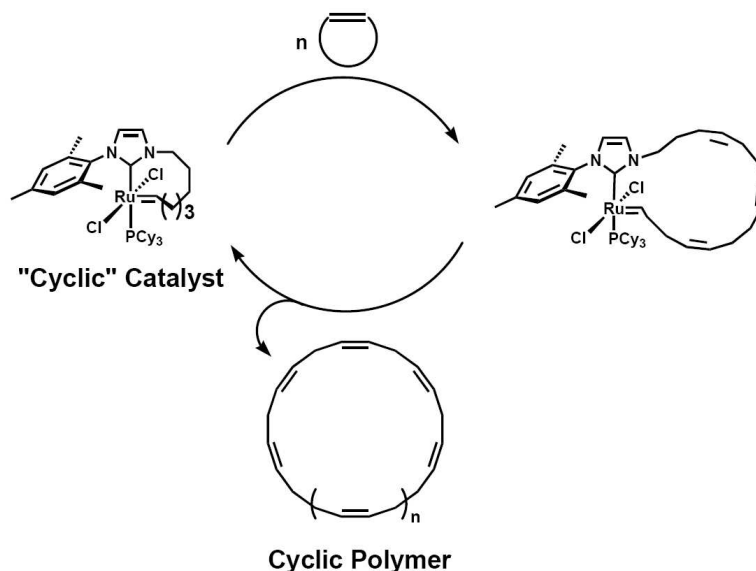
Introduction

Many of the important physical properties of a polymeric material, such as mechanical strength and viscosity, are the result of long-chain entanglements.¹ The end groups of a polymer chain are instrumental in this distinctively polymeric behavior, and, therefore, can have a considerable effect on the characteristics of the material. Consequently, a cyclic architecture, which lacks end groups entirely, may expand the scope of applications of well-established linear materials such as polyethylene or polyesters. Moreover, it has already been demonstrated that due to their different topology, ring polymers (of different chemical compositions) are less viscous, exhibit higher glass transition temperatures, and have smaller hydrodynamic volumes than their linear analogs.² However, this data is still too scarce for generalized predictions, due to 1) the limited availability of cyclic backbones,³⁻⁶ especially when compared to the current pool of linear polymers, and 2) the lack of efficient synthetic methods towards the clean (free of linear contaminants) production of cyclic polymers.⁷⁻¹⁰

A novel route to cyclic polymerization via ring-expansion olefin metathesis (REMP) with a “cyclic” catalyst (Scheme 5.1) has recently been developed by our group.¹¹ The method is similar to the ring-opening polymerization (ROMP) of strained cyclic alkenes, but it requires a specially designed, end-less, olefin metathesis catalyst. This direct polymerization route avoids the use of linear precursors, which are often employed in the construction of large rings,⁷⁻¹⁰ and, therefore, can provide access to multi-gram amounts of well-defined, pure cyclic polymers, whose physical properties can be extensively investigated.¹¹ In addition, the experimental data obtained from the study of a cyclic architecture, relative to a linear analogs, can facilitate a deeper understanding of macromolecular behavior and polymer properties in general.^{2,12} However, any exhaustive polymer structure-property relationship consideration necessitates access to a wide range of chain sizes with a low polydispersity index (PDI), which, in turn, requires good molecular weight control of the polymerization reaction of interest. However, molecular weight control of “end-less” REMP is an ongoing challenge. This chapter highlights two different rheological studies towards a better understanding of the physical properties of cyclic

polymers. Furthermore, the challenges associated with the synthesis of very large and very small polymers via REMP are also discussed.

Scheme 5.1. Ring-expansion polymerization.¹¹



Results and Discussion

Part 1: Studies of shear-induced crystallization processes in polyethylene and the need for large cyclic polymers.

Properties of semicrystalline polymeric materials, such as polyethylene (PE) and polypropylene (PP), are strongly dependent on processing conditions.¹³ For example, the shearing stresses experienced by molten polymers during extrusion and molding affect the spatial arrangement and alignment of crystallites in the final product, defining its morphology and, consequently, its physical characteristics. Therefore, properties such as strength, permeability, and transparency can be tuned by altering the processing conditions.

The Kornfield group at Caltech has studied the effect of flow shearing stresses on the nucleation and crystallization in semicrystalline polymers. Furthermore, the group has designed and built an instrument that can impose high wall shear stresses for a controlled length of time at specified temperatures; the apparatus allows for shear-mediated crystallization studies to be performed with unusually small amounts of material (5g per loading/~0.5g per experiment).¹⁴ This methodology was used to demonstrate that

incorporation of a small amount of long chains into a resin of much shorter chains of linear isotactic polypropylene (iPP) greatly enhances the orientation in the sample's outer layer/skin (where the effect of shear stresses is greatest during flow).¹⁵ Presumably, this morphology is the result of the shear stresses forcing the long chains to stretch into the threadlike precursors to crystallites, thereby orienting the short chains which cling to them (Figure 5.1b). Furthermore, this effect is not observed in systems where the molecular weight distribution is mono-modal. Moreover, the phenomena was shown to be cooperative, rather than single chain, and it has been attributed to the overlap of the long chains stretching under a shear force.¹⁵

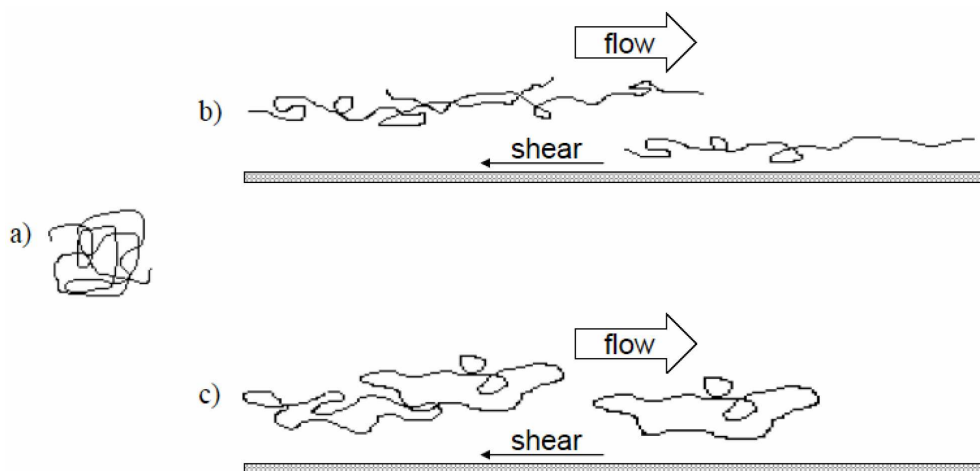


Figure 5.1. The effect of shear stress on polymer chain orientation. a) A relaxed polymer chain, b) linear chains under shear stress, c) cyclic chains under shear stress.

In light of these findings, it would be very instructive to examine the behavior of cyclic polymers under shear stress conditions. Of particular interest is the effect that large cyclic chains might have on the flow-induced crystallization of a host of short linear chains. As a result of its unique topology, each cyclic chain is expected to provide a shorter and thicker crystallization precursor, compared to a linear chain of the same size (Figure 5.1). Consequently, a large single ring might be able to act as two overlapped long linear chains, enhancing the crystallite growth and orientation in a sample to a greater extent than a linear chain.

In order to probe the effect of cyclic polymers on the flow induced morphology of PE, blends with varying fractions of large cyclic and long linear chains must be prepared in

a host of short linear polymers. Unlike industrial PE, which is traditionally prepared via Ziegler-Natta polymerization, polymers prepared via ROMP of plain, cyclic alkenes have absolutely no branches from the main chain and a much lower PDI. Consequently, since branching and polydispersity determine material's physical properties, the wealth of available information on the properties of industrial PE cannot be taken for granted in the investigation of PE architectures obtained via olefin metathesis. Therefore, all of the polyethylenes used for the studies—large, small, linear and cyclic—have to be prepared via olefin metathesis for a fair comparison of the two topologies.

The molecular weights required for flow-induced crystallization experiments were found to be 60–75 kDa for the short chain matrix and > 400 kDa for the long blend additives (as determined in a series of preliminary experiments with short linear PE chains of 21 kDa and 66 kDa). Molecular weight control of ROMP of strained cyclooctenes with ruthenium-based catalysts **1** and **2** (Figure 5.2) is well established, so the desired medium to large sized linear chains can be effortlessly obtained through the use of the appropriate catalyst loading. In fact, subjecting cyclooctene to **1** in 3630 monomer to catalyst ratio, successfully produced corresponding polyalkenamers with $M_w \sim 450$ kDa (slightly larger than the calculated 400 kDa) (Scheme 5.2A). However, the smaller polycyclooctenes (with $M_w < 100$ kDa) can be synthesized more efficiently with the aid of a chain transfer agent (CTA) and a more active catalyst **2**. Therefore, this method was used to make a short chain matrix material with $M_w \sim 58$ kDa (Scheme 5.2B). The molecular weights of all of the final polyethylene products (Scheme 5.2) were assumed to remain very close to those of the corresponding polyalkenamers; they could not be measured directly in our laboratory due to the low solubility of PE in common Size-Exclusion Chromatography (SEC) solvents at room temperature.

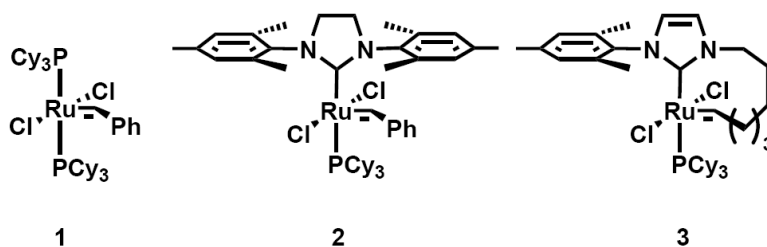
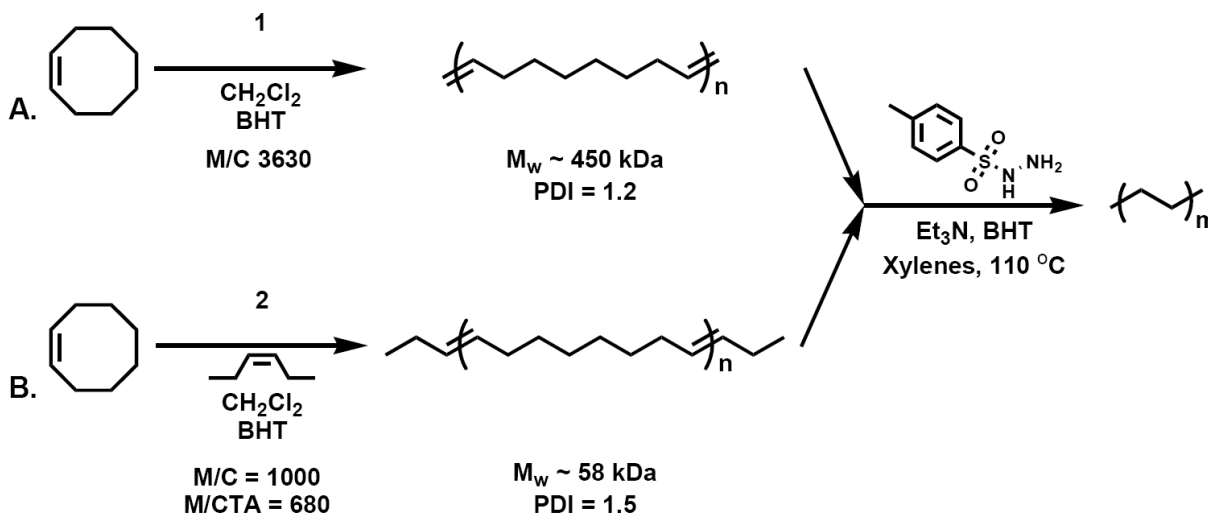


Figure 5.2. Catalysts required for the preparation of linear and cyclic polyalkenamers.

Scheme 5.2. Synthesis of long (A) and short (B) linear PE chains.



Molecular weight control of REMP with **3** is less straightforward than molecular weight control of ROMP with **1** and **2**. At the time of this study, the activity of the “cyclic” catalyst **3** was not yet well understood, and the synthesis of a polymer with the desired molecular weight of ~ 400 kDa required an additional polymerization conditions survey. Furthermore, since “cyclic” polymerization cannot rely on chain ends for size control, factors other than amount of the catalyst and use of CTA were considered; initial monomer concentration was one known factor.¹⁶ In addition, since our final synthetic goal was plain, fully reduced polyethylene, we chose to investigate the effect of the ring strain of various cyclic alkenes on the final molecular weight of the REMP products.

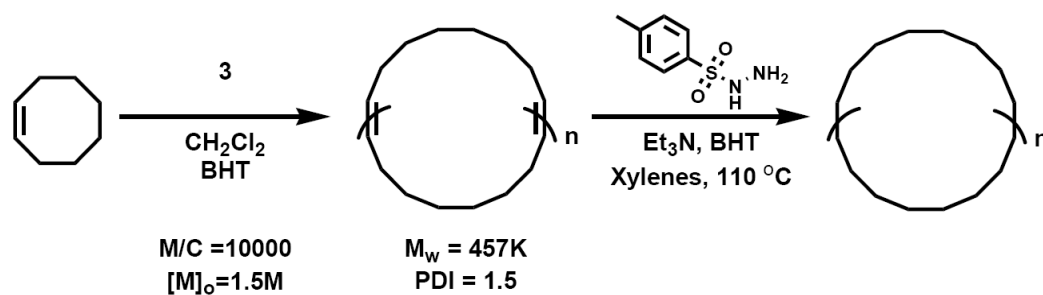
Table 5.1 summarizes the results of the study in which four cyclic alkenes with different ring strains were polymerized from a range of initial monomer concentrations and constant amount of **3**. It is immediately evident from this table that the more strained rings produce polymers of higher molecular weights in better yields. Furthermore, the data appears to confirm that the initial monomer concentration has a considerable effect on the molecular weight of the polymerization products. For example, polymerization does not occur in very dilute solutions ($[M]_0 = 0.1 \text{ M}$) of any of the considered monomers. On the other hand, the reaction of neat, strained cycloheptene and cyclooctene produces poorly soluble gels, which contain chains of very high molecular weight. Although the neat

polymerization of the less strained cycloheptene gels to a lesser extent than the neat polymerization of cyclooctene, and allows some material recovery, the obtained polymers have a smaller than expected size. The lower molecular weights of the products isolated from these gels are probably artifacts from inefficient stirring due to the high reaction viscosities of neat polymerizations. The exposure of cyclopentene to **3** produced only short oligomers in poor yields even at the highest monomer concentration, due to a lack of sufficient ring strain for ROMP ring strain. Based on this survey, the desired cyclic polymer with a molecular weight (M_w) of 457 kDa was successfully prepared from cyclooctene at a 1.5 M concentration (Scheme 5.3).

Table 5.1. Results (M_w / yield) for REMP of cyclic alkenes with **3**. Polymerization conditions: M/C = 2500 was used as a catalyst loading, and the reaction was conducted at 45 °C for 6 h. NP—no polymerization observed.

M/C = 2500		Monomer ring size (as # of carbons)		
		5	7	8
[M] ₀	Neat	2.2 kDa / 30 % (11.3 M)	Gel + 213 kDa (8.7 M)	Gel (7.7 M)
	5 M	1 kDa / 5 %	231 kDa / 60 %	Gel
	2.5 M	NP	90 kDa / 40 %	677 kDa / quant.
	1 M		NP	350 kDa / quant.
	0.5 M			75 kDa / 80 %
	0.1 M			NP

Scheme 5.3. Synthesis of large PE rings.



Initial investigation with all linear olefin metathesis-derived blend components (5% by weight of 450 kDa chains in a matrix of 58 kDa) confirmed the appropriateness of the selected molecular weights for the studies of PE samples. This study also provides guidance for future experimental conditions (temperature, shear stress, time). As can be seen from Figure 5.3, polarized optical microscopy confirms that a higher shear pressure (Figure 5.3a vs. 5.3b) and longer shearing times (Figure 5.3c vs. Figure 5.3d) result in greater alignment in the PE sample's skin. Moreover, these micrographs appear to suggest that the long chains do enhance the skin's orientation even at the low doping of 5% concentration (Figure 5.3b vs. 5.3c). Experiments with higher concentrations of long chain and with cyclic polymers are currently underway.

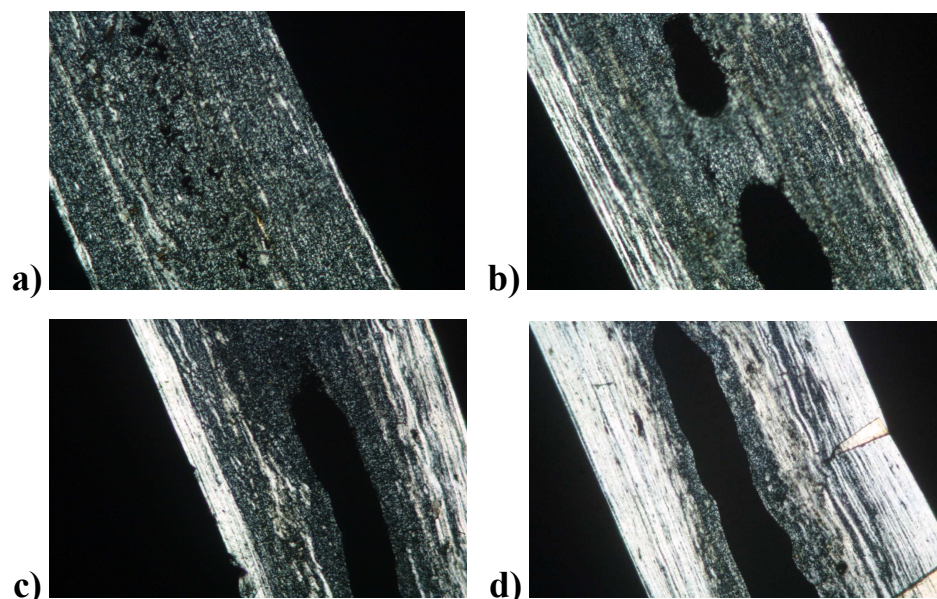


Figure 5.3. Polarized optical microscopy of selected samples. All blends are 5 % long ($M_w \sim 450$ kDa) linear chains in a matrix (~ 58 kDa) linear chains. Long white threads indicate chain alignment. a) Matrix only, 124 °C, 40 psi, 3 s; b) matrix only, 126 °C, 80 psi, 2 s; c) blend, 126 °C, 80 psi, 2 s; d) blend, 126 °C, 80 psi, 4s.

Part 2: Studies of the viscoelastic properties of cyclic polyethylene and the need for small cyclic polymers.

The reptation^{1,17} or tube¹² theory was first proposed by de Gennes in 1971 in an attempt to explain the effects of entanglement between long chains on the dynamical

properties of polymer melts. This powerful model suggests that each chain in the high molecular weight polymer melt is confined to a topological tube, which is defined by the polymers around it. Moreover, since the chain in question is not allowed to cross any of the boundaries of this three-dimensional, network-imposed constrain, it can only reptate along the tube in a snake-like movement, as one chain end follows another. The reptation model greatly simplifies melt rheology considerations, and offers a very good prediction for chain relaxation times and molecular size dependence of zero-shear viscosity ($\eta_0 \sim M^3$ vs. the experimentally derived $\eta_0 \sim M^{3.4}$) for polymeric materials consisting of chains capable of entanglement.

Rheological studies of cyclic polymers, which cannot reptate in the conventional sense, due to a lack of ends, should greatly improve the current understanding of the fundamentals of polymer chain dynamics. Although some experimental data on the melt behavior of macromolecular rings has been collected to date, it is limited to polymers 1) of very few chemical compositions such as poly(dimethylsiloxanes),^{2,18,19} polystyrene,^{20,21} and polybutadiene²², and 2) of limited sizes (usually on the smaller side), and 3) of, sometimes, questionable purity²³ (due to synthetic routes which involve linear precursors). Nevertheless, the existing data suggests that the cyclic polymers have lower zero-shear rate viscosities relative to corresponding linear analogs. However, the relevance of the η_0 - M_w relationship remains under debate, although the rings are believed to be less capable of entanglements due to the lack of chain ends.

The linear viscoelastic properties of cyclic polyethylene prepared by REMP with **3** were investigated in collaboration with the McKenna group at Texas Tech University (Figure 5.4a). Contrary to any previous reports on cyclic polymers, the cyclic PE in the molecular weight range from 85 to 380 kDa (which are all well above the critical PE chain entanglement sizes), appeared to be more viscous than the linear analogs (red dots in Figure 5.4a). To explain the observed phenomena, we hypothesized that, any possibility of linear contaminants aside, the rings tested were large enough to entangle much more than their linear analogs due to the “loop-loop interpenetration” effect implied by a lattice-tree model (Figure 5.4b).²⁴ Furthermore, smaller rings with sizes below some yet unknown critical molecular weight should have reduced “loop interpenetration” capabilities and entangle

less than large cyclic polymer or corresponding linear chains, much like previously reported small cyclics. To test this theory (red line in Figure 5.4a), cyclic polymers covering range of molecular weights below 85 kDa need to be studied.

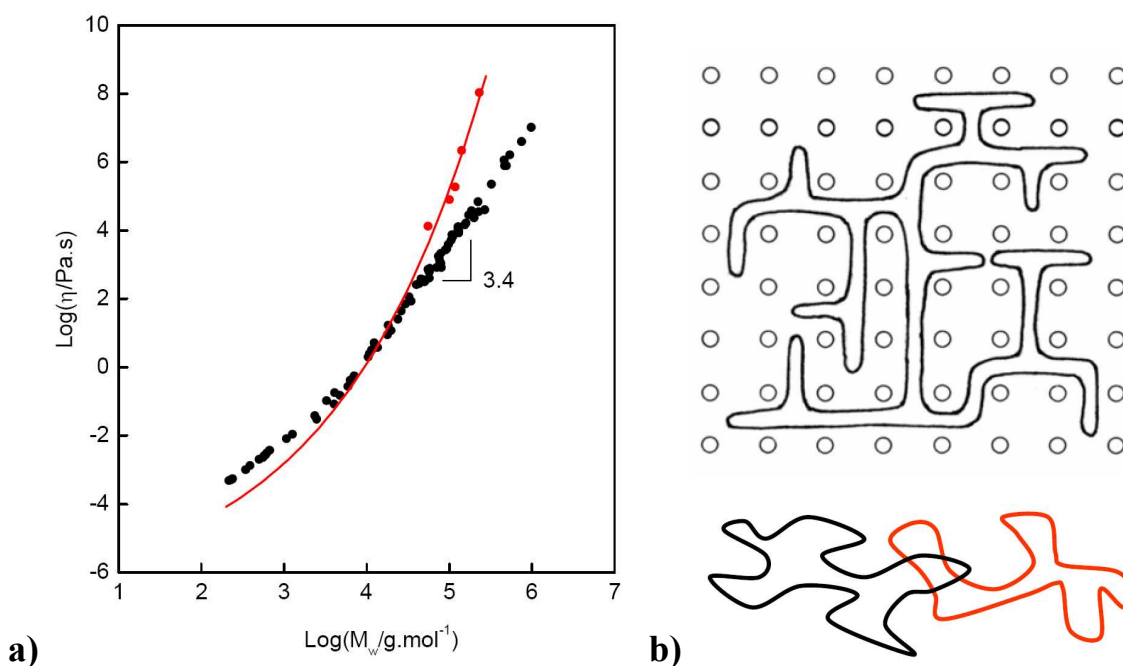


Figure 5.4. The results of the viscoelastic properties investigation of cyclic PE prepared by REMP. a) Plot of zero-shear-rate viscosity vs M_w (at 154 °C). Red dots represent experimental data for cyclic polymers, while red line represents the predicted $\eta_0 \sim M$ dependence; black dots represent the data for a metallocene polymerization derived linear PE reported elsewhere.²⁵ b) Lattice-tree animation theory.²⁴ Open circles represent the polymeric network/obstacles.

Although initial monomer concentration allows for reasonable control of REMP with **3** in the synthesis of large cyclic chains, this method of molecular weight control is very inefficient for the production of polymers smaller than 80-100 kDa. However, some of our studies of the polymerization behavior of **3** indicate initial rapid molecular weight build-up, followed by a slow decrease over the course of reaction (presumably due to the catalyst's re-insertion activity of the catalyst). Therefore, a second generation cyclic catalyst, which is more stable, long-living, and efficient than **3**, might be instrumental in the

synthesis of smaller rings (among other advantages).²⁶ Catalysts **4** and **5** (Figure 5.5) might satisfy these criteria.

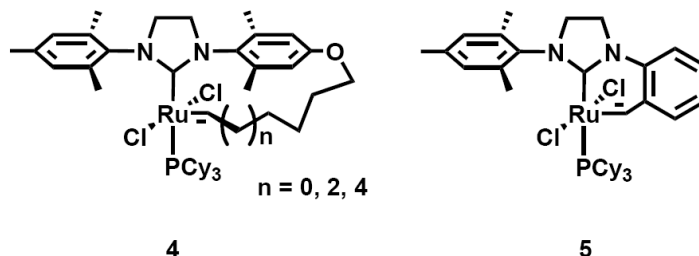
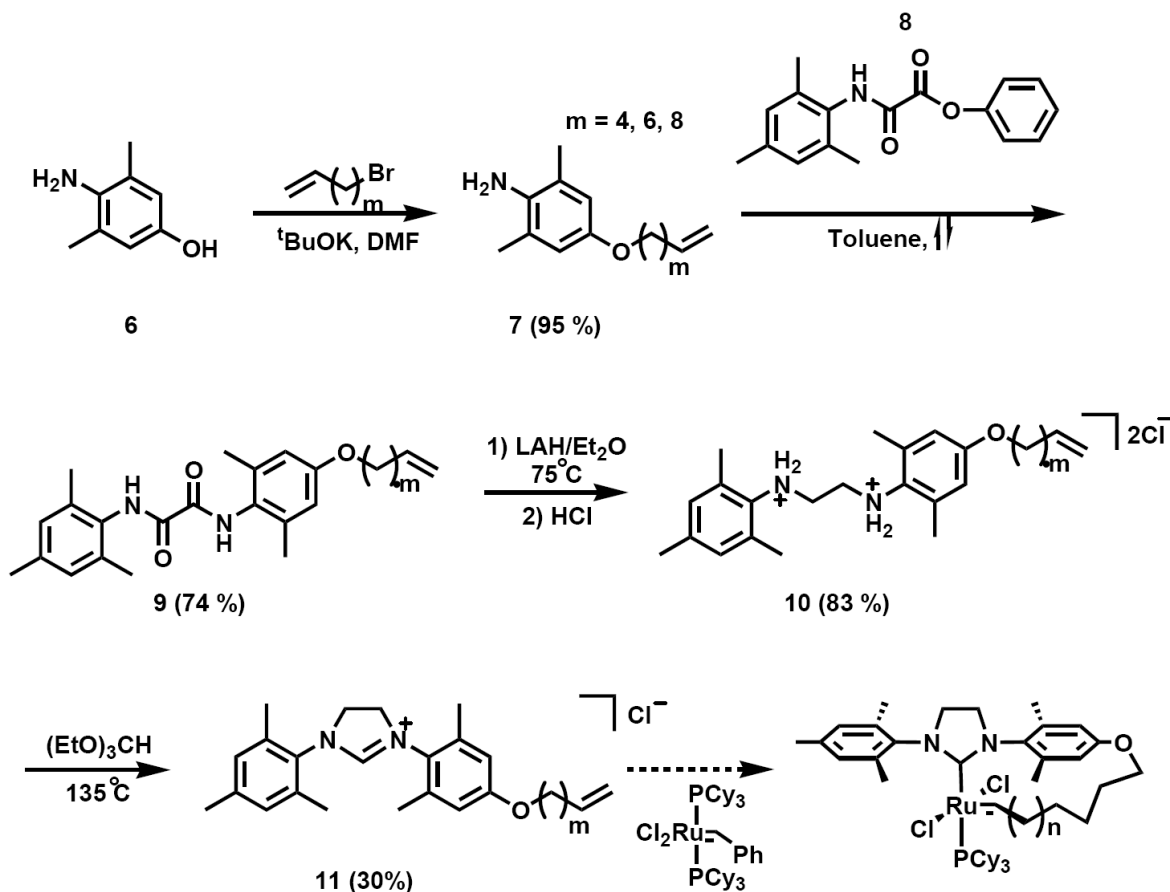


Figure 5.5. Proposed 2nd generation REMP catalysts.

Both catalysts **4** and **5** (Figure 5.5) boast a fully saturated imidazolyl ring and an aryl-fortified Ru-to-N tether. The saturation of the NHC-backbone should enhance the catalyst's activity,^{27,28} while the inserted dimethyl phenol should improve its stability, by preventing decomposition via C-H insertion by the ruthenium into the alkyl tether. In addition, **5** is a benzylidene, rather than an alkylidene-type catalyst, and, thus, might prove to be even more stable.²⁹ Although, there has been a report indicating that a phosphine-free, iso-propyloxy variant of **5**, is too stable to be metathesis active,³⁰ **5** might strike an appropriate balance between activity and stability.

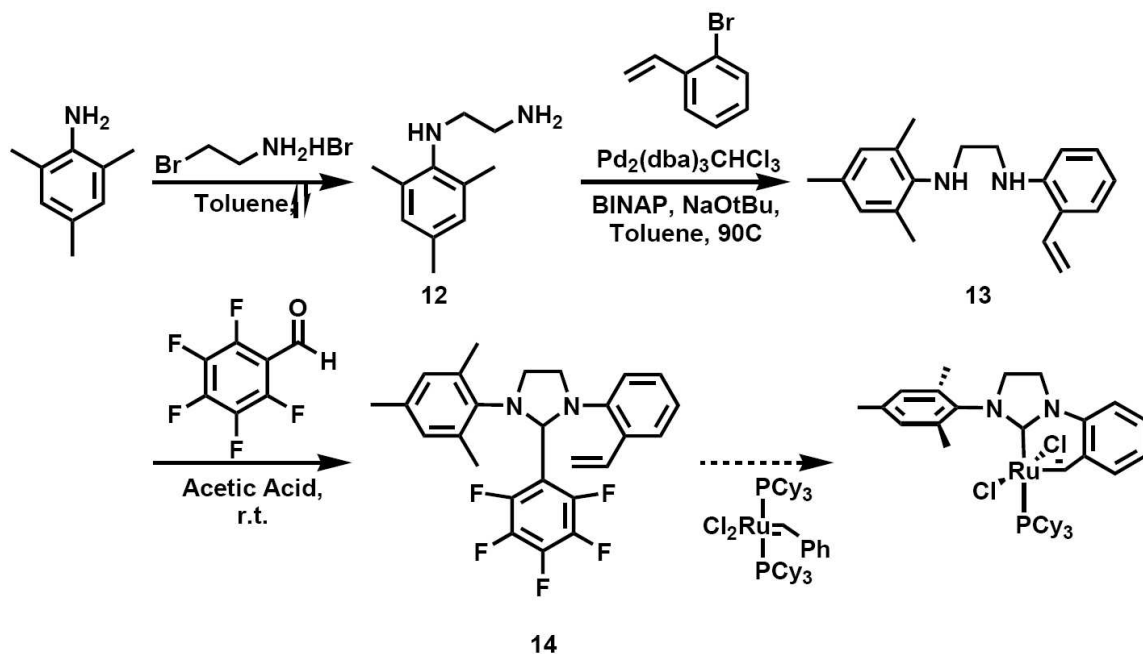
A synthetic route towards **4** is outlined in Scheme 5.4. Since the influence of the aryl moiety on the alkyl tether flexibility is unclear, three ligands with different linker lengths were prepared. Cyclic catalyst assembly usually proceeds via phosphine ligand exchange on **1**, followed by the intramolecular metathesis cyclization of the tether.^{26,31} However, despite evidence for a successful ligand exchange in some cases, no ring-closed species **4** could be obtained from any conditions or linker lengths tested.

Scheme 5.4. Synthetic route towards 2nd generation REMP catalyst **4**.



The synthetic route towards **5** is outlined in Scheme 5.5. Initially, an imidazolium salt, similar to **11** (Scheme 5.4), was attempted, but the cyclization reaction with triethyl orthoformate produced only brightly fluorescent oligomeric materials. Next, a pentafluorobenzaldehyde adduct **14**, which could be used to cleanly generate a carbene under very mild conditions^{32,33} was tested. Unfortunately, it appears that at the elevated temperature required for carbene generation from **14**, hydrolytic de-cyclization to **13** competes with carbene formation and prevents the efficient synthesis of **5**. However, a variety of reaction conditions are currently being tested and this route remains promising for the synthesis of **5**.

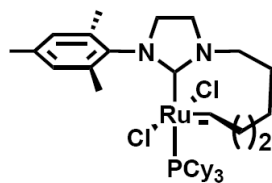
Scheme 5.5. Synthetic route towards 2nd generation REMP catalyst **5**.



Conclusion

REMP of strained cyclic alkenes can provide multi-gram quantities of well-defined, cyclic polymers containing a wide variety of backbones. These can then be utilized to probe issues which are fundamental to polymer science. Furthermore, the rheological properties of cyclic polyethylene produced by this method are already being tested by a number of research groups and initial results indicate interesting behavior. Nevertheless, to fully realize the potential of this architecture for such investigations, polymer samples in a wide range of sizes and with a narrow PDIs are required. However, molecular weight control of REMP is difficult since there are no chain ends in the polymerization to rely upon. Although chains of larger sizes can be controllably produced by empirical variations in the reaction conditions, these methods fail to yield polymers much smaller than ~ 85 kDa. A number of 2nd generation REMP catalysts, which are expected to be more stable and active thereby affording small polymers, are currently being developed. Moreover, the recently reported complex **6** (Figure 5.6), which features a saturated NHC backbone and shortened tether, is promising and exhibits much improved stability and activity.²⁶ Taken

together, these data and observations underscore the potential of olefin metathesis for preparation of cyclic polymers with excellent molecular weight control.



6

Figure 5.6. First accomplished 2nd generation REMP catalyst.²⁶

Polymerization Experimental Procedures

Materials. All reagents, except for *cis*-3-hexene, were purchased from Aldrich at the highest available purity grade and used without further purification, unless otherwise noted. *Cis*-3-hexene was purchased from Fluka. CH₂Cl₂ was purified by passage through a solvent column and degassed with argon prior to use.

Instrumentation. NMR spectra were obtained using a Varian Mercury-300 spectrometer; samples were dissolved in CD₂Cl₂.

Size exclusion chromatography (SEC) analysis was performed using a Viscotek triple detector system (model 270), equipped with a right angle laser light scattering (RALLS) detector, a differential viscosity detector, and a refractive index (RI) detector—all operating at 25°C. American Polymer Standards AM-GEL linear columns were used for SEC with CH₂Cl₂ as the eluent and a Shimadzu LC-10AD pump operating at 1 mL/minute.

Synthesis of High Molecular Weight Linear Polyoctenamer. A 100 mL disposable vial was charged with dry, degassed *cis*-cyclooctene (5.0 g, 45.5 mmol), dry, degassed CH₂Cl₂ (35 mL), 2,6-di-*tert*-butyl-4-methoxyphenol (BHT analog) (0.53 g, 2.27 mmol), and catalyst **1** (10.3 mg, 13.0 μmol, M/C = 3630). The mixture was heated to 45°C under argon atmosphere with stirring. The solution became very viscous within 15 min of heating, so 12 mL of CH₂Cl₂ was added to ensure efficient stirring and polymerization followed by an additional 12 mL of CH₂Cl₂ after another 30 min. After 12 h, the reaction solution was cooled to room temperature and poured over acetone. A white precipitate was collected on a Büchner funnel and washed with acetone. The product was redissolved in hot THF, precipitated from acetone, filtered, and dried under vacuum to produce 4.0 g (80% yield) of a white polymer. SEC: M_w = 450 Kg/mol, PDI = 1.2.

Synthesis of Low Molecular Weight Linear Polyoctenamer—Chain Transfer Agent (CTA) Mediated Polymerization. *cis*-Cyclooctene (50.0 g, 0.45 mol) was degassed with argon and combined with dry CH₂Cl₂ (650 mL), 2,6-di-*tert*-butyl-4-methoxyphenol (5.3 g, 22.5 mmol), 3-*cis*-hexene (56 mg, 0.67 mmol, M/CTA = 680) and catalyst **2** (0.38 g, 0.45 mmol, M/C = 1000). The solution was purged with argon for an additional 0.5 h and heated to 45 °C. After 12 h of stirring under a positive argon pressure,

the mixture was cooled to room temperature and poured over acetone. The white precipitate was collected on a Büchner funnel and thoroughly washed with acetone. The product was then re-dissolved in CH_2Cl_2 , precipitated from acetone, filtered, and dried under vacuum to give 39.0 g (75% yield) of a white polymer. SEC: $M_w = 58 \text{ Kg/mol}$, PDI = 1.56.

Synthesis of Cyclic Polyoctenamer. Cyclic polyoctenamer was prepared and isolated according to the same procedure as described for the High Molecular Weight Linear Polyoctenamer from degassed *cis*-cyclooctene (5.0 g, 45.0 mmol), dry CH_2Cl_2 (25 mL + 10 mL added during the polymerization), 2,6-di-*tert*-butyl-4-methoxyphenol (0.53 g, 2.27 mmol), and catalyst **3** (3.3 mg, 4.5 μmol , M/C = 10000). SEC: $M_w = 456 \text{ Kg/mol}$, PDI = 1.28.

Representative Hydrogenation Procedure (Matrix PE). Polyoctene (39.0 g, 0.35 mol of olefinic units), xylenes (1000 mL), and 2,6-di-*tert*-butyl-4-methoxyphenol (4.2 g, 17.7 mmol) were combined in a flask and purged with argon for 30 min, during which time the polymer partially dissolved. The solution was heated to 70 °C and vigorously stirred with argon purging for an additional 45 min, until all of the polymer completely dissolved. Tripropylamine (390 mL, 2.6 mol) and *p*-toluene-sulfonylhydrazide (260 g, 1.4 mol) were added to the reaction mixture and the flask was heated to 110 °C. After 6 h more *p*-toluene-sulfonylhydrazide (260 g, 1.4 mol) was added and the solution was stirred for more 12 h. The reaction vessel was cooled to room temperature, and the solution was poured over acetone. The resulting white precipitate was collected on a Büchner funnel, thoroughly washed with acetone, CH_2Cl_2 , and isopropanol; and then dried *en vacuo* to produce an off-white powder in quantitative yield. $^1\text{H NMR}$ (300MHz, toluene- d_8 , 100 °C, ppm): δ 1.33 (s).

References

- (1) Sperling, L. H. In *Introduction to Physical Polymer Science*; 2nd ed.; Wiley: New York, 1992, p 104-105.
- (2) *Cyclic Polymers*; 2nd ed.; Semlyen, J. A., Ed.; Kluwer Academic Publishers: Dordrecht, The Netherlands, 2000.
- (3) Kudo, H.; Sato, M.; Wakai, R.; Iwamoto, T.; Nishikubo, T. *Macromolecules* **2008**, *41*, 521-523.
- (4) Jeong, W.; Hedrick, J. L.; Waymouth, R. M. *J. Am. Chem. Soc.* **2007**, *129*, 8414-8415.
- (5) Kricheldorf, H. R.; Lee, S.-R.; Schittenhelm, N. *Macromol. Chem. Phys.* **1998**, *199*, 273-282.
- (6) Kricheldorf, H. R.; Eggerstedt, S. *Macromol. Chem. Phys.* **1998**, *199*, 283-290.
- (7) Tezuka, Y.; Komiya, R. *Macromolecules* **2002**, *35*, 8667-8669.
- (8) Oike, H.; Imaizumi, H.; Mouri, T.; Yoshioka, Y.; Uchibori, A.; Tezuka, Y. *J. Am. Chem. Soc.* **2000**, *122*, 9592-9599.
- (9) Roovers, J.; Toporowski, P. M. *Macromolecules* **1983**, *16*, 843-849.
- (10) Geiser, D.; Höcker, H. *Macromolecules* **1980**, *13*, 653-656.
- (11) Bielawski, C. W.; Benitez, D.; Grubbs, R. H. *Science* **2002**, *297*, 2041-2044.
- (12) McLeish, T. C. B. *Adv. Phys.* **2002**, *51*, 1379-1527.
- (13) Kornfield, J. A.; Kumaraswamy, G.; Issaian, A. M. *Ind. Eng. Chem. Res.* **2002**, *41*, 6383-6392.
- (14) Kumaraswamy, G.; Verma, R. K.; Kornfield, J. A. *Rev. Sci. Instrum.* **1999**, *70*, 2097-2104.
- (15) Seki, M.; Thurman, D. W.; Oberhauser, J. P.; Kornfield, J. A. *Macromolecules* **2002**, *35*, 2583-2594.
- (16) Bielawski, C. W.; Benitez, D.; Grubbs, R. H. *J. Am. Chem. Soc.* **2003**, *125*, 8424-8425.
- (17) de Gennes, P. G. *J. Chem. Phys.* **1971**, *55*, 572-579.
- (18) Orrah, D. J.; Semlyen, J. A.; Ross-Murphy, S. B. *Polymer* **1988**, *29*, 1452-1454.
- (19) Orrah, D. J.; Semlyen, J. A.; Ross-Murphy, S. B. *Polymer* **1988**, *29*, 1455-1458.

- (20) McKenna, G. B.; Hostetter, B. J.; Hadjichristidis, N.; Fetters, L. J.; Plazek, D. J. *Macromolecules* **1989**, *22*, 1834-1852.
- (21) Roovers, J. *Macromolecules* **1985**, *18*, 1359-1361.
- (22) Roovers, J. *Macromolecules* **1988**, *21*, 1517-1521.
- (23) Lee, H. C.; Lee, H.; Lee, W.; Chang, T.; Roovers, J. *Macromolecules* **2000**, *33*, 8119-8121.
- (24) Rubinstein, M. *Phys. Rev. Lett.* **1986**, *57*, 3023.
- (25) Aguilar, M.; Vega, J. F.; Sanz, E.; Martínez-Salazar, J. *Polymer* **2001**, *42*, 9713-9721.
- (26) Boydston, A. J.; Xia, Y.; Kornfield, J. A.; Gorodetskaya, I. A.; Grubbs, R. H. *J. Am. Chem. Soc.* **2008**, *130*, 12775-12782.
- (27) Sanford, M. S.; Love, J. A.; Grubbs, R. H. *J. Am. Chem. Soc.* **2001**, *123*, 6543-6554.
- (28) Bielawski, C. W.; Grubbs, R. H. *Angewandte Chemie International Edition* **2000**, *39*, 2903-2906.
- (29) Schwab, P.; Grubbs, R. H.; Ziller, J. W. *J. Am. Chem. Soc.* **1996**, *118*, 100-110.
- (30) Vehlow, K.; Gessler, S.; Blechert, S. *Angew. Chem. Int. Ed.* **2007**, *46*, 8082-8085.
- (31) Fürstner, A.; Ackermann, L.; Gabor, B.; Goddard, R.; Lehmann, C. W.; Mynott, R.; Stelzer, F.; Thiel, O. R. *Chem. Eur. J.* **2001**, *7*, 3236-3253.
- (32) Blum, A. P.; Ritter, T.; Grubbs, R. H. *Organometallics* **2007**, *26*, 2122-2124.
- (33) Nyce, G. W.; Csihony, S.; Waymouth, R. M.; Hedrick, J. L. *Chem. Eur. J.* **2004**, *10*, 4073-4079.

Appendix A
Towards AB_n-Based Hyperbranched Polyethylene

Facile access to different polymeric architectures of chemically well-established macromolecules can expand their applications. Moreover, comparative studies of polymers with the same chemical composition but different chain structure can contribute to a better understanding of polymer physics and aid in the design of new materials. In particular, the large volume, industrial polymers, such as polyethylene (PE) or polypropylene (PP), stand to benefit from structural changes since their simple aliphatic backbones do not allow other types of alterations. For example, the vast array of properties demonstrated by PE is based on the amount and extent of branching that is introduced into its main chains during the polymerization. However, the structure and functionality of this polyolefin are also very difficult to manipulate in a precise manner, because of PE's chemical simplicity and the lack of any kind of anchoring or repeat unit-defining functional groups.

Olefin metathesis is a reaction ideally suited for the construction of model polyolefins since it joins well-defined monomers via an alkene functionality, which can be “erased” at will by subsequent hydrogenation. In fact, ADMET has previously been used for precise branch placement in an ethylene/propylene copolymer model study.¹ Moreover, Chapter 5 of this thesis includes a discussion on the synthesis of previously unattainable cyclic PE via ring-expansion metathesis polymerization. However, to the best of our knowledge, hyperbranched PE with a well-defined AB_n unit has never been prepared via olefin metathesis or any other method.^{2,3,4}

Scheme A1 outlines a route to hyperbranched polyethylene via ADMET of a specially designed monomer **3**, followed by hydrogenation. The general method for this polymerization is based on the selectivity of catalyst A (Figure A1) towards different types of alkenes, which is described in Chapter 2 of this thesis. However, the AB_n monomer design described in Chapter 2 must be adjusted for the preparation of hyperbranched PE. To be able to reduce the polymerization product to the bare aliphatic backbone of polyethylene, ester linkages must be avoided. Therefore, the acrylate “B” functionalities have to be exchanged for vinyl ketones.

The desired monomer **3** was prepared in three simple steps from commercially available, inexpensive dimethyl glutaconate. However, its polymerization with **A** stalled, presumably due to the very slow rate of metathesis of the very electron-deficient vinyl

ketones. Nevertheless, according to ^1H NMR analysis, this polymerization proceeds to some extent when a more active and stable, phosphine free catalyst **B** is employed under dilute conditions (Figure A2).⁵ The optimization of polymerization conditions with **B** is currently underway and appears promising.

Scheme A1. Synthetic route towards the hyperbranched polyethylene via ADMET.

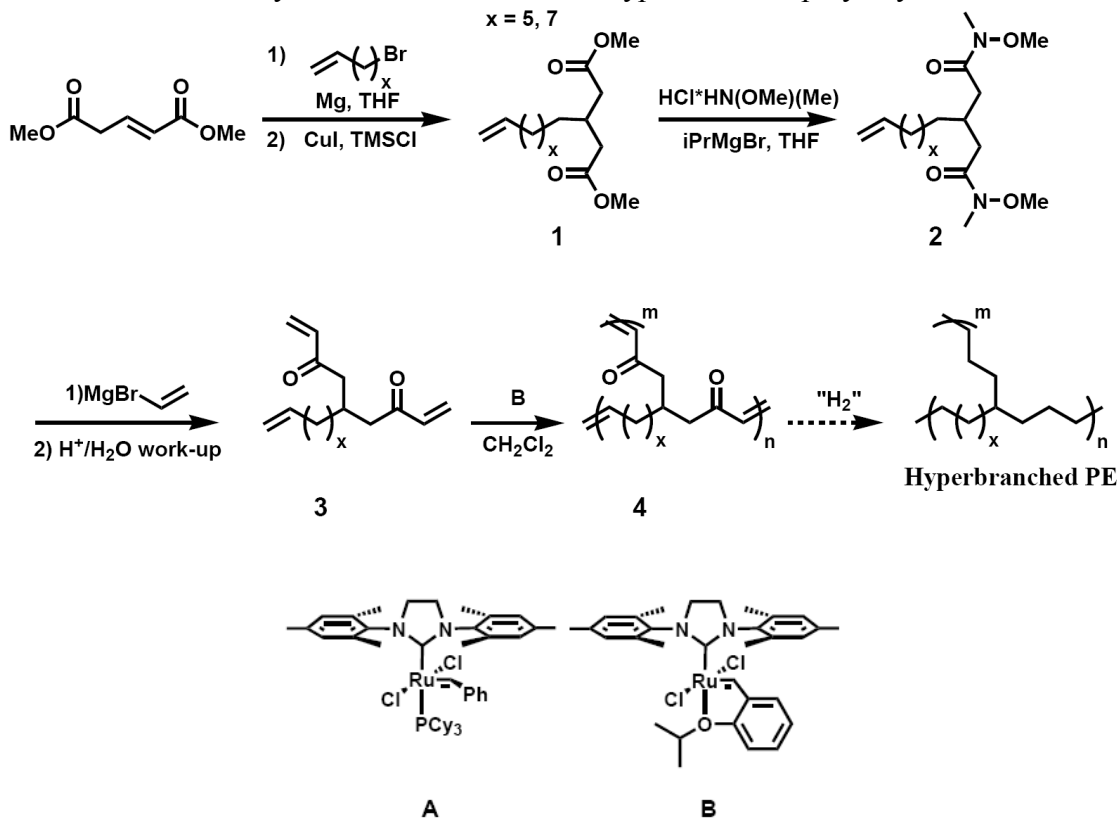


Figure A1. Hyperbranched ADMET catalysts.

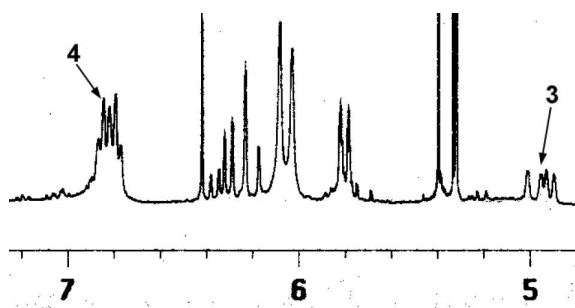


Figure A2. ^1H NMR evidence for polymerization of **3** to **4**.

Experimental Procedures

Materials and Instrumentation. All reagents were purchased from Aldrich at the highest available purity grade and used without further purification. NMR spectra were obtained using a Varian Mercury-300 spectrometer; samples were dissolved in CD₂Cl₂.

(1). A dry, 50 mL, round bottom flask equipped with a stir bar was charged with magnesium turnings (2.0 g, 82.3 mmol) and purged with argon for 15 min. 15 mL of dry THF was added to this reaction vessel and the mixture was heated to 50 °C. After the reaction mixture was stirred at 50 °C for another 15 min, a few drops of magnesium-activating 1,2-dibromoethane were added to the flask, and the solution was checked for gas evolution. Once it was established that the addition of C₂H₄Br₂ produced gas, 10-bromo-1-decene (4.2 g, 19.2 mmol) was slowly added to the vessel. The reaction solution was stirred for 3 hours at 50 °C before being transferred to a dry, 100 mL, round bottom flask charged with CuI (0.37 g, 1.9 mmol), 25 mL of dry THF, and a stir bar. The resulting suspension was stirred at room temperature until the dark color persisted (~ 2 min) before being cooled to -78 °C. After the consecutive addition of TMSCl (2.8 g, 25.7 mmol) and dimethyl glutaconate (1.0 g, 6.3 mmol), the mixture was stirred at -78 °C for 2 h and allowed to warm to room temperature. A solution of NH₄Cl (sat. aq.) was then added to the reaction flask and the solution was stirred for ~ 1 h until it became clear (bright orange in color). The products were extracted in EtOAc three times. The combined organic layers were washed with brine and dried over anhydrous MgSO₄. The solution was then filtered, concentrated, and purified by silica gel chromatography. Elution with 1 to 5 % EtOAc in hexane afforded 1.23 g of **1** (x = 7; 65 % yield). NMR (300 MHz, CD₂Cl₂, ppm): δ 5.82 (m, 1H), 5.02–4.90 (m, 2H), 3.63 (s, 6H), 2.33–2.31 (m, 4H), 2.03 (m, 2H), 1.37–1.27 (m, 15H). ¹³C NMR (300 MHz, CD₂Cl₂, ppm): δ 173.45, 139.88, 114.37, 51.85, 38.84, 34.54, 34.36, 32.68, 30.15, 30.01, 29.97, 29.68, 29.52, 27.09. HRMS(FAB+) *m/z*: 299.2213 [M+H].

(2). **1** (1.23 g, 4.12 mmol) was combined with N,O-dimethylhydroxylamine hydrochloride (1.21 g, 12.4 mmol) in 9 mL of dry THF. The reaction mixture was cooled to -20 °C, a 2M solution of isopropylmagnesium chloride in THF (12.4 mL) was added dropwise to the flask, and the solution was stirred for additional 30 min. A saturated

aqueous solution of NH_4Cl was added to the reaction mixture, and it was allowed to warm to room temperature. Thereafter, the mixture was diluted with Et_2O , and the products were extracted with Et_2O three times. The combined organic layers were dried over anhydrous MgSO_4 , filtered, and concentrated. Purification by silica gel chromatography, eluting with 25 to 50 % EtOAc in hexane afforded 1.24 g of oil **2** ($x = 7$; 84 % yield). NMR (300 MHz, CD_2Cl_2 , ppm): δ 5.82 (m, 1H), 5.01–4.90 (m, 2H), 3.66 (s, 6H), 3.12 (s, 6H), 2.41–2.37 (m, 4H), 2.03 (m, 2H), 1.39–1.21 (m, 15H). ^{13}C NMR (300 MHz, CD_2Cl_2 , ppm): δ 174.09, 139.91, 114.33, 61.66, 36.72, 35.06, 34.75, 34.36, 31.81, 30.33, 30.13, 30.02, 29.70, 29.53, 27.38. HRMS(FAB+) m/z : 357.2747 [M+H].

(3). **2** (0.35 g, 0.98 mmol) was dissolved in 5 mL of dry THF, and the solution was cooled to $-78\text{ }^\circ\text{C}$. A 1M solution of vinylmagnesium bromide in THF (10 mL) was added to the reaction flask, and the mixture was allowed to warm to room temperature. The resulting solution was then slowly poured over a saturated aqueous solution of NH_4Cl , and the products were extracted with CH_2Cl_2 three times. The combined organic layers were consequently washed with saturated aqueous solutions of NaHCO_3 (once) and NaCl (once), before being dried over anhydrous MgSO_4 , filtered, and concentrated. Purification by silica gel chromatography, eluting with 5 to 20 % EtOAc in hexane, afforded 115 mg of oil **3** ($x = 7$; 40 % yield). NMR (300 MHz, CD_2Cl_2 , ppm): δ 6.38–6.17 (m, 4H), 5.89–5.75 (m, 1H), 5.81 (dd, $J = 10.2\text{ Hz}$, $J = 1.6\text{ Hz}$, 2H), 5.03–4.91 (m, 2H), 2.58–2.40 (m, 4H), 2.03 (m, 2H), 1.39–1.18 (m, 15H). ^{13}C NMR (300 MHz, CD_2Cl_2 , ppm): δ 200.62, 139.87, 137.35, 128.37, 114.40, 44.49, 35.22, 34.75, 34.39, 31.01, 30.27, 30.01, 29.71, 29.54, 27.35. HRMS(FAB+) m/z : 291.2336 [M+H].

Notes and References

(1) Sworen, J. C.; Smith, J. A.; Wagener, K. B.; Baugh, L. S.; Rucker, S. P. *J. Am. Chem. Soc.* **2003**, *125*, 2228-2240.

(2) Pseudo-hyperbranched polyethylene has been prepared via "chain-walking" methods, which employ transition metal catalysts and are described in references 3 and 4. However, these methods produce statistical, random branching with no defined AB_n monomers in the backbone.

(3) Guan, Z.; Cotts, P. M.; McCord, E. F.; McLain, S. J. *Science* **1999**, *283*, 2059-2062.

(4) Sunder, A.; Heinemann, J.; Frey, H. *Chem. Eur. J.* **2000**, *6*, 2499-2506.

(5) Choi, T.-L.; Lee, C. W.; Chatterjee, A. K.; Grubbs, R. H. *J. Am. Chem. Soc.* **2001**, *123*, 10417-10418.